LUT UNIVERSITY
LUT School of Energy Systems
LUT Mechanical Engineering

Luka Ivanovskis

SYSTEMATIC SELECTION OF PERSPECTIVE SOLID WASTE MECHANICAL SEPARATION TECHNOLOGIES FOR MATERIAL RECOVERY

Examiners: Prof. Timo Kärki
D.Sc. (Tech.) Ville Lahtela

ABSTRACT

LUT UNIVERSITY
LUT School of Energy Systems
LUT Mechanical Engineering

Luka Ivanovskis

Systematic Selection of Perspective Solid Waste Mechanical Separation Technologies for Material Recovery

Master's Thesis

2019

103 pages, 69 figures, 5 tables and 3 appendices

Examiners: Prof. Timo Kärki
D.Sc. (Tech.) Ville Lahtela

Keywords: material recovery, mechanical separation, solid waste, technology selection, construction and demolition waste

Material recovery from waste streams is an important element of the circular economy. It relies on efficient liberation and separation of materials, which remains challenging for commingled solid waste streams. LUT University intends to research and develop new mechanical separation technologies, so an understanding of the state of the art, as well as research and development in the field in industry and academia is required.

For objective review and comparison of available and emerging mechanical separation technologies, a database of a new tree-like structure was created and filled with performance figures achieved by different technologies. Custom software written in Julia parsed the database into a tabular format for easy filtering and visualization.

The database allowed to describe technologies in terms of separation efficiency, suitable particle size, material categories and connections between these and other parameters. Alongside with technology performance, their underlying principles were characterized in terms of used effects, target material properties and affecting factors, that has led to insight into new possibilities for research. Considering both existing and future technologies, a feasible arsenal of techniques for separation of construction and demolition waste was proposed.

Limits of direct sorting methods were identified. Ways to achieve economical multimaterial separation with sensors were discussed. The database showed potential as a decision support tool suitable for systematic selection and comparison of technologies, extendable to keep up with future technological progress.

TABLE OF CONTENTS

LIST OF SYMBOLS AND ABBREVIATIONS

a	Particle acceleration [m/s^2]
B	Magnetic flux density [T]
F	Electroadhesion force [N]
F_{MA}	Magneto-Archimedes levitation force [N]
FN	False negative rate [-]
FP	False positive rate [-]
g	Acceleration of free fall [m/s^2]
G	Purity grade [-]
m	Particle mass [kg]
$m_{in,tar}$	Mass of target material in input material stream [kg]
m_{out}	Mass of output material stream [kg]
$m_{out,tar}$	Mass of target material in sorted product [kg]
r	Air compression ratio [-]
R	Recovery rate [-]
T	Levitation temperature [K]
TN	True negative rate [-]
TP	True positive rate [-]
T_0	Initial temperature [K]
z	Vertical coordinate [m]
μ_0	Magnetic permeability of free space [H/m]
ρ	Fluid density [kg/m^3]
ρ_0	Air density at 1 bar, 300 K [kg/m^3]
ρ_m	Material density [kg/m^3]
χ	Magnetic susceptibility of fluid [-]
χ_0	Magnetic susceptibility of air at 1 bar, 300 K [-]
χ_m	Magnetic susceptibility of material [-]
ABS	Acrylonitrile butadiene styrene
CCA	Chromated copper arsenate
CDW	Construction&demolition waste

DE-XRT	Dual energy X-ray transmission
ELV	End-of-life vehicle
EVA	Ethylene-vinyl acetate
IR	Infrared
FIR	Far infrared
FR	Flame retardant
HDPE	High-density polyethylene
HIPS	High impact polystyrene
HSI	Hyperspectral imaging
LIBS	Laser-induced breakdown spectroscopy
LIF	Laser-induced fluorescence
LDPE	Low-density polyethylene
LWIR	Long wave infrared
MWIR	Midwave infrared
MRF	Material recovery facility
MSW	Muncipal solid waste
NIR	Near infrared
NDE	Non-destructive evaluation
PA	Polyamide
PBT	Polybutylene terephthalate
PC	Polycarbonate
PCB	Printed circuit board
PCL	Polycaprolactone
PE	Polyethylene
PET	Polyethylene terephthalate
PHBV	Poly(3-hydroxybutyrate-co-3-hydroxyvalerate)
PLA	Polylactic acid
PMMA	Polymethyl methacrylate
PO	Polyolefin
POM	Polyoxymethylene
PP	Polypropylene
PPO	Polyphenylene oxide

PS	Polystyrene
PTFE	Polytetrafluoroethylene
PU	Polyurethane
PVC	Polyvinyl chloride
SAN	Styrene-acrylonitrile resin
SWIR	Short wave infrared
TPI	Terahertz pulsed imaging
UV	Ultraviolet
WEEE	Waste electric and electronic equipment
WPC	Wood-plastic composite
XRF	X-ray fluorescence

1 INTRODUCTION

In the following motivation for waste recycling is be explained. Terminology, separation equipment examples and its selection strategies are given. Aims of the present study are stated.

1.1 Material recovery from waste

Solid waste management is a part of sustainable development. There are numerous options to treat waste streams, starting with a least-favourable option, such as landfilling and ending with the utmost goal of total waste elimination. In the latter case, so-called cradle-to-cradle, or principle of circular economy, is achieved, when output of every single production activity is a source for the next one, thus material circulates in a closed loop (unlike with cradle-to-grave, when everything ends up being waste). Scarcity of natural resources, pollution of the environment with slowly degradable and hazardous materials, steadily increasing global production force to get higher in the waste management hierarchy (see Figure 1). Because of socio-economical constraints and technological limitations a significant amount of solid wastes do not get above basic landfilling and energy recovery. The next stage above that is material recovery.

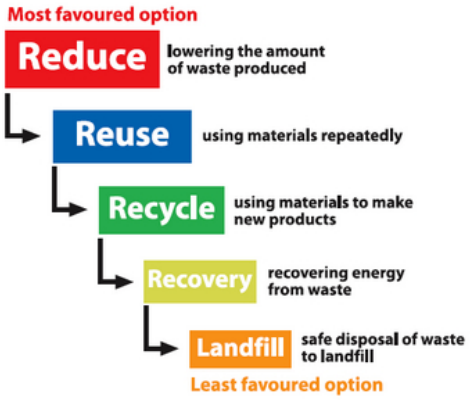

Figure 1. Waste treatment hierarchy (Brighton & Hove n.d.)

Recycling, or material recovery from waste, contributes a lot to sustainability. In particular,

- it decreases demand in virgin materials and natural resources like rare metal elements,
- reprocessing of waste into raw materials has lower energy consumption compared to the production of raw materials (Ragaert et al. 2017),

- less area is needed for landfilling,
- material recovery industry creates workplaces for people.

There are established routes for recycling of certain products like end-of-life vehicles (ELV), plastic and glass packaging, waste paper and cardboard. These are mostly products for which source-based separation was successfully implemented, when consumers deliver their items to separate collection points with targeted subsequent treatment. Acknowledgement of the waste composition also simplifies recycling of industrial waste, such as polymer manufacturing residues (Singh et al. 2017). On the other hand, commingled waste streams like municipal solid waste (MSW) and construction&demolition waste (CDW) have rich and broadly varying composition.

Despite established collection and processing facilities challenges remain in material recovery. Abundance of material grades used today overwhelms sorting capacities. Most of the rare alloying elements are lost in the recycling of steel and aluminium from ELVs. Only platinum and palladium are functionally recycled because of special care of catalysts, while cobalt, gold, manganese, molybdenum, rhodium, silver are lost (Andersson et al. 2017). Estimation for global recycling rates of metals yields 40% recycling of aluminium, 38% copper, 47% steel, 47% lead, 34% nickel and 36% zinc – all below 50% (Reuter & Kojo 2012).

In the packaging waste challenges are posed by materials like multi-layered laminates, polylactic acid (PLA), black plastic containers, full shrink wrap labels, metallized tubes, coloured opaque polyethylene terephthalate (PET) bottles, cardboard trays in plastic films. Foils in general complicate separation because of their low density and ability to cover underlying thick-walled items that leads to misclassification. Tight binding between layers in laminates force to sacrifice polymers in pyrolysis in favour of aluminium recovery. Biodegradable PLA plastic is replacing other plastics in packaging, but it is not accepted for composting and contaminates streams of currently recycled plastics. The production of PLA plastic itself has not yet reached sufficient volume for separate recycling. Black plastics are not recognizable nor distinguishable for optical sorters. Coloured PET contaminates the dominant stream of clear PET. (PacNext 2014.)

Special care has to be taken with respect to materials used in the past but violating environmental legislation now. Presence of plastics with brominated flame retardants (FR)

(Peeters et al. 2014), glass with high lead content from cathode ray tubes (Dully 2011), wood with chromated copper arsenate (CCA) treatment (Solo-Gabriele et al. 2004) is unwanted in general purpose recycling and should be treated for safe disposal or reprocessed into products with similar requirements.

Commingled multimaterial waste streams like MSW, CDW as well as sophisticated postconsumer products (like waste electric and electronic equipment (WEEE)) do not attain high enough recycling rates for material recovery. With application of information theory, it was shown that items possessing high entropy due to material mixing remain out of recycling when contained materials are valued low on the market (Dahmus & Gutowski 2006). In Figure 2 an apparent boundary between recycled and non-recycled items is drawn supporting this idea. As material prices go higher the recycling area should have consumed some of the products not recycled at that time, but there is still a long way to make full recycling of laptop computers and cell phones economically attractive. Progress in robotics allowed Apple company to develop a disassembling robot for recycling of postconsumer phones produced by that company (Apple Inc. 2018). However, cheaper and more general purpose separation solutions are in demand.

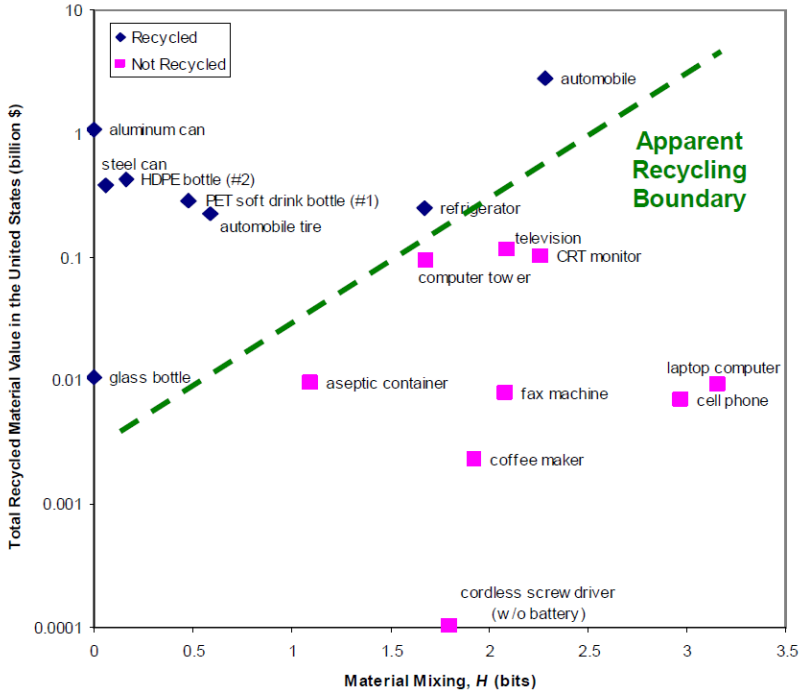

Figure 2. Apparent recycling boundary for products in the US (Dahmus & Gutowski 2006).

1.2 Terms of material separation

In order to avoid ambiguity in the meaning of terms used, the list below provides definitions of those in the way they are used in the present work. The terms are in common use in literature about waste separation, though different variants of some terms can be used.

- Comminution (also fragmentation) – reduction in size of waste fragments by crushing, shredding, milling etc.
- Sorting – general term about getting pure material streams out of a waste stream.
- Manual/automatic sorting – sorting by trained human workers (manual) or dedicated machinery (automatic).
- Liberation – breaking connection between different materials found together in one fragment of waste, often achieved by comminution, precedes separation.
- Separation – splitting of the waste stream into streams with less commingled content.
- Differential – action that affects differently various materials allowing to separate them, like differential fragmentation.
- Positive/negative sorting – removal of the target (positive) or non-target (negative) material from the waste stream in a material recovery facility (MRF).
- Target material – material that is aimed to be separated from the non-target one (waste).
- Macro/Microsorting – sorting of whole waste items (like plastic containers) or comminuted waste fragments.
- Direct/indirect sorting – separation of materials by use of forces acting differently on various materials in the waste stream (direct) or sensors identifying and locating materials in the stream and subsequent picking up or ejection by mechanical devices (indirect).
- Binary/multiway sorting – sorting of waste stream into two/many fractions.
- Up/downcycling – conversion of recovered materials into products with higher (up-) or lower (down-) requirements for material quality and purity compared to the products the materials were recovered from.
- Recovery (also yield) – fraction of extracted material from its amount in the feed stream.
- Purity (also grade, content) – fraction of target material in the product stream.
- Accuracy – prediction power of sensor-based material identification in the context of sensor-based material classification.

The last three terms are measures used to assess the performance of separation equipment. Accuracy term was brought from computer science where different classification algorithms are used. The classification algorithm yields positive (P) or negative (N) result whether the item belongs to some class (material) A. Imperfection of the algorithm and measuring equipment introduces some false (F) classification results in addition to the correct true (T) results for both positive and negative classification outcomes. In total there are four fractions in binary classification from which accuracy, purity G and recovery R are defined by equations:

$$Accuracy = \frac{TP + TN}{TP + FP + TN + FN} \tag{1}$$

$$Purity\ G = \frac{TP}{TP + FP} = \frac{m_{out,tar}}{m_{out}} \tag{2}$$

$$Recovery\ R = \frac{TP}{TP + FN} = \frac{m_{out,tar}}{m_{in,tar}} \tag{3}$$

Purity grade and recovery were brought from the mineral industry, so they are usually expressed in terms of mass ratios: $m_{in,tar}$ and $m_{out,tar}$ are masses of the target material in the unsorted input and sorted output streams, but m_out is mass of the whole sorted output. R and G values together with the content of each material in the feed stream allow to solve the problem of computing masses and composition of outcoming streams. Sometimes separation efficiency is reported, although definitions vary: it can be products recovery and purity for both materials in a binary separation $R_1G_1R_2G_2$ (Dodbiba et al. 2005), geometric mean of both material recoveries $\sqrt{R_1R_2}$ (He et al. 2011), Newton's efficiency $R_1 + R_2 - 1$ (Tsunekawa et al. 2005b), difference between the percentage of correctly ejected material and mistakenly rejected material (Abbasi et al. 2010) and some other.

1.3 Layout of MRF

In this section, a general overview of the state of the art techniques and waste processing stages used at MRF is given. Unlike chemical recycling that breaks materials into basic elements

(like monomers in case of polymers treatment), mechanical recycling split materials by mechanical forces and does not alter the chemistry of materials (Ragaert et al. 2017). The first operation in mechanical recycling is comminution which reduces particle size down to the preferred range. Smaller particles can be more easily manipulated than bulky parts and each individual particle tends to be more homogeneous in composition (materials are liberated this way). Coarse comminution is done by hammer mills, shear shredders and crushers (recycling of ELV and CDW). Mills have high-speed rotor impacting the incoming waste. The waste can exit mill only when its size allows to go through the grate at the bottom. Shear shredders are made of multiple shafts rotating in opposite directions and cutting items with cutting extensions on their surface. Shear shredders tend to consume less energy compared to milling equipment. Crushers use some kind of reciprocating motion to break items in pieces. Some dedicated machinery for bag debaling can be included prior to comminution. (Chang & Pires 2015.)

Separation follows the comminution stage. It is often required to classify particles by size before the following treatment. This is done by screens of various construction: vibrating screen, rotating trommel (or drum), disc (or roller) screen. Vibrating and rotating screens are inclined sieves with holes of different size, starting with a smaller one. Waste moves along the device and finer particles fall through the screen first, while coarser ones proceed further until they pass through holes. Disc screen is comprised of a series of rotating non-circular shafts that disentangle particles and let smaller ones to fall through gaps. Shafts can be specifically designed to break fragile items like glass cullet so that they are removed from the stream. (Chang & Pires 2015.)

Rough classification by apparent density allows to separate mineral part from wood and plastic, light foils and paper from plastic containers etc. Air knife, air cyclone achieve this by aerodynamic forces. The ballistic separator consists of inclined sieves in reciprocating motion that segregate waste into heavy (slides down), light (jumps upward) and fine fraction (falls through). Further separation of materials with density close to water is done in sink-float tanks filled with water or salt solution with density lying between that of separable materials. (Chang & Pires 2015.)

Magnetic and eddy current separators are aimed at removal of, respectively, ferrous and

non-ferrous metal particles. A permanent magnet mounted above conveyor or inside conveyor pulley attracts ferromagnetic particles (typically steel and iron). The alternating magnetic field produced by the high speed rotating magnetic drums with alternating poles induces eddy currents in conductive materials (copper, aluminium alloys and stainless steel) and eject them from the stream. (Chang & Pires 2015.)

The presented list of direct sorting methods is not an exhaustive one but presents the major techniques which are in use despite their lack of specificity. The following stages typically involve manual separation by human workers or sensor based separation (or combination of them). Sensors may recognize conductivity properties of materials (inductive sensors), but typically they operate by detecting reflected or transmitted parts of the electromagnetic spectrum – visual, infrared (IR), X-ray (Pretz & Julius 2008). Measured spectral profiles and images are fed to classification or machine vision algorithms that operate ejection mechanisms, usually blow bars – arrays of pneumatic valves blowing out the target (in the positive sorting) or non-target (in the negative sorting) items. Examples of how different separation stages are included into real MRF are shown in Figures 3 and 4.

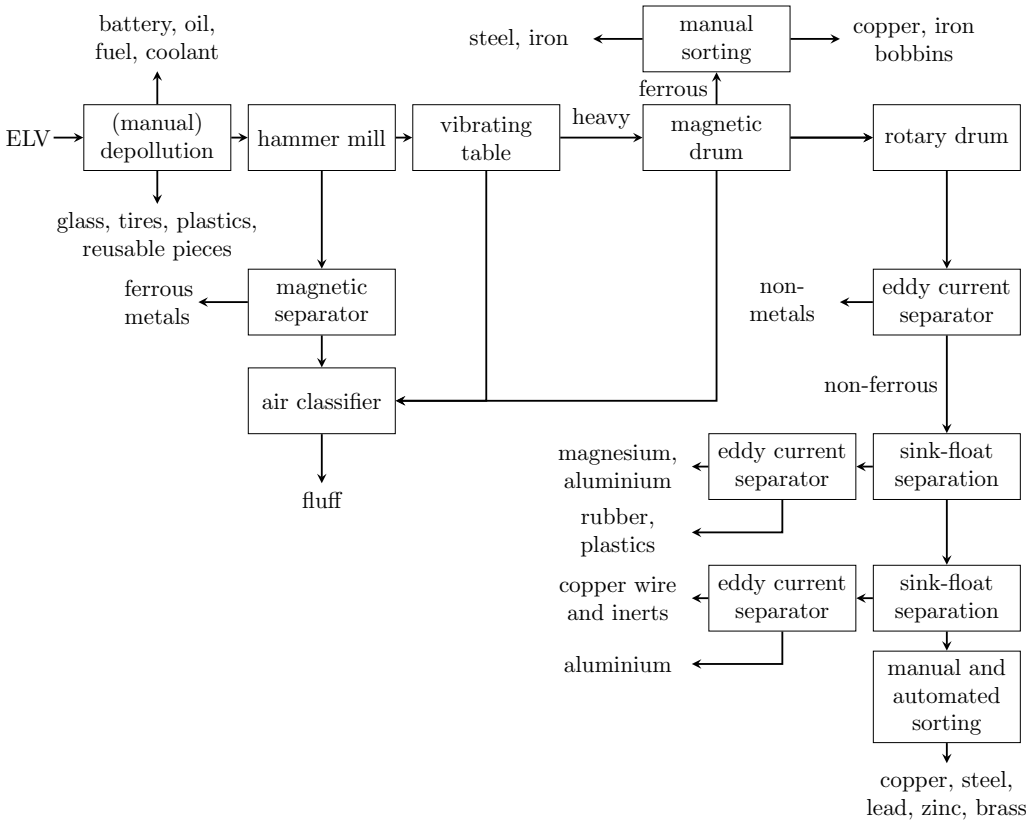

Figure 3. Flow sheet of ELV recycling (Chang & Pires 2015).

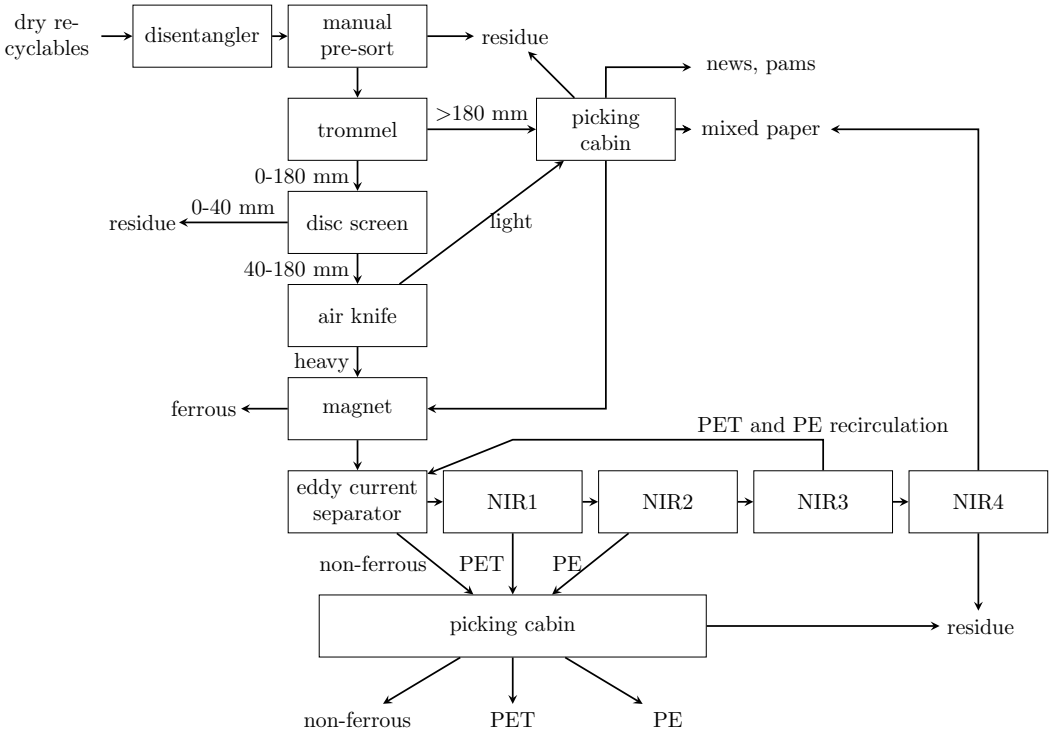

Figure 4. Flow sheet of an MRF in United Kingdom processing kerbside collected dry recyclables (WRAP 2010).

1.4 Frameworks for MRF planning

The efficiency of MRF depends on the choice of equipment as well as its layout. Various studies aimed at modelling and optimization of solid waste treatment. Mellor et al. (2002) developed a mathematical model and decision-support framework for material recovery, recycling and cascaded use. The model described material flow through activity units. Material flow comprised material categories together with their utilities (properties). Activity units (like separators) were characterized by acceptance criteria for the input materials and effects on their utilities. The model (called CHAMP – CHAin Management of Materials and Products) focused on polymer materials, although authors claimed its applicability for metals.

Coates & Rahimifard (2009) modelled post-fragmented waste stream in the scale of MRF in the United Kingdom. The model considered several mechanical separation methods with certain target parameter of sorting (like density, particle size, electrical conductivity): eddy-current, air classification, screening, magnetic separation, dense media separation. Both inefficiencies of separation equipment as well as incomplete material liberation incorporated

in the model. The proportion of resulting waste streams was accurately predicted.

Metal recycling was analyzed by van Schaik & Reuter (2010). Mathworks Simulink program simulated material liberation based on engineering data of ELV. The program took as input material clusters in vehicle components with their connection types and predicted material recovery rates with the state of the art technologies. Physical and chemical material description were incorporated in the model.

Dully (2011) presented automated searching in the internet for potential technologies for treating specific waste. Algorithm used sample text documents to extract terms specific for the studied material fraction, recycling and recovery, technology novelty. Afterwards, requests from randomly selected terms of those three categories were sent to an internet search engine. Search results were assessed by experts for feasibility. In the case study, lead-rich glass from waste cathode ray tubes was found to be economical for reprocessing into protection shields for medical radiography equipment.

Combinatorial approach for optimizing the layout of MRF was done by Ip et al. (2018). Calculation of material flow being separated into the target and non-target fraction at each separator resulted in the prediction of resulting purity and recovery of materials (so-called Bayesian separation model presented by Wolf et al. (2010)). Uncertainty analysis, sensitivity analysis, maximization of MRF revenue by rearranging separators in sequence and adjusting their separation thresholds for higher purity or recovery (see Figure 5) were completed.

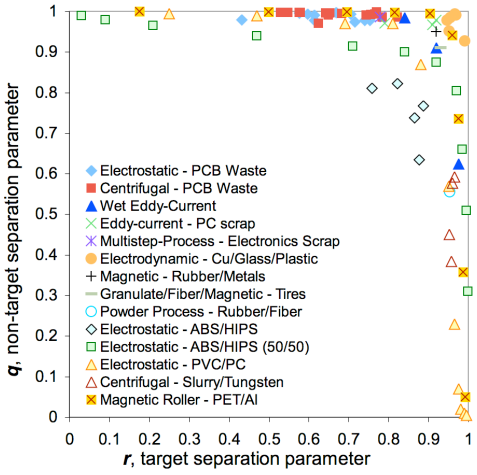

Figure 5. Separation performance for different processes in terms of target and non-target separation efficiencies (Wolf et al. 2010)

Table 1. Material recovery decision support.

	Mellor et al. (2002)	Coates & Rahimifard (2009)	van Schaik & Reuter (2010)	Dully (2011)	Ip et al. (2018)	present study
Scope	present plastic product lifecycle	present waste separation	present separation and treatment	perspective waste fraction processing	MRF layout (present)	present/perspective separation equipment
Soft-ware	no data	MS Excel VBA	Matlab/Simulink	IPA-Scout, RapidMiner, Java	Java, genetic algorithm	Julia, Jupyter, data in JSON-format
Mate-rials	polymer "utilities" (properties)	target parameters for common materials	physical and chemical description of 28 materials	verbal description	mass flow	material categories from experiment description
Libe-ration	"reprocessing" activity with acceptance criteria, alters utility values	models material entanglement through interaction matrix	material clusters and particle compositions prediction, based on the joint types	none	none	none
Sepa-ration	"reprocessing" activity with acceptance criteria, alters utility values	binary separation based on one target parameter for each technology	based on material physical properties	none	coefficients for mass flow through binary separator	quantitative and qualitative facts about material separation
Out-come	cost/environmental assessment for material selection, recycle/re-use options	effect of materials entanglement on separation, material sizing, composition of recyclates	prediction of mass flows, recyclate quality, recycling/recovery	best available technique for recycling problem from automated internet search	MRF layout, internal recycling loops for best purity/recovery/profit	comparison of technologies from facts

1.5 Aims of study

LUT University intends to build a pilot separation line for research purposes. Aforementioned frameworks for technology assessment had limited applicability for the research questions at LUT. Therefore, planning of the laboratory scale separation plant needed a better-tailored framework for the needs of the research institution. Aims of the study comprised:

- review existing and suggest new waste material mechanical separation principles and technologies to bring in the field of recycling,
- apply tools and knowledge acquired in the previous step to propose a layout of separation equipment for a particular research problem.

Development of the tailored approach is described in detail in the following chapters, but its place among the presented frameworks is summarized in table 1. Chapter 2 describes software development and literature search procedure. Chapter 3 presents results concerning the technology landscape, new technologies and technology selection in a case study. Chapter 4 summarizes results and Chapter 5 states final conclusions.

2 METHODS

The procedure of the current study was based on the creation of a database that could store and process information about waste separation technologies and related techniques. Details of its composition and interface are presented below.

2.1 Database contents

Although databases often have tabular form and are stored and processed in spreadsheets (like Excel), this approach would have limited applicability to document performance data of different technologies. Hierarchical (or tree-like) structure suits the purpose better, as it allows to nest the data: a general description of technology as the root and further branching into subtypes, instances and experimental trials with associated details. In this case, every leaf of the tree (for example, purity value achieved in a single experiment) has an association with all the information located on the path from the root to this particular leaf. There is practically no duplication of information because information in the root characteristic to multiple instances does not need to be repeated for every instance, unlike it is with tabular data storage. Also, the level of details in information sources varies and covers different aspects, making it challenging to follow one strict tabular format but rather forces to bind multiple tables.

There are numerous general-purpose hierarchical file formats: XML, JSON, HDF5 (Fridrich & Urban 2018). XML and JSON both store information in human-readable text format (can be viewed and edited in a simplest text editor like Notepad) and can be mapped into variable types provided by many programming languages. HDF5 stores data in binary format and has widespread use for scientific data. XML and JSON are plain text data formats that serve for data exchange over the internet or in databases like CouchDB or PouchDB. From those three JSON was chosen because of its simplicity and straightforward import into many programming languages (it is native for JavaScript), which gives freedom for implementation of custom data analysis algorithms. Extension of the database is possible by manual entry of data in text following the implemented syntax.

The JSON file stores a collection of name-value pairs and ordered lists of values. Since value

can be a collection or a list itself, nesting is achieved by simple delimiting with brackets. The single values can be of type string, number, boolean (true/false) or null. Names and strings are put in double quotes, collections in { } brackets and lists in [] (Introducing JSON 2017).


```
{
	"guide": {
		"action": {
			"detect": "senses and produces signal",
			"enrich": "remove remaining (like 5%) contaminants from the target stream",
			"feed": "a mean of conveying",
			"route": "selectively routes items to the right bin",
			"sort": "separation by some force field"
		},
		"brief": "short (2-3 sentences) description of the process",
		.
		.
		.
	},
	"materials" : {
		"board": {
			"cardboard": {},
			"paper": {
				"newsprint": {},
				"notebook paper": {},
				"glossy paper": {},
				"white free sheet": {},
				"coated sheet": {},
				"colored free sheet": {}
			}
		},
		.
		.
		.
	},
	"technologies" : {
		"active pulsing air classification": {
			"brief": "Intermittent airflow fed into a column with shredded waste particl
			"action": "sort",
			"continuity": "online",
			"medium": "air",
			"pressure": "normal",
			"temperature": "room",
			"property": "density",
			"factors": ["drag", "density", "size", "shape", "terminal velocity"],

			"effects": [
				"drag",
				"free fall",
				"gravity",
				"inertia",
				"pump",
				"valve",
				"vibration"
			],

			"instances": [
				{
					"reference": "Lee & Rahimifard 2012",
					"maturity": "research",
					"trials": [
						{
							"waste": "footwear",
							"size": [0, 5],
							"materials": ["rubber", "leather"],
							"shape": "flake",
							"parameter": [[0.9, 1.4], [0.7, 0.8]],
							"recovery": [0.96, 0.93, 0.87],
							"purity": [0.82, 0.91, 0.93]
						},
						.
						.
						.
	}
}
```


Figure 6. JSON file with data, an overview.

The JSON file created for data storage in this work consists of three sections: a guide, a materials classification and description of technologies. The guide tells about used names (data fields) and conventions to fill them. Although it is aimed at humans that will come to read and write the file, it is written in the very same JSON format and is partly used by

file parser. Materials classification is a tree with material names that are encountered in the following description of technologies and it makes possible to replace very specific material types used in experiments with more generic ones (like AL-1100 is mostly aluminium which belongs to non-ferrous metals). At last, the technologies section deals with technologies found relevant throughout the study. Figure 6 gives an overview of the file structure.

A description of technology is a collection named by technology name. After that follows brief description, action type (sort for direct sorting, detect for indirect sorting and so on), process continuity (batch/online), medium (air/gas/supercritical, water/solution/liquid or none when technology does not rely on that), pressure (vacuum/normal/elevated), temperature (cryo/elevated/room), property by which materials are separated and factors that affect the separation. "Effects" field lists generally known effects and techniques that take place in the process. After that instances follow. Every instance is supposed to have a reference. The reference name has to coincide with a pdf-file name of the source and possibly with a png-image name containing some illustrative information. A single instance must predominantly belong to one technology and operate with the same equipment, so one reference may appear in different instances if needed.

The maturity level of an instance is a rough assessment of how close the presented information is to industrial implementation. It can be research, laboratory, pilot or industrial (Gundupalli et al. 2017a). Research level corresponds to experiments with custom equipment at a tiny scale with specially prepared test materials and aims at the proof of concept. Laboratory level goes further and either uses commercial or larger scale equipment, materials from real waste (which can be indicated in free text for "waste" field). The pilot level is close to the industrial one but still experimental. In addition to those four, "patent" level is added to specify information from patents without clear evidence of real use and "external" for those industrial solutions used elsewhere (not in recycling). At any place, there can be a remark that provides a textual comment about experiment conditions, observations. The word "note" is introduced for comments about transferring data from a reference into the database when there is no straightforward way to do it, like if only the highest value is taken.

"Device" field and "cost" are special remarks with information about commercially available equipment and expenses. Characterization of materials is given in terms of their names,

particle size in mm (either single number or [minimum, maximum]), wavelength range in nm (for sensors using electromagnetic radiation), parameter (value of material property, if given, with units specified in the "guide" section of the file), content in the feed (called "input"), particle shape (flake/granule/sheet/sphere/strand), recovery, purity, accuracy and efficiency rates, depending on what is available (rounded to the second decimal place). Since many results can be reported in a single publication, those fields can be organized into two-dimensional structures, so that correspondence between single values can be deduced. For example, a note in the form of

```
"materials" : ["PP", "PE"],
"input" : [0.4, 0.6],
"purity" : [[0.8, 0.91], [0.85, 0.88]]
```

can be interpreted as "a 40%/60% polypropylene/polyethylene (PP/PE) mixture was sorted with 80% PP purity in the first experiment, 91% PE purity in the first experiment, 85% PP purity in the second experiment, 88% PE purity in the second experiment". Internal brackets should group results of a single experiment. Since researchers may report results for only one (target) fraction of waste, it is possible to describe as follows:

```
"materials" : ["PP&PE", "aluminium", "copper"],
"purity" : [0.7, 0.75, 0.72, 0.74]
```

In this case, PP and PE are considered as a single fraction and 70%, 75%, 72% and 74% purity signifies purified PP and PE content obtained in four experiments (dimension mismatch suggests that purity grades cannot be mapped to the materials). More complex cases can be split using "trials" keyword:

```
"materials": ["PVC", "PET"],
"shape": "flake",
"trials": [
    {
        "size": [0.9, 4],
```

```
        "input": [[0.5, 0.5], [0.1, 0.9], [0.9, 0.1]],
        "recovery": [[1, 0.91], [0.94, 1], [1, 0.82]],
        "purity": [[0.92, 1], [0.97, 0.99], [0.98, 0.97]]
    },
    {
        "remark": "two-stage flotation",
        "size": [[3.2, 4], [2.5, 3.2], [2, 2.5]],
        "recovery": [[0.97, 0.99], [0.88, 0.99], [0.95, 0.95]],
        "purity": [[0.99, 0.97], [0.99, 0.9], [0.95, 0.95]]
    }
]
```


In all the lines the first number in [] is related to polyvinyl chloride (PVC), while the second one to PET, except size for which number pairs indicate the minimum and maximum size by default. Both materials in all experiments are in flake form. In the first trial, the size of particles is the same for all experiments, while it varies throughout the second trial. Using the aforementioned conventions, there exist a more or less compact way for documenting achieved performance results without repeating information very frequently. Some fields may appear several times on the way from technology name down to particular result, however, not within the same collection. They may combine with each other (like remarks or effects) or override when the latter occurrence exclude the former one by definition (like the medium in a particular instance may differ from the one typically used for that technology). The JSON file can be checked for correct syntax and reviewed in different online tools like JSONLint (Crockford & Carter 2018) or Code Beautify (Code Beautify n.d.).

2.2 Database filling

The database file was filled manually by going through valid references for the topic. Search of technologies was done first by creating a list of them from recent review articles: Gundupalli et al. (2017a), Ragaert et al. (2017), Singh et al. (2017), Vrancken et al. (2017). Collected titles were then searched primarily in LUT Wilma Finna database, references in the articles extended the list of technologies and associated references. References mostly published after the year 2000 were considered with some exceptions. Because of broad scope and large

amount of data some articles were not documented in the database, preference was given to more recent, innovative and better documented numerical results. In total, 199 references were collected.

The "effects" field in the database should have provided an insight into what principles are used in the respective technologies. Since the term "principle" is very broad, a list of those effects with annotations was taken from databases collected by Aulive (Aulive 2019) and Oxford Creativity (Oxford Creativity n.d.) companies. Additionally, a list of material properties was created for the systematic description of target properties for separation methods (Matmatch n.d.).

Patent information was used occasionally when they were found through similarity search provided by Teqmine software (Teqmine n.d.). The service searches for patents filed in English through natural language processing, thus allowing to find technologies similar to those described in scientific publications by copying whole texts into the search field. Search in the web allowed to collect some examples of available industrial equipment and commercial technologies. Review by Fantoni et al. (2014) on robotic grippers provided search terms for material handling and routing technologies.

Ideas for new technologies were drawn from an additional search about used and unused effects, problem areas of existing technologies, analogous technologies developed for other fields. Their technical feasibility assessment was done based on available evidence of their performance.

2.3 Database use

There are data processing tools used for hierarchical data. Relational databases do this by connecting multiple tables to each other. Pivot tables in Excel have limited applicability to work with nested data, Gneiss (Chang & Myers 2016) is an experimental software for intuitive work with pivot tables stored in JSON format, but not very usable for so many custom fields. For this reason, a dedicated data parser was developed in Julia – free general purpose programming language developed since 2012 for high-performance computing (Julia n.d.). It has Matlab-style syntax convenient for operation with vectors and matrices. The parser and related tools were put into Jupyter notebook (Jupyter 2019) that run in a web

browser and combine text annotations (styled with Markdown or Latex), short executable code scripts and their interactive outputs. Altogether this allows to review database, filter results by specific criteria and produce plots for exploratory data analysis. Because of the programming environment, a custom processing can be implemented in Julia code.

The core idea of database processing lies in "factualization" of the tree-like technology structure stored in it. That is, every possible path from the root of the tree to the leave is turned into a row of a table. The table of facts contains all the same columns like the keywords in the JSON files, like technology, brief, effects and others with minor changes to serve the tabular format best: size is split into minimum and maximum size columns (same for the spectrum and parameter columns), missing efficiency was computed as geometric mean of available performance figures (accuracy, recovery, purity) to give a vague performance estimate where no better option is present. Separation of materials was treated as there was one target fraction in each trial separated from the rest (called "trash" for short). Thus, one trial of sorting a ternary mixture resulted in three lines (not to confuse with cases where multiple materials may occur in the same fraction). For example, separation of PP, PE and PET mixture is equivalent to the separation of PP from PE&PET, PE from PP&PET, PET from PP&PE. Only target material parameter values were taken in each line (split into minimum and maximum values). Additionally, parameter difference value was computed as a distance from the mean target material parameter to the closest material in the "trash". Extra columns for the year (extracted from the reference name), as well as instance and trial identification numbers were created (data about the same instance were given the same instance number, about the same separation trial – the same trial number) to make clear how results are connected. Fields occurring multiple times were either concatenated or overridden. List-like fields, such as effects and factors are kept as a list in the respective cell. Missing values are implemented in Julia as a special variable type.

Conversion of the database into a table is driven by the ease of filtering of table rows and columns. For that, a graphical interface was implemented in the Jupyter environment. The interface consists of Filtering, Table view and Plotting blocks, preceded by short annotation. In the Filtering (Figure 7) allowable values for different columns are set after the JSON file is read and parsed. Graphical interface covers the most probable use cases – inequalities for numerical values, checkboxes for values with few possible options. Text boxes are provided

to limit technologies, effects, factors, materials. All filters are applied with AND operation, except for the fields organized in columns (like online OR batch continuity). Material category level controls replacement of specific materials with more generic ones (the level equals the maximum depth of materials in the material classification tree, level=0 results in total substitution of everything with "materials", level=1 consists of plastics, metals..., level=2 – PE, aluminium, copper..., level=3 – LDPE, HDPE...). There is a possibility to search a keyword (or a phrase) that must have a perfect match within the table entries. Finally, exclusion of missing values requires the obligatory presence of values in the marked columns (by default missing value does not lead to filtering the respective row out).

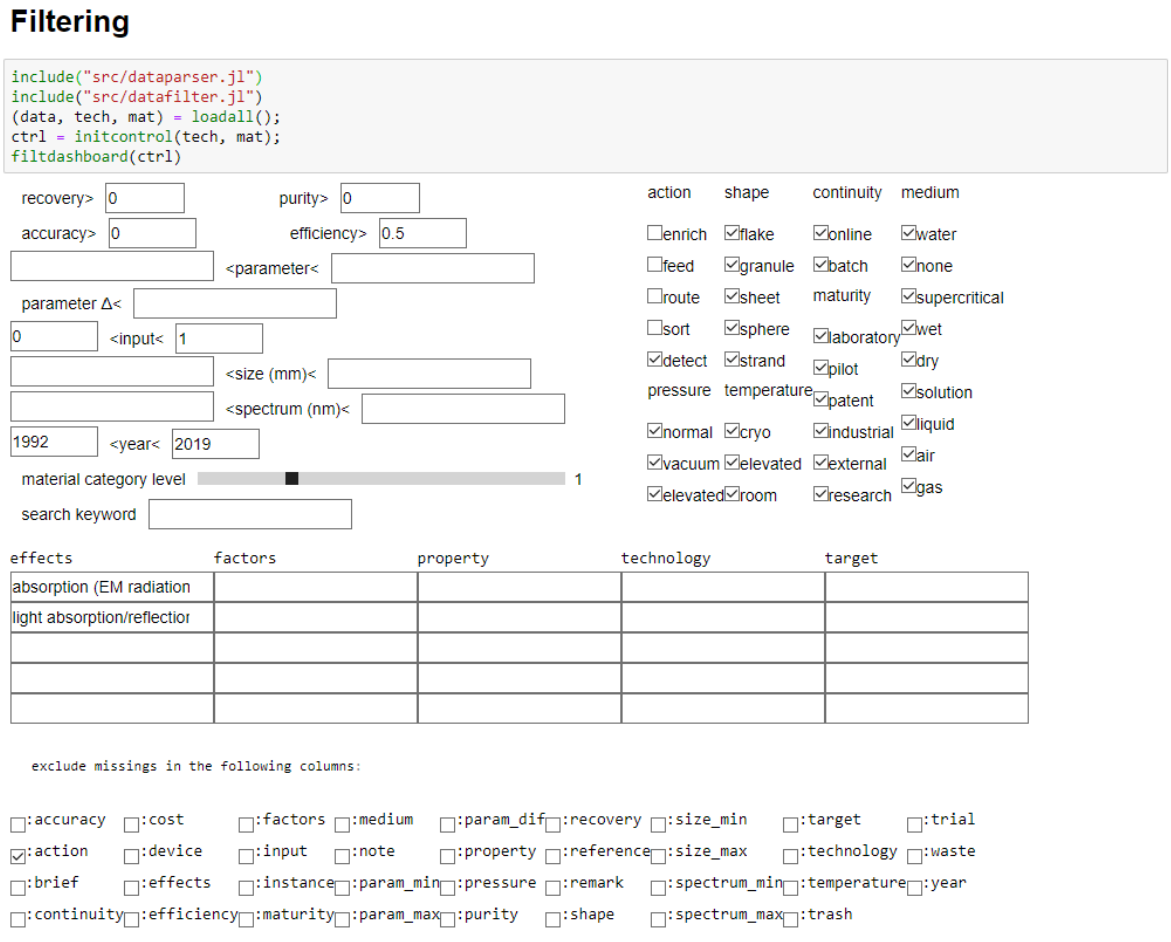

Figure 7. Filtering interface, see parsing and filtering code in Appendices I and II.

In the Table view (Figure 8) the filtered table can be reviewed by selecting columns and pressing "update". The filtered data can be accessed in Julia code from `df[]` data frame, the shown table is contained in `tb[]` variable (updated after each manipulation). The displayed table can be exported to an Excel file (all rows are saved, also those cropped by the preview).

When the reference column is included, the respective file can be opened by providing the line number.

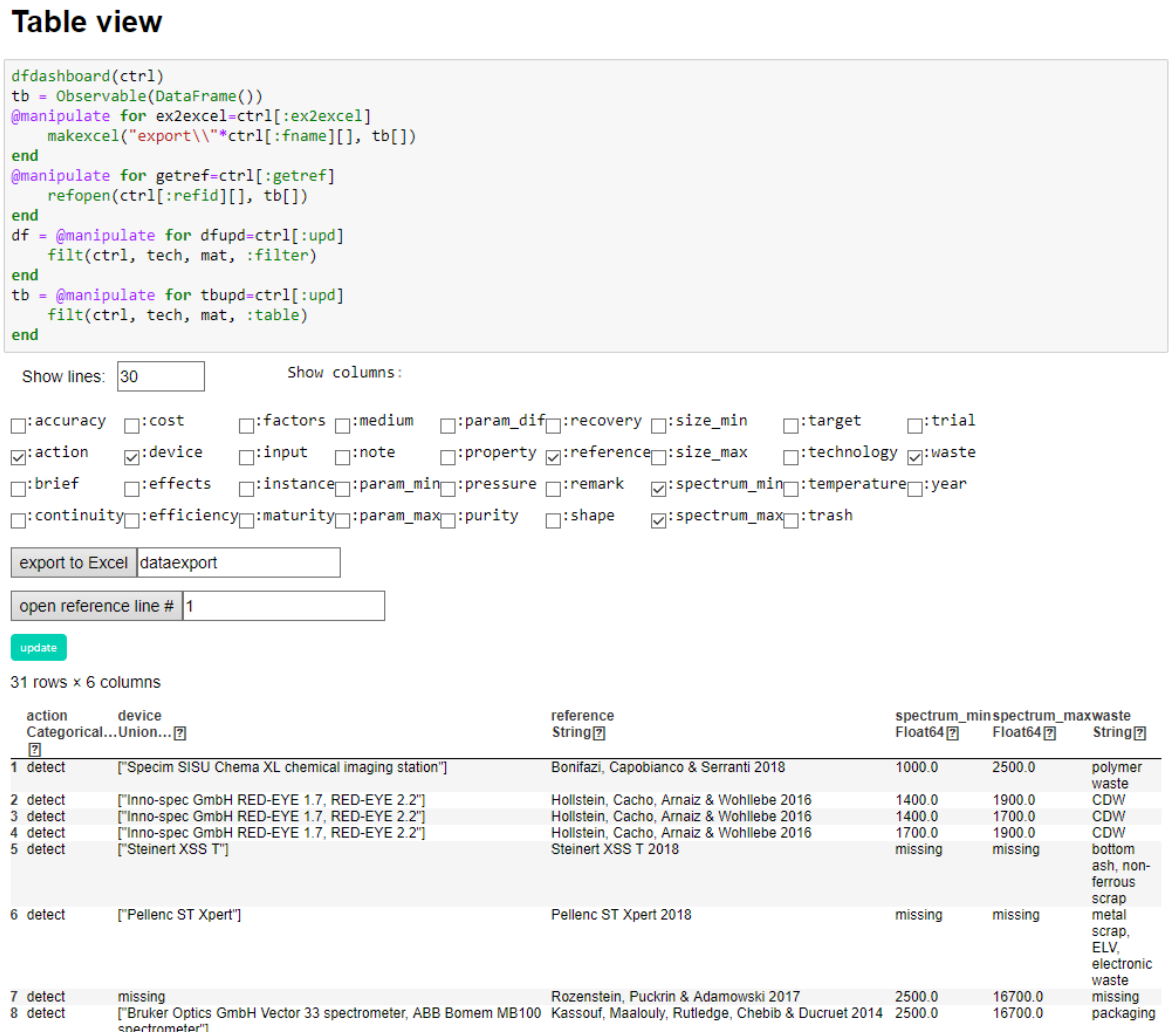

Figure 8. Table view interface.

In the Plotting (Figure 9) the filtered table can be visualized. Bubble, scatter and range plots are implemented. Bubble plot works with categorical values for both axes, range plot works with min-max values for the x-axis. Grouping eliminates repeated counting of elements with the same x, y and grouping values in the bubble plot. Grouping for the range and scatter plots induces colouring of markers based on the grouping value (and the legend is added). Rows with missing in x, y or grouping columns are eliminated before plotting. Saving produces .pdf and .png images. The current plot can be accessed and edited with Julia via `plt[]` variable.

Plotting

```
include("src/dataplotter.jl")
plotdashboard(ctrl)
plt=Observable(plot())
@manipulate for ex2image=ctrl[:ex2image]
    savefig(plt[], "export\\"*ctrl[:iname][] * ".pdf")
    savefig(plt[], "export\\"*ctrl[:iname][] * ".png")
end
plt = @manipulate for pltupd=ctrl[:upd]
    filt(ctrl, tech, mat, :plot)
end
```

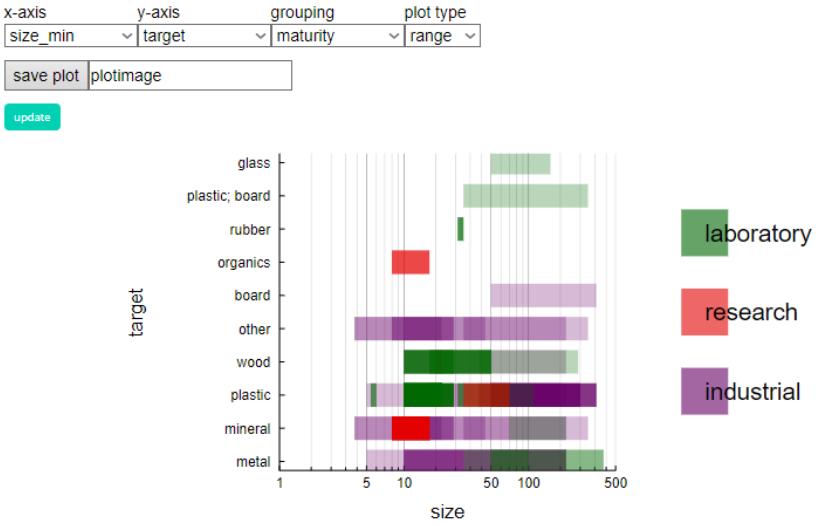

Figure 9. Plotting interface, see the respective code in Appendix III.

Database usage includes searches for target materials, technologies, getting an idea about hot topics of research, assessing maturity and performance of technologies, their sensitivity with respect to the target parameter, particle size and so on. For interest in a particular result, the reference file can be opened in an external viewer. With proper filter and visualization settings, the database can aid in both review of technological landscape as well as a case study for a particular separation problem. It is to be noted, however, that the absence of any result in the database does not mean it is impossible. The database just affirms that somebody has obtained certain data, extrapolation and interpolation of those results must be within the user's capabilities. The database in conjunction with external sources was used to derive a technological landscape, generate ideas for new technologies and select perspective technologies for the case study.

3 RESULTS

Findings from the database filling and usage are described in the following.

3.1 Technology landscape

Separation technologies in research and industrial applications are grouped based on the target material property for sorting.

3.1.1 Wet density-based separation

Separation of materials by density stems from centuries long mining applications. The very basic technology is sink-float separation, simple and efficient binary separation when:

- density distribution of separable materials do not overlap each other, see how close densities decrease separation efficiencies in Figure 10,
- there is fluid with density between those of materials (water has the dominant use),
- material particles are not too small, otherwise, they agglomerate or get disturbed by hydrodynamic forces,
- particles are wetted well and do not hold air bubbles adding buoyancy.

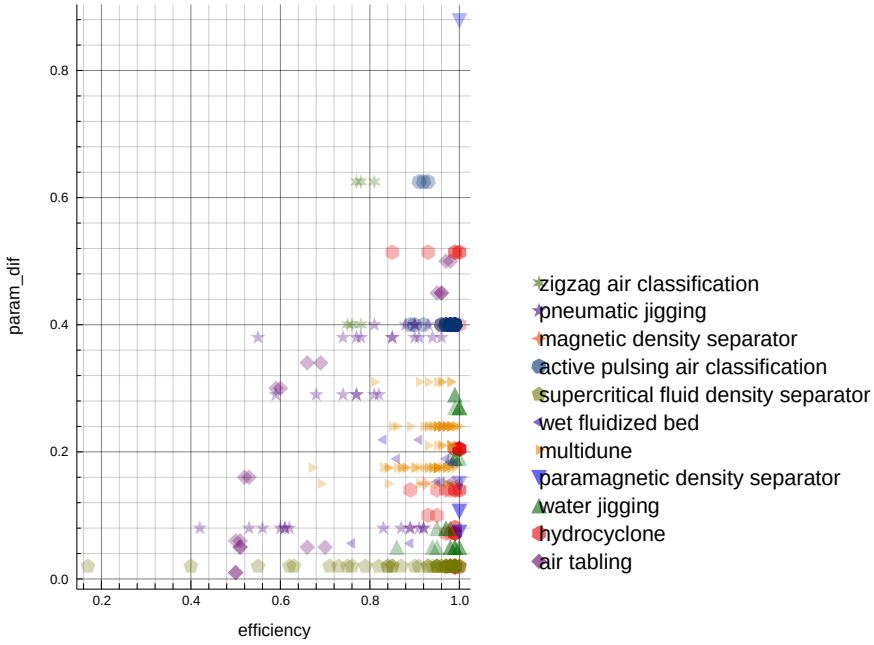

Figure 10. Difference in density (g/cm^3) and obtained efficiency for different technologies, from the database.

Separation in a sink-float tank occurs because of different buoyancy due to Archimede's force.

However, the acceleration of particles in the sinking or floating direction is quite low when there is little difference in density between the fluid and materials. For spherical particles acceleration cannot exceed the value from the equation:

$$a = -2g\frac{\rho - \rho_m}{\rho + 2\rho_m} \tag{4}$$

where ρ – fluid density, ρ_m – material density, g – acceleration of free fall (assumed positive), full derivation is given in Manida (2001). Sphere with zero density may go up with finite acceleration of $2g$, in practice, little difference in density makes the process susceptible to secondary factors, see Figure 11.

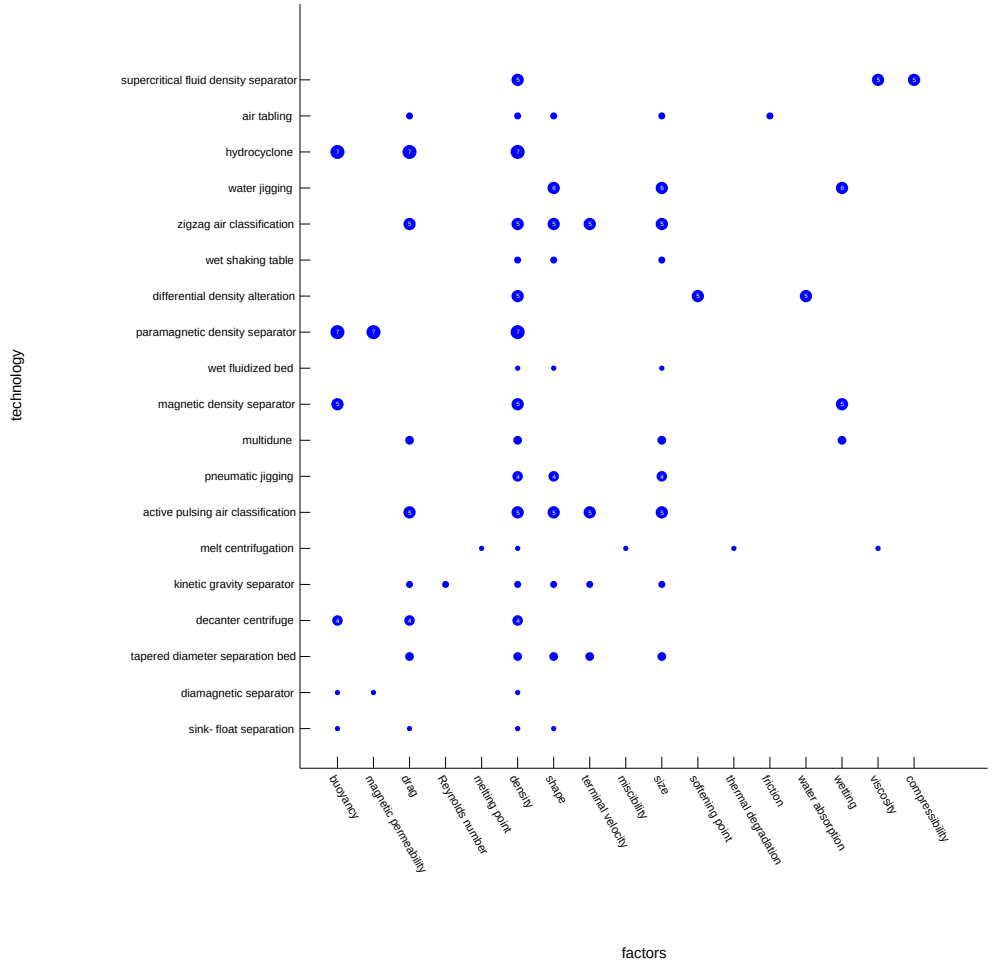

Figure 11. Density separation and affecting factors, fewer factors – less obscured separation, bubble size indicates instance count, from the database.

Evolution of wet density-based separation methods suggested the following advancements:

- replace gravity force with centrifugal force in hydrocyclones and decanter centrifuges,
- replace hydrostatic (Archimede's) force with floating-settling by hydrodynamic forces in wet shaking table, multidune, water jigging, wet fluidized bed,
- allow particles to follow different settling trajectories in tapered diameter separation bed, kinetic gravity separator.

Hydrocyclones use a circular flow of liquid with particles suspended. The free fall acceleration (the g) is replaced by centrifugal acceleration and influence of hydrodynamic forces and bubbles is reduced. Industrial hydrocyclones are used for coal beneficiation and can process particles up to 120 mm in size (Gent et al. 2009). Decanter centrifuge relies on mechanical rotating parts with screws transporting heavy and light fractions in opposite axial directions (Figure 12). Mechanics of decanter centrifuge has the advantage of decreased water content in the output because of incorporated centrifuge (Andritz n.d.). Both technologies are in industrial use. Intensification of the basic sink-float comes at the cost of higher energy consumption (Herbold n.d.). For comparison: Herbold sink-float tank uses 1,5 kW (drives of loading-unloading drums) at throughput of 2,5 t/h plastic, while Herbold hydrocyclone consumes 15 kW (vortex pump) at 1,5 t/h throughput (cyclone diameter 250 mm). The equipment cost per unit throughput is of the same order (~100 k€ /(t/h)) (MBA Polymers 1998). Salt solution (up to 3,1 g/cm^3 with sodium polywolframate (Stadtschnitzer & Flachberger 2008)) or fine mineral suspension can be used to increase fluid density, although high suspension concentration increases viscosity.

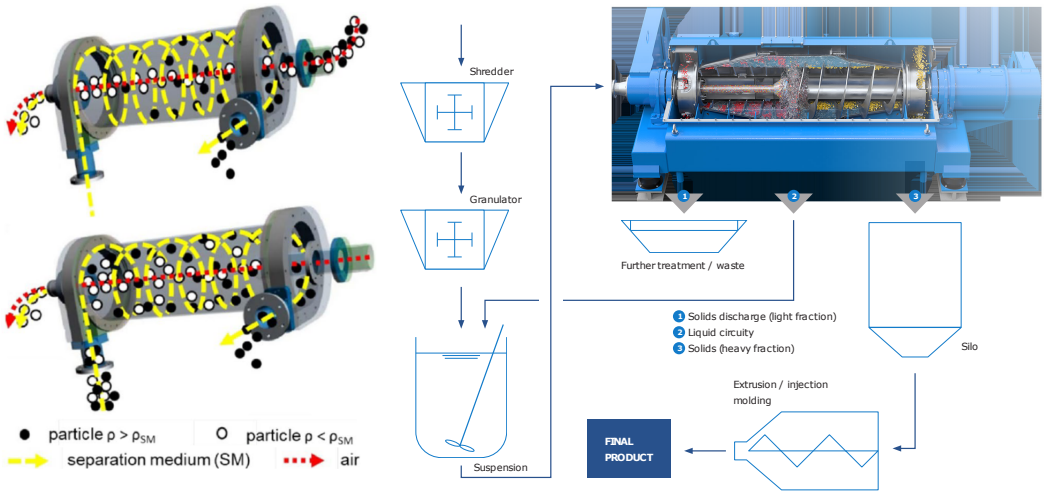

Figure 12. Left: possible material flow in hydrocyclone, adapted from Bauer et al. (2018), right: commercial decanter centrifuge with auxiliary stages (Andritz n.d.).

Wet shaking table comprises inclined in both direction table with rifles, which is shaken along the rifles. Water is fed across the rifles from the upper edge in a thin layer, materials are fed from the upper corner. Fractions move diagonally (vibrations are asymmetric) and exit table at different rifles, heavier close to the input (Carvalho et al. 2007). Multidune (Figure 13) develops this principle by enclosing the rifles from the upper side and omitting the vibration. Intricate properties of water flow let materials to settle in different channels (Lupo et al. 2016).

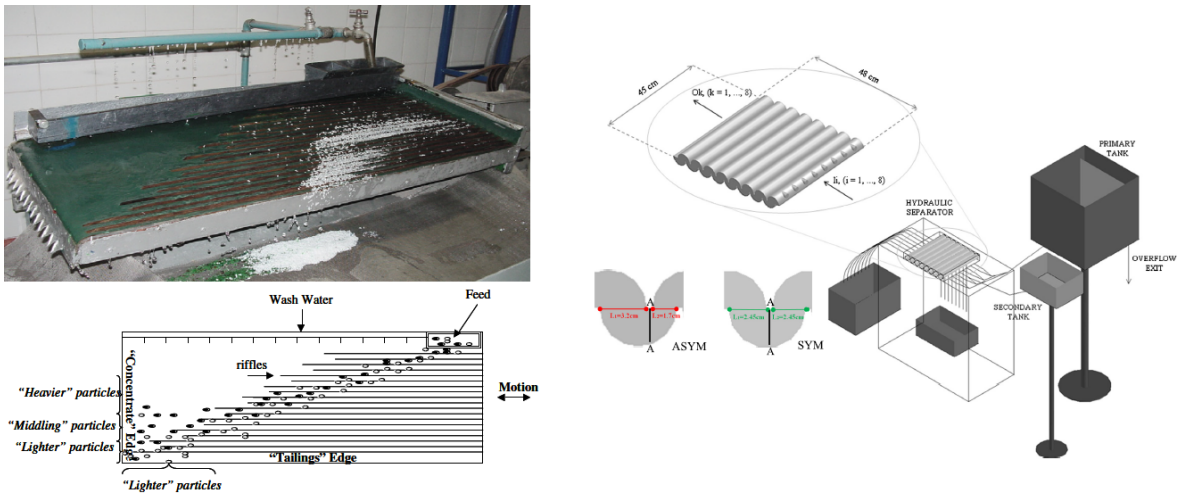

Figure 13. Left: wet shaking table, laboratory equipment and schematic, adapted from Carvalho et al. (2007), right: multidune experimental equipment (primary tank – for water, secondary tank – for material, exits directed downward), both symmetric and asymmetric channel profiles were used by Lupo et al. (2016).

In water jigging, pulsed water jets are forced vertically up through the perforated bottom of a water-filled vessel. Heavier particles concentrate at the bottom, lighter in the overflow. The intermittent flow is produced with air blow from below. In Japan equipment was developed to separate CDW in multiple fractions (known under names TACUB jig and RETAC jig), see Figure 14. Methods with any kind of reciprocating motion or vibration make use of particles inertia as a quasi-substitute for their mass and the cross-sectional area as a quasi-substitute to the volume. Fluidized bed lets particles settle in layers in the order of density – flow from the bottom fluidizes particles bed so that they behave in a quasi-fluidic way (Ito et al. 2010). There is little or no industrial application for the technologies in recycling, research continues. Hydrodynamic forces depend on the particle shape and cross sectional area, so these technologies require narrow particle size ranges. On the other hand, processes use

water without additives (prewashing or wetting agent is desired, though). Processes like the fluidized bed and water jigging rely on relative densities between fractions, so the feed should always contain light and heavy particles.

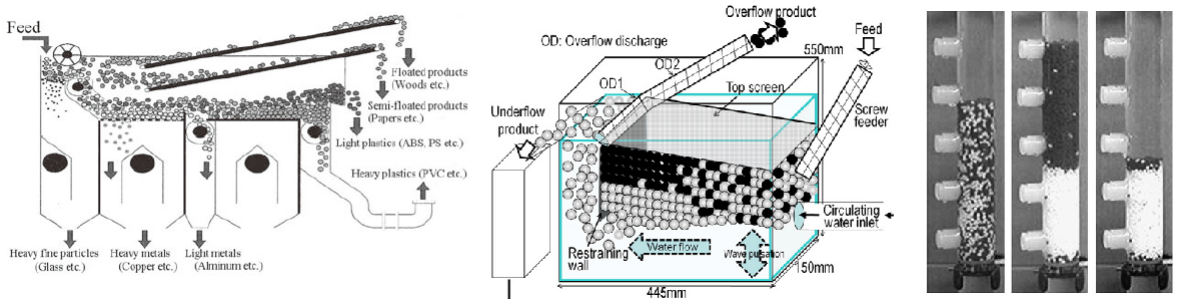

Figure 14. Left to right: TACUB jig for CDW (Tsunekawa et al. 2005a), layout of a modified commercial RETAC jig (Ito et al. 2010), PVC/PET mixture separation and discharge in a laboratory fluidized bed (Kinoshita et al. 2006).

Falling in water occurs at different speed depending on particle densities. Kinetic gravity separator lets particles fall through water in rotary motion, see Figure 15. The bottom of the circular separation tank is divided into sectors (feeding occurs above the first one). Heavier particles end up in the first sector, lighter – in the sector located further along the angular coordinate (van Kooy et al. 2004). Tapered diameter water column uses both water flow and air feed to force particles to settle at different discharge ports (Duan et al. 2014).

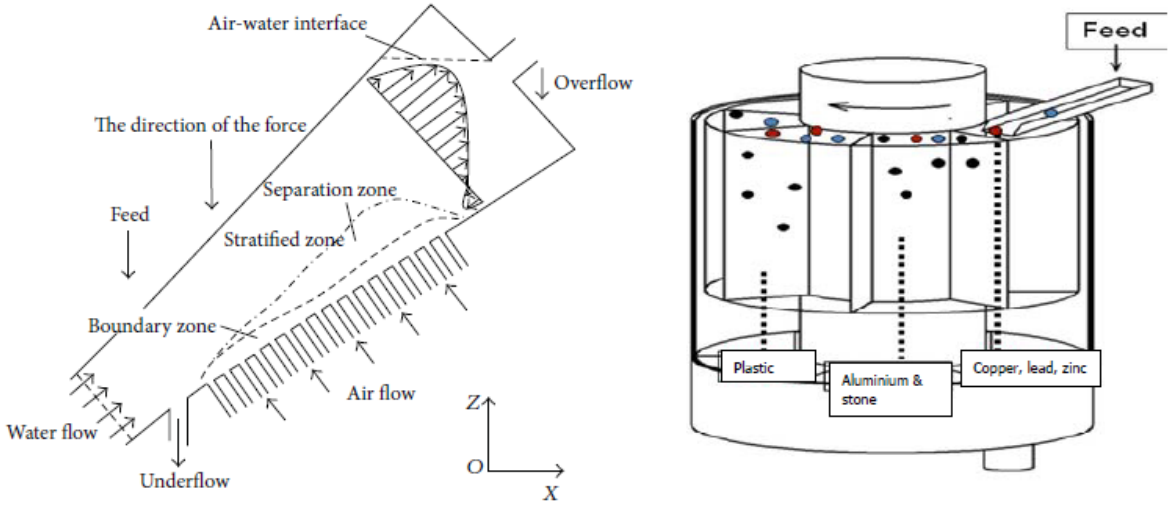

Figure 15. Left: tapered diameter separation bed flow layout (Duan et al. 2014), right: example of material trajectories in kinetic gravity separator (WRAP 2009).

Sorting performance of methods with a liquid medium (also with some special features

described next) is presented in Figure 16. Separators that passed proof-of-concept stage were tested for suitable particle sizes (Figure 17).

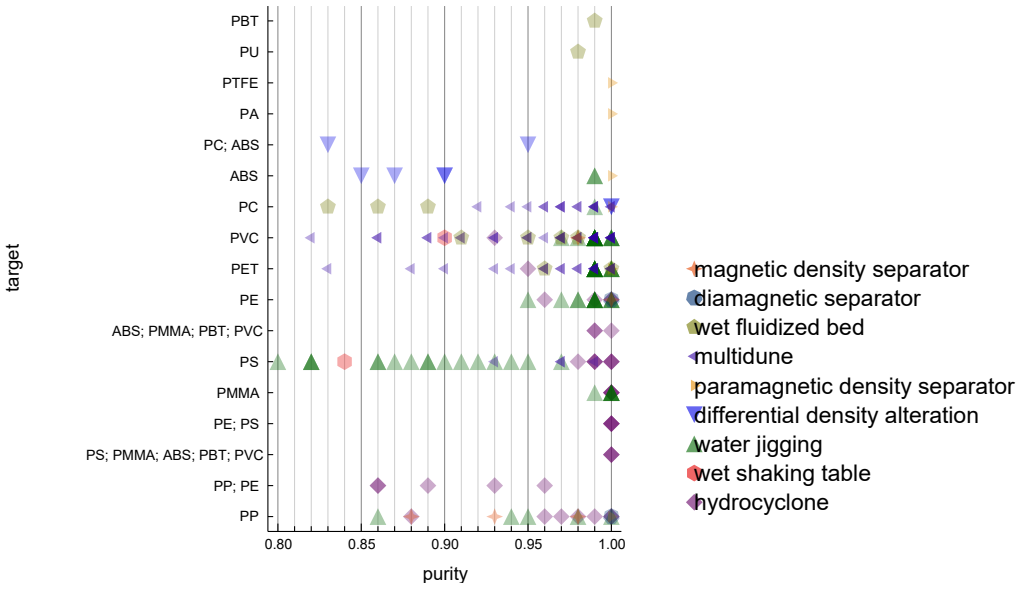

Figure 16. Purity of plastics separated by density in some liquid, from the database. Abbreviations: PBT – polybutylene terephthalate, PU – polyurethane, PTFE – polytetrafluoroethylene, PA – polyamide, PC – polycarbonate, ABS – acrylonitrile butadiene styrene, PMMA – polymethyl methacrylate, PS – polystyrene.

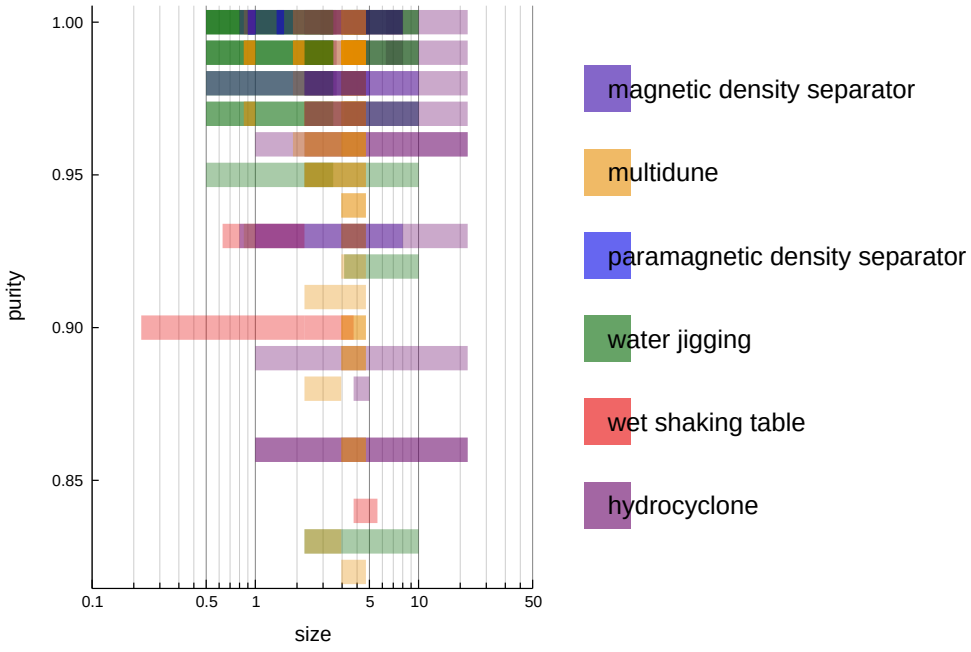

Figure 17. Particle size ranges for wet density separation brought to the laboratory stage and further, from the database.

3.1.2 Dry density-based separation

Use of water in wet density-based separation makes materials literally wet (post-drying is needed) and requires wastewater treatment. Dry methods using air as working medium resemble hydrodynamic methods, see Table 2. Air classifiers used in the mining industry are given by Shapiro & Galperin (2005), their use in recycling is still in research with the exception of generic air classifier (foil blow-out) and zigzag classifier.

Table 2. Complementary wet and dry separation methods.

Wet method	Dry method	Dry method description
sink-float	fluidized bed	Archimede's law holds in fluidized bed (fine glass beads act as fluid). Fluidization occurs from airflow or ultrasound (Huerta et al. 2005). Fluidization of shredded waste showed ~80% efficiency in separation into combustible/incombustible fractions (Sekito et al. 2006).
wet shaking table	air tabling	Airflow is fed through porous inclined deck to fluidize light fraction and let it slide downhill. Eccentric drive induces asymmetrical longitudinal vibration to let heavy fraction move uphill, see Figure 18.
multidune	zigzag air classification	Air column separator with a zigzag shaped column (Figure 19).
water jigging, wet fluidized bed	pneumatic jigging, active pulsing air classification	Both methods use air flow interrupted by valve. Pneumojig lets particles settle in the order of density (Figure 18), classifier makes particles go up or down in a column (Figure 19).
kinetic gravity separator	air knife for film removal	Removal of difficult-to-handle foils by blowing them out.

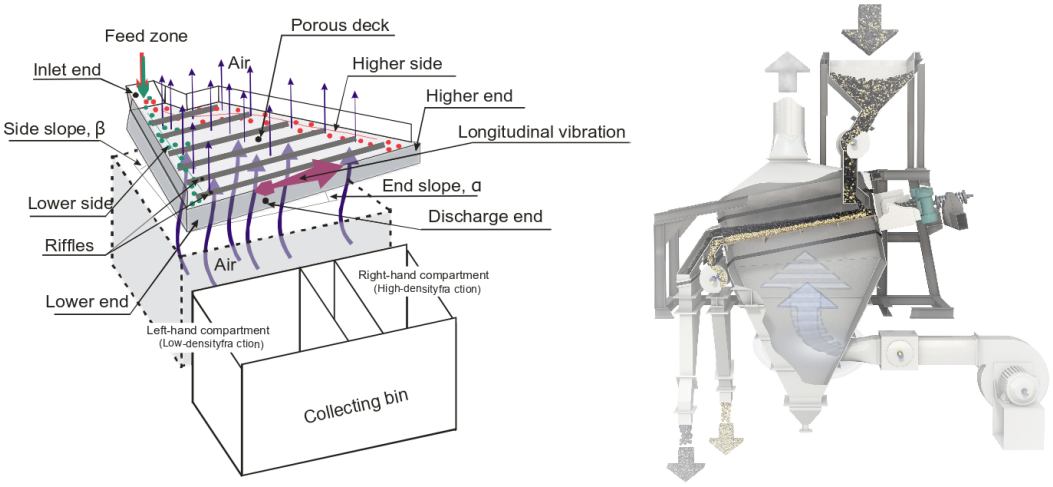

Figure 18. Principle of air tabling, left (Dodbiba et al. 2005) and commercial pneumatic jig, right (AllMineral 2019).

In air classifiers air acts as a material carrier, so they need relatively high air consumption and cyclone filtering at the air exit. Industrial pneumatic jig by Allmineral GmbH for coal beneficiation was tested in the separation of CDW aggregates, purity and recovery rates exceeded 80-90% for gravel and gypsum fractions (Ambros et al. 2017).

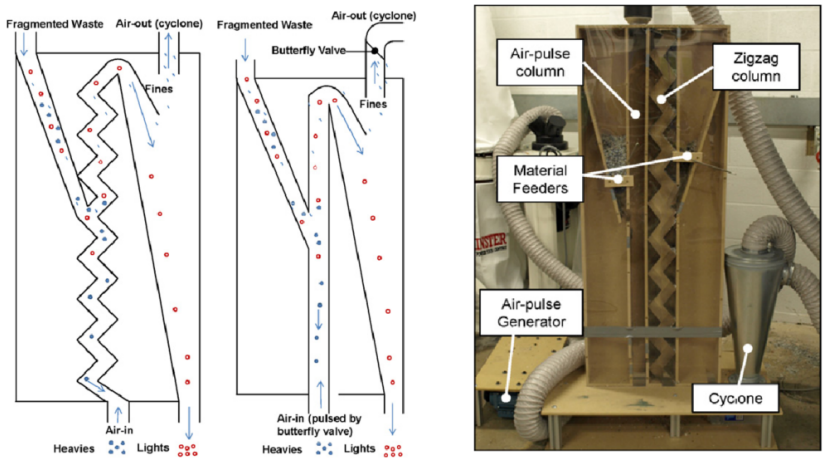

Figure 19. Zigzag column and active pulsing air classifier: layout (left) and laboratory equipment (right) with a switchable mode of operation (Lee & Orr 2009).

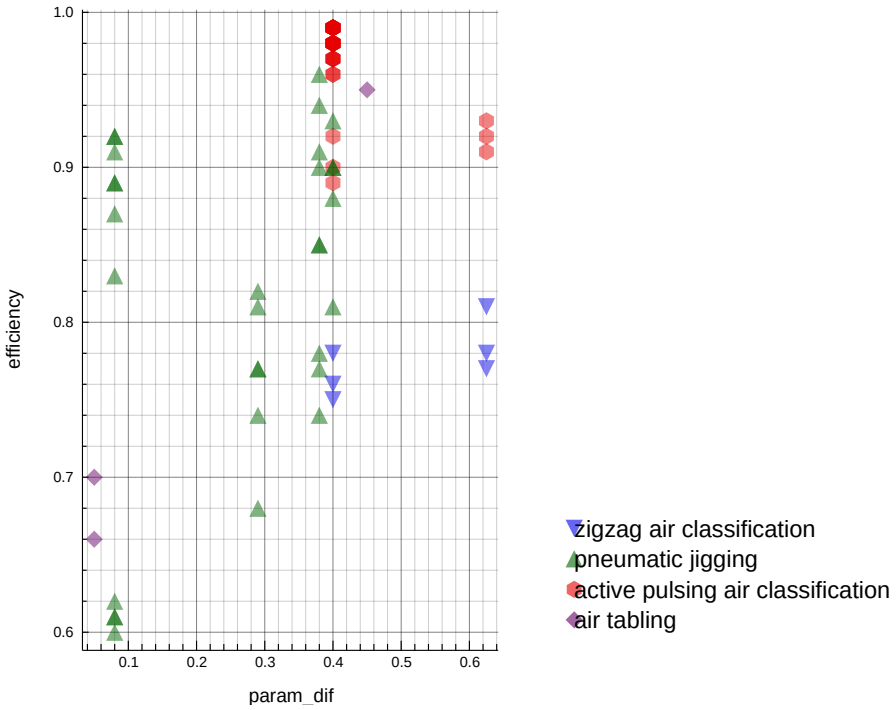

Figure 20. Efficiency against difference in density (g/cm^3) for dry density separation, from the database.

Infographics from the database (Figures 21 and 20) provides comparison about tested particle

size ranges and sensitivity to density difference across technologies.

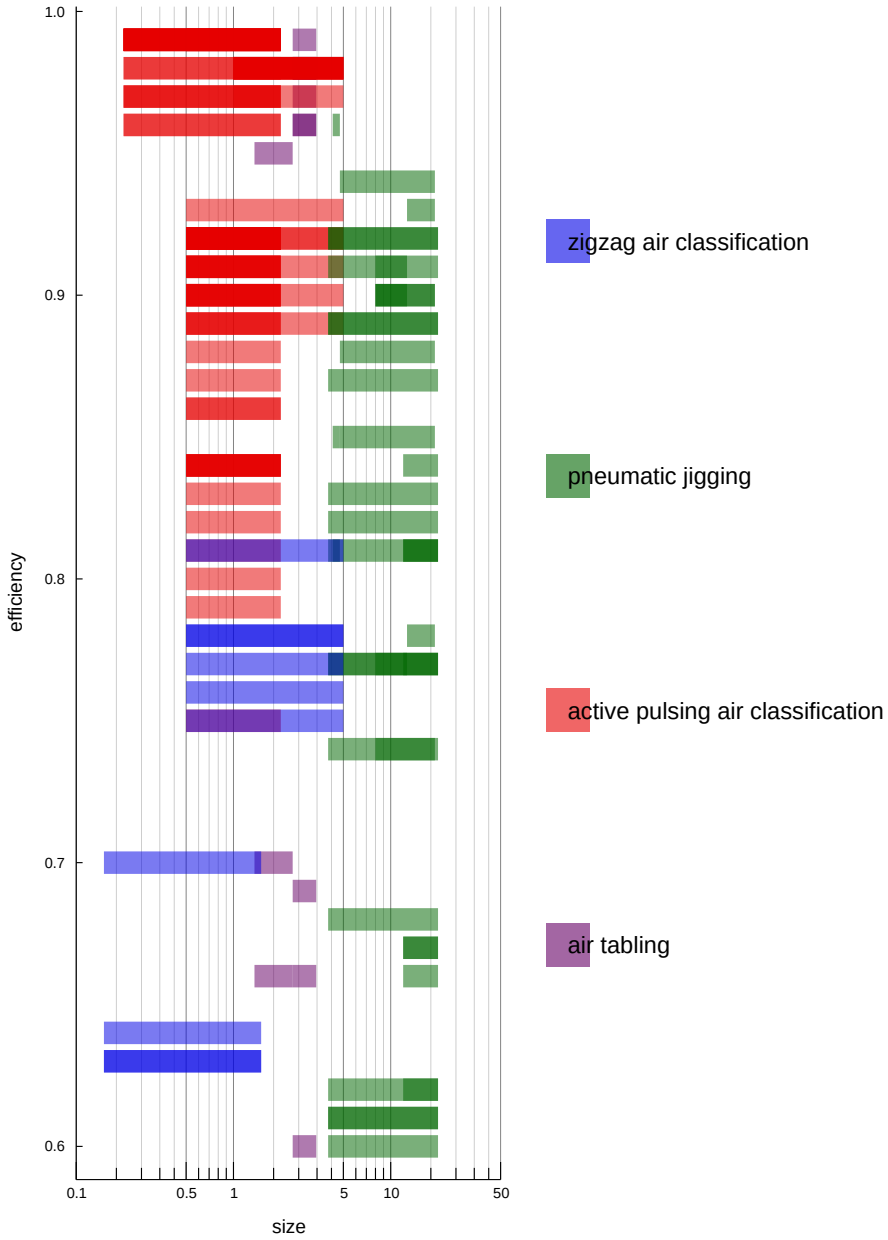

Figure 21. Efficiency against particle size (mm) for dry density separation, from the database.

A method proposed by (Dobrovszky & Ronkay 2014) gets rid of separation medium by centrifugation of polymers in a molten state. Custom-built equipment applied 30-100 *g* acceleration to separate PET/LDPE (low-density polyethylene) mixture. Temperature increase to 290 °C, well above the melting point of PET (260 °C) was necessary for successful separation into pure fractions. At 310 °C even polymer blend was separated.

3.1.3 Material and separation medium density alteration

Some plastics often encountered together in waste streams have close or overlapping densities, like PP and PE (0,90-0,91 and 0,91-0,97 g/cm^3), PS and ABS (1,04-1,05 and 1,01-1,21 g/cm^3), PC and PMMA (1,14-1,21 and 1,16-1,22 g/cm^3), PET and PVC (1,29-1,40 and 1,19-1,58 g/cm^3) (Gent et al. 2015). Separation of these materials by density requires either fine tuning of separation medium density or selective material density modification to push densities further away from each other. The latter approach is called differential density alteration (term coined in Pat. US 6335376 (2002)).

ABS and PS, PC and PMMA will have sufficient difference in density when conditioned in water or steam (at elevated pressure) and then rapidly heated above the softening point of one of the plastics. The water diffused in the polymer will foam it upon heating at low pressure, making its apparent density considerably lower. Plastic flakes must be pre-classified by size for adequate foaming that occurs mostly at the surface. Another technique makes supercritical carbon dioxide to dissolve in PVC at 73-300 bar pressure and 30-150°C temperature (where the carbon dioxide is beyond the critical point and has liquid-like density and gas-like viscosity) to foam it upon depressurization and make it lighter than PET (Pat. US 5462973 1995).

The separation medium density can be altered by physical methods. Super et al. (1993) used compressibility of carbon dioxide in the supercritical state to acquire density between samples of HDPE (high-density polyethylene), LDPE and PP. Supercritical carbon dioxide density can reach 1000 kg/m^3 (pressure about 300 bar), for denser plastics like PET and PVC supercritical sulfur hexafluoride can be added (maximum density 1700 kg/m^3). Separation was run in batch mode (Figure 22), the separation vessel could be loaded up to 40% by volume. Supercritical fluids are advantageous for sink-float separation because of low viscosity and non-polarity (no problems with wetting of polymers), but the need for high pressure is the main disadvantage. Operation costs of ~170 €/t with pure carbon dioxide were estimated (Karmana et al. 1997).

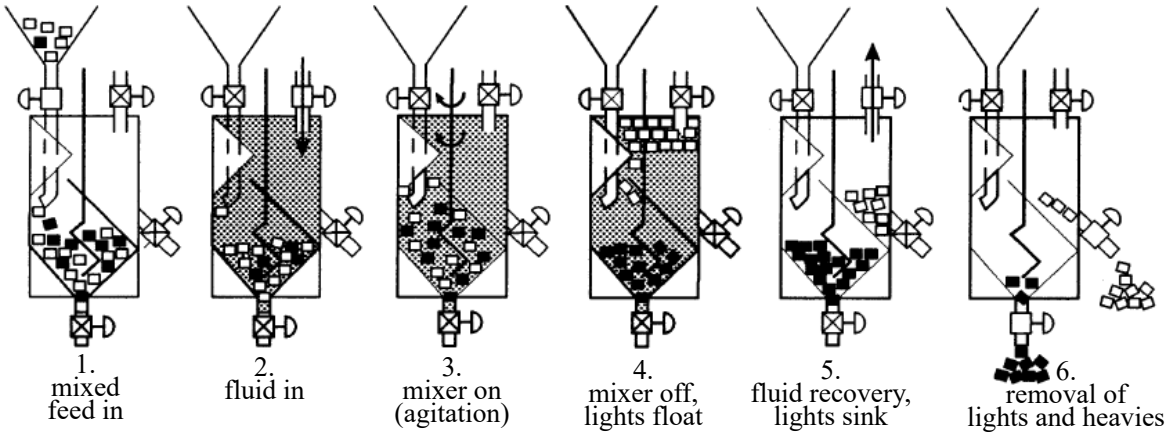

Figure 22. Stages of sink-float separation with supercritical fluid (Karmana et al. 1997).

Instead of changing fluid density, effective gravity acting on the fluid can be changed when the fluid possesses profound magnetic properties. Magneto-Archimedes levitation force F_{MA} is given then by equation (Catherall et al. 2005):

$$F_{MA} = \left(\frac{\chi}{\mu_0} B \frac{dB}{dz} + \rho g \right) V \tag{5}$$

where ρ, $\mathrm{kg/m^3}$ – fluid density, V, $\mathrm{m^3}$ – floating body volume, χ – magnetic susceptibility of fluid, $B\frac{dB}{dz}$, $\mathrm{T^2/m}$ – magnetic field (flux density) and its vertical gradient product, μ_0, $\mathrm{H/m}$ – magnetic permeability of free space and g, $\mathrm{m/s^2}$ – acceleration of free fall. The equation holds when the floating material is a weak diamagnetic (like most materials are), so that its interaction with the magnetic field is negligible. The fluid can be a paramagnetic salt water solution or ferrofluid – a suspension of iron oxide nanoparticles in water. The latter medium was used in a pilot scale (200 kg/h throughput) plastic separation line, separating PE, PP, PET and PS at cost of about 100 €/t (Hellemans 2013). A permanent magnet placed above the separation channel with ferrofluid decreased its apparent density. Additional steps of boiling for wetting the polymer waste and reclaiming of ferrofluid afterwards were implemented.

Paramagnetic salt solutions are used in research experiments (Figure 23), often with superconducting magnets able to produce up to ~1400 $\mathrm{T^2/m}$ field-gradient product (Catherall et al. 2005), permanent magnets have practical limit at 20 $\mathrm{T^2/m}$ (Ueda et al. 2014). Strong magnetic fields can make use of weak diamagnetic properties of materials and fluids like it was shown by Ueda et al. (2014) that separated PP and PE in ethanol solution, both in

vertical and lateral directions. However, such experiments do not only require cryogenic environment for superconducting magnets (liquid nitrogen) but also cannot be scaled up because the creation of strong magnetic field gradient in a large space is challenging in view of technology and expenses. The advantage of magnetic density separation is the creation of layers of different apparent density in the fluid, so that separation into multiple fractions can be done at once. On the other hand, it has all the same problems as the generic sink-float method and cannot be intensified in a similar way (by centrifugal force, for example).

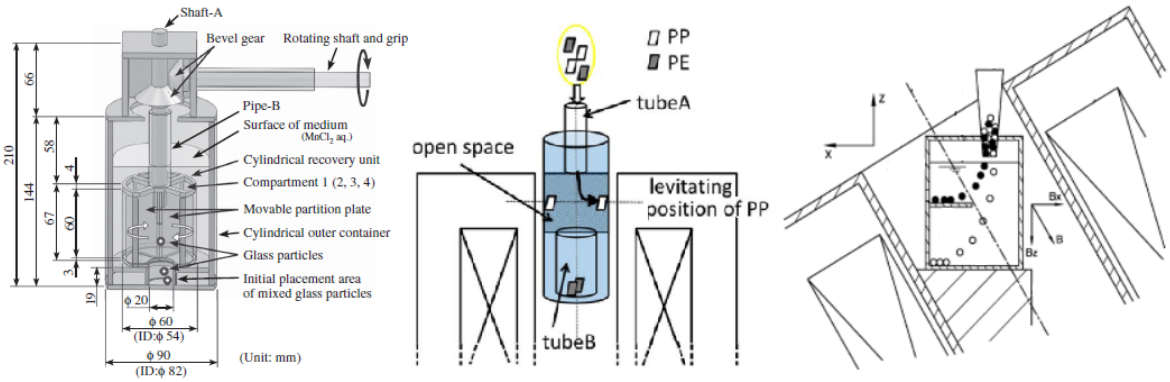

Figure 23. Separation layouts with use of strong magnetic fields (left to right): vane rotor mechanism to catch particles in different sectors upon their floating in increasing magnetic field (Ando et al. 2015), PP and PE separation in ethanol solution (Ueda et al. 2014), inclined superconducting magnet forces particles to follow oblique layers of the same apparent density, so no horizontal propulsion is needed (Pat. EP 2679310 2014).

3.1.4 Wetting (flotation)

Insufficient wetting of plastics that causes attachment of air bubbles and shift of apparent density in sink-float and similar separation methods can be used for separation of plastics denser than water. Chemical or physical treatment may selectively make particles of one polymer hydrophilic while another remains hydrophobic. When submerged in a water tank with a constant supply of air bubbles from below particles with hydrophilic properties will likely to remain in the bottom, unaffected by bubbles, unlike the hydrophobic ones. This is the method of froth flotation. A variation of it is dissolved air flotation where the air is first dissolved in water under pressure (Figure 24) and turns into the gas when the pressure is released (Guo et al. 2016).

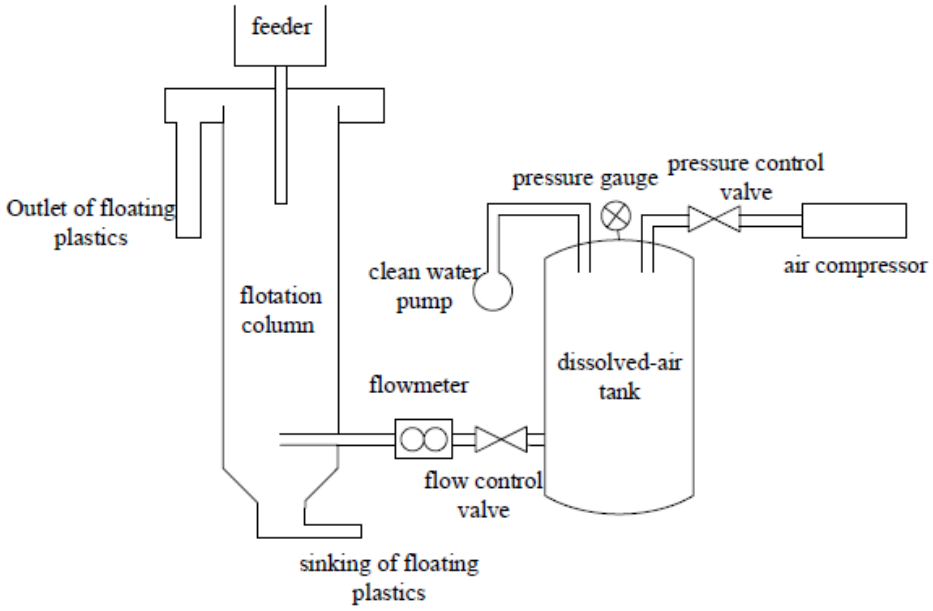

Figure 24. Layout of dissolved air flotation (Guo et al. 2016).

Froth flotation makes use of chemical differences in materials for direct sorting, so it can be made very selective, see Figure 26. For example, PVC was separated from ABS, PET, PS, HIPS (high impact polystyrene), PMMA, SAN (styrene-acrylonitrile resin), PA and POM (polyoxymethylene) mixture (Mallampati et al. 2016), a ternary mixture of PET, PVC and PS was shown to be separable in multiple steps with appropriate wetting agents (Negari et al. 2018).

Use of chemical wetting and froth agents is a drawback of froth flotation. Multiple reuses of water solution were found to be effective up to 10 times in some cases (Wang et al. 2018b). Physical pretreatment methods tested for certain plastics were flame treatment (Pascoe & O'Connell 2003), boiling Wang et al. (2014), application of activated carbon with heating in the oven or with microwaves (Thanh Truc & Lee 2016), ozone treatment with calcium and calcium oxide nanoparticles (Mallampati et al. 2016). Froth flotation depends on surface effects, thus it is sensitive to contaminants and requires a thorough washing of materials coming from waste, while research is often done with shredded virgin plastics (Wang et al. 2015), see Figure 25. A profit estimate for separation of PC, PVC and PMMA yields about 520 €/t, with 110 €/t expenses on crushing, chemicals and labour (Wang et al. 2017a).

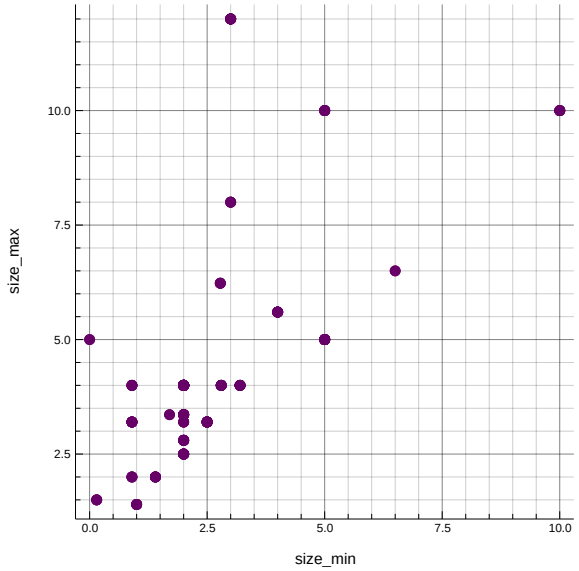

Figure 25. Minimum and maximum particles sizes used in froth flotation, from the database.

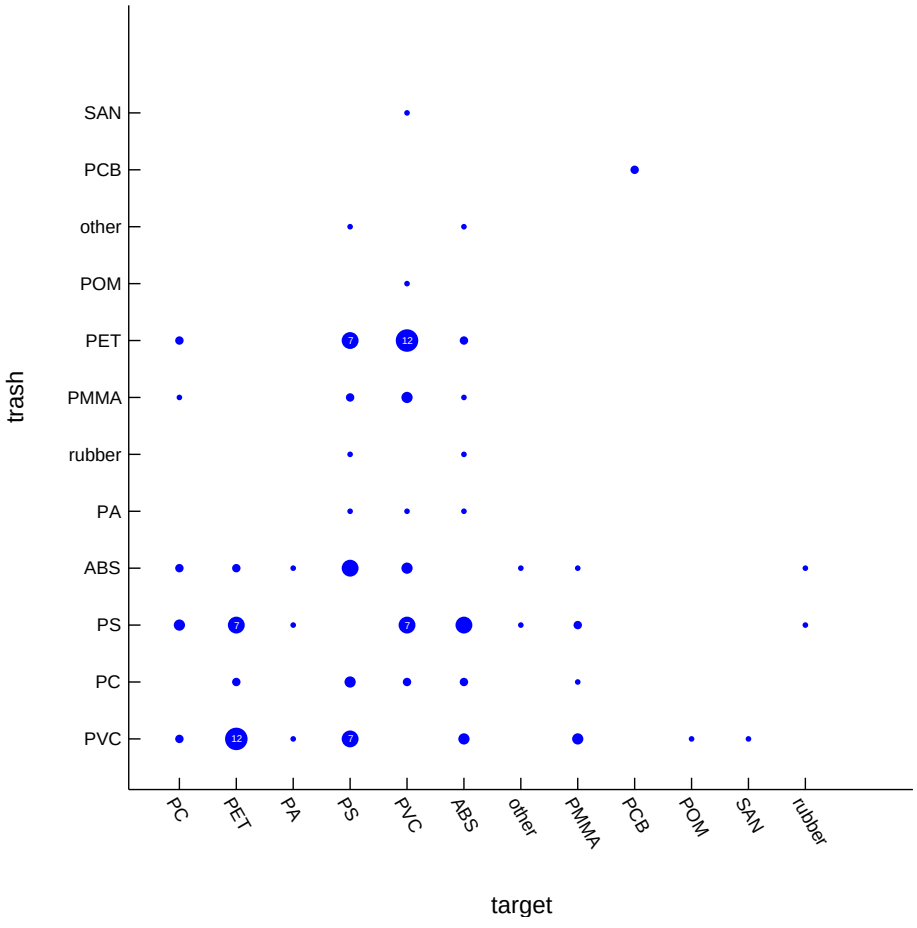

Figure 26. Pairs of materials separable by froth flotation, bubble size indicates the number of research instances, from the database.

3.1.5 Ferromagnetism

Ferromagnetic materials (primarily iron alloys) are separated from other materials in either permanent magnet or electromagnet field. The latter approach has a feature of switching the field off, which may outweigh the drawback of energy consumption for electromagnet coil. Magnetic separation is a mature technology that has a different embodiment: block magnet above the conveyor for accumulation of ferrous contaminants, overbelt magnets with dedicated conveyor to take attracted ferrous particles away from the magnet, head roll magnet – magnetic pulley of the conveyor and magnetic drum – a sector magnet is hidden inside rotating hollow drum, see Figure 27. Commercial systems provide magnetic field below 0,5 T and capture 3-300 mm pieces of steel and iron. For capturing small (0,1-30 mm) particles or weakly ferromagnetic alloys (such as stainless steel) high gradient magnetic separators are used with a stronger magnetic field (0,6-0,9 T). (Goudsmit Magnetic Separators n.d.)

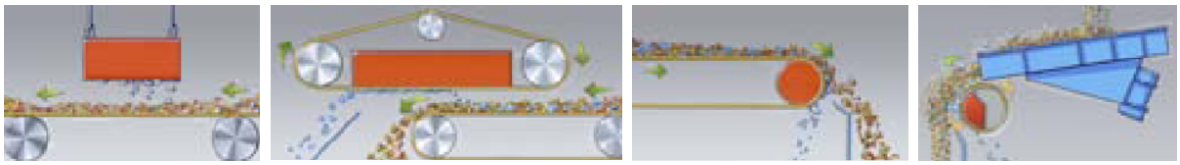

Figure 27. Magnet installations (left to right): block, overbelt, head roll, magnetic drum, adapted from Goudsmit Magnetic Separators n.d.

3.1.6 Electrical conductivity and triboelectricity

Specific electrical conductivity values span from orders of 10^{-16} S/m (ABS) to 10^{7} S/m (copper). Recently developed conductivity-based separation methods allow to separate materials within one category (poor conductors from strong conductors and poor insulators from strong insulators). Eddy current separation is a mature technology that uses repulsion of conductive particles from the alternating magnetic field (by Lenz's law). In commercial systems alternating field is produced by the high speed rotating drum with alternating magnetic poles and can eject metallic particles of 0,5-300 mm size (Goudsmit Eddy Current Separators n.d.), either horizontal or vertical (Wang et al. 2013).

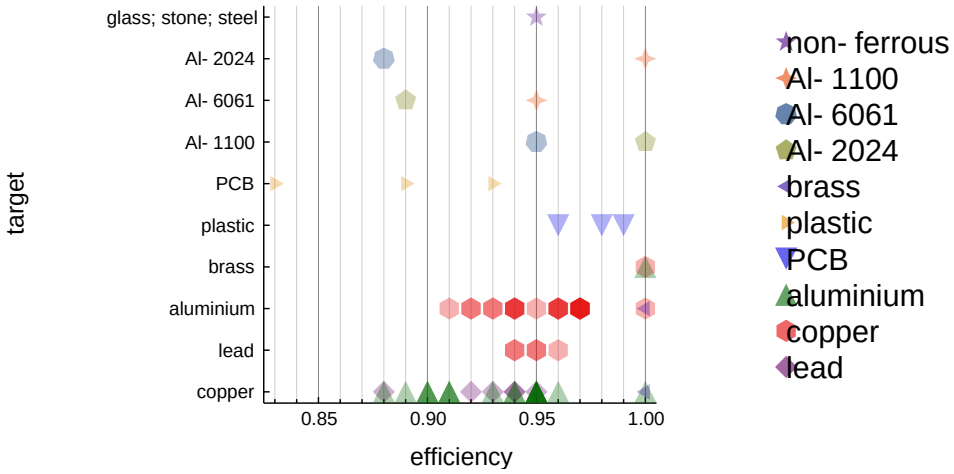

Figure 28. Eddy current efficiency in the separation of target materials from non-target, from the database.

Researchers aim to simplify the construction and increase the selectivity of eddy current separation, see Figure 28. Different conductivity-to-density ratio of aluminium, copper and lead alloys force them to follow different trajectories in separators by Lungu & Rem (2002) and Lungu (2005), see Figure 29. Instead of ballistics, the Magnus effect was used to force particles to follow different paths in Lungu & Neculae (2018). Magnus effect is the lateral force acting on object flying through gas or liquid while spinning (what conductive particles actually do in the alternating magnetic field). Increase in alternating field frequency to 50 kHz for better separation was shown to be possible with electromagnet instead of magnetic drum (Dholu et al. 2017).

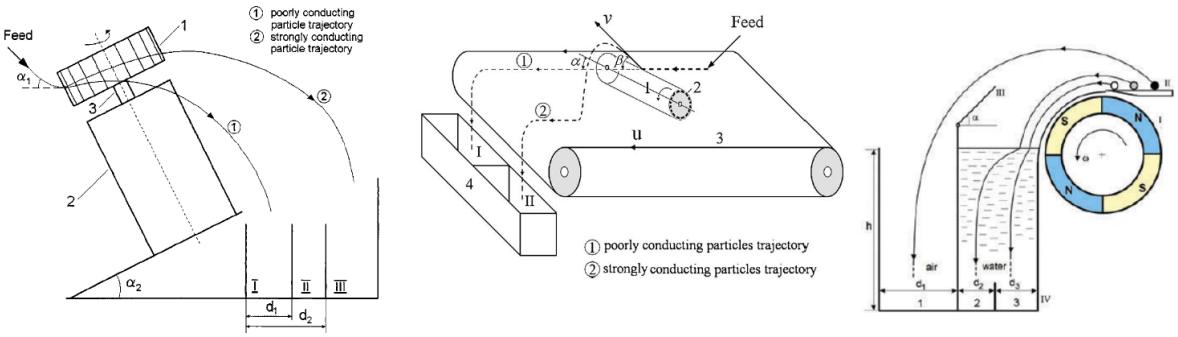

Figure 29. Particle trajectories in (left to right): inclined rotor eddy current separator (Lungu & Rem 2002), separator with rotor underneath the belt (Lungu 2005), Magnus effect-assisted separator with air and water (Lungu & Neculae 2018).

Corona electrostatic separation uses charge leakage from particles charged by corona

treatment. Particles are deflected depending on the remaining charge by a high-voltage electrode. This technology was tested for both conductive and non-conductive particle separation. Copper separation from aluminium with 69% recovery and 99% purity was estimated to cost 810 €/t with 90 kWh/t energy consumption (Salama et al. 2018). Laboratory scale electrostatic separator costs about 60 000 € (Eriez Magnetics 2019). The principle of charge leakage was further developed in charge-decay electrostatic separation (Li et al. 2017), where non-conductive particles of PVC (10^{12} Ω m), PP (10^{14} Ω m) and ABS (10^{16} Ω m) have prolonged time (300 s) to discharge on a grounded conveyor belt, see Figure 30.

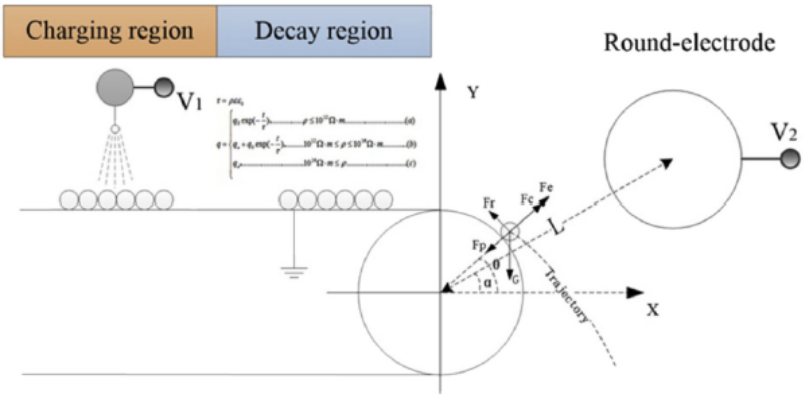

Figure 30. Charge-decay electrostatic separation (Li et al. 2017).

Triboelectrostatic separation makes use of charge build-up when dissimilar materials are rubbed against each other. Charge polarity and density depend on material properties in friction contact. There are multiple ways to charge the particles: in a fluidized bed, in a cyclone (Zhang & Chen 2017), by rotating drum or propeller (Fekir et al. 2017), on a vibratory feeder. The target charging mechanism can be rubbing of particles against each other or against walls of the vessel. Subsequent deflection by high voltage electrodes let the particles to end up in multiple collection bins. Commercial equipment separates PS/ABS, PVC/rubber, HDPE/PP, PET/PVC, PP/PS, ABS/PMMA, PVC/PE mixtures of clean, free from dust particles in 2-10 mm size range (Hamos EKS n.d.). In research, flake size usually stays below 5 mm (Figure 31), but sorted materials nomenclature is quite broad, see Figure 32. Ternary mixtures like PA/PC/PVC and PA/HIPS/PVC were separated in a single step by Fekir et al. (2017).

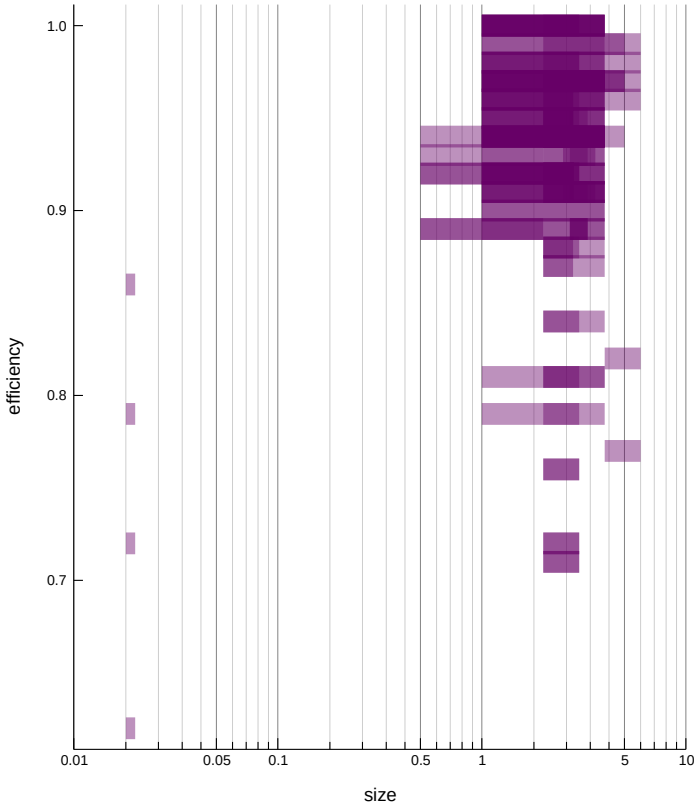

Figure 31. Triboelectrostatic separation efficiency and particle size range, from the database. Abbreviations: PHBV – poly(3-hydroxybutyrate-co-3-hydroxyvalerate), PCL – polycaprolactone.

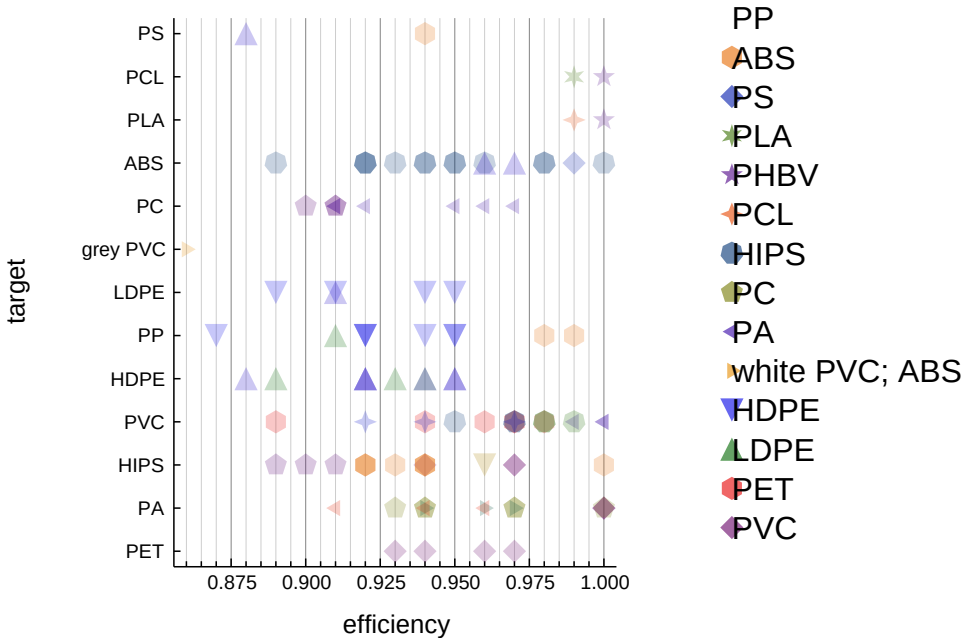

Figure 32. Efficiency of triboelectrostatic separation, target materials against non-target, from the database.

One way to quantify triboelectricity is by charge affinity, a material-specific value of charge build-up per unit of friction energy. The resulting amount of charge can be calculated as a sum of charge affinities of materials in friction contact and multiplied by the friction energy, see values for about 50 materials in Lee & Orr (2009). However, when compared to qualitative triboelectric series of polymers collected from separation experiments (Silveira et al. 2018), some inconsistencies arise, see Figure 33. It was also found that antistatic additives may change polarity or suppress the charge build-up, while talc makes charge polarity independent on the polymer type, although polymer irradiation with electrons may neutralize these effects (Reinsch et al. 2014). Separation methods involving electrostatics are sensitive to ambient humidity, in laboratory trials relative air humidity is deliberately kept at levels below 50-60% to avoid a decrease in separation efficiency, see Figure 34.

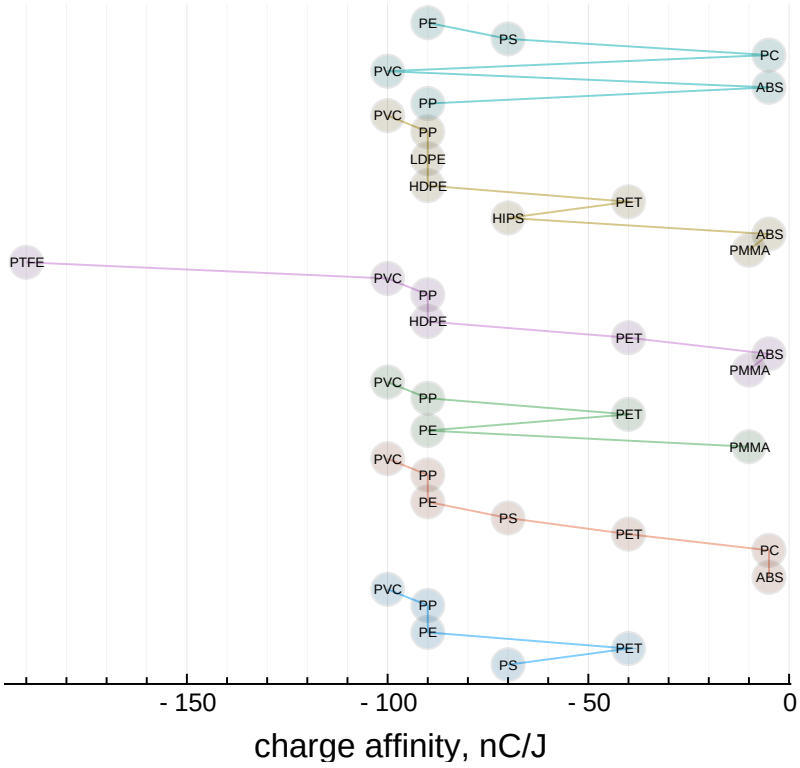

Figure 33. Triboelectric series of polymers from literature (Silveira et al. 2018), plotted in coordinates of charge affinity (Lee & Orr 2009).

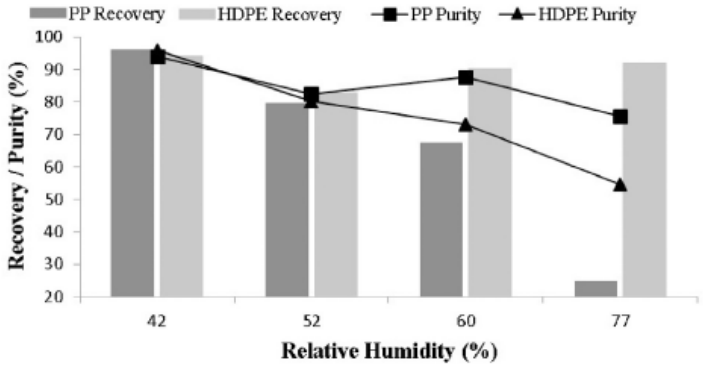

Figure 34. Effect of air relative humidity on triboelectrostatic separation (Silveira et al. 2018)

3.1.7 Electromagnetic wave sensors – operation principles

Since there a wide range of electromagnetic waves (see Figure 35) and their interaction with matter, the main principles are explained as follows. Upon irradiation several processes occur to a greater or lesser extent (Berwanger et al. 2014):

- reflection – radiation goes back from a surface without penetration,
- fluorescence – emission from energized atoms at a wavelength different from irradiation,
- absorption – partial or full energy uptake by material,
- transmission – radiation goes through.

The results of interaction can be quantified for the whole sample and at the selected wavelength (in laboratory tests), however, in recycling individual measurements are taken simultaneously across one spectral and two spatial coordinates. Resolution of such hyperspectral imaging (HSI) depends on available radiation sources and detectors. A hyperspectral camera can be of area scan type as well as push broom scanner (which takes linear frames of a moving belt).

X-rays are ionizing radiation (harmful for biological tissues) that is used in transmission and fluorescence measurements. X-rays are produced in X-ray tubes by bombarding a metal plate with accelerated electrons. Dual energy X-ray transmission (DE-XRT) recognizes different atomic densities in the materials. In DE-XRT, X-rays of two wavelengths are passed through the sample and intensities of transmitted rays are measured. The ratio between those intensities is a material-specific constant. X-ray fluorescence (XRF) technology excites materials with X-rays and measures emitted radiation. Depending on the technique (energy-dispersive or wavelength-dispersive) quantitative elemental analysis is possible for

elements starting with atomic weight 11 (sodium) or 4 (beryllium). Lasers comprise the essential part of the following techniques. Laser-induced fluorescence (LIF) excites materials with intense monochromatic light (often in the ultraviolet region, UV) and detects emission at specific wavelength together with its decay profile, characteristic for the target substance. Laser-induced breakdown spectroscopy (LIBS) uses a pulse of a focused laser beam to turn a few micrograms of sample into the plasma of high temperature (up to 25 000 K). Upon cooling down electrons return from their energized state and emit light of characteristic wavelength (200-800 nm) analyzed by a spectrometer. Ultraviolet, visual and infrared radiations are used for HSI. Reflection of these radiations is influenced by absorption at specific wavelengths due to resonant vibration of molecules in the substance (where the radiation energy goes to), thus creating spectrum specific to the analyzed substance. (Berwanger et al. 2014.)

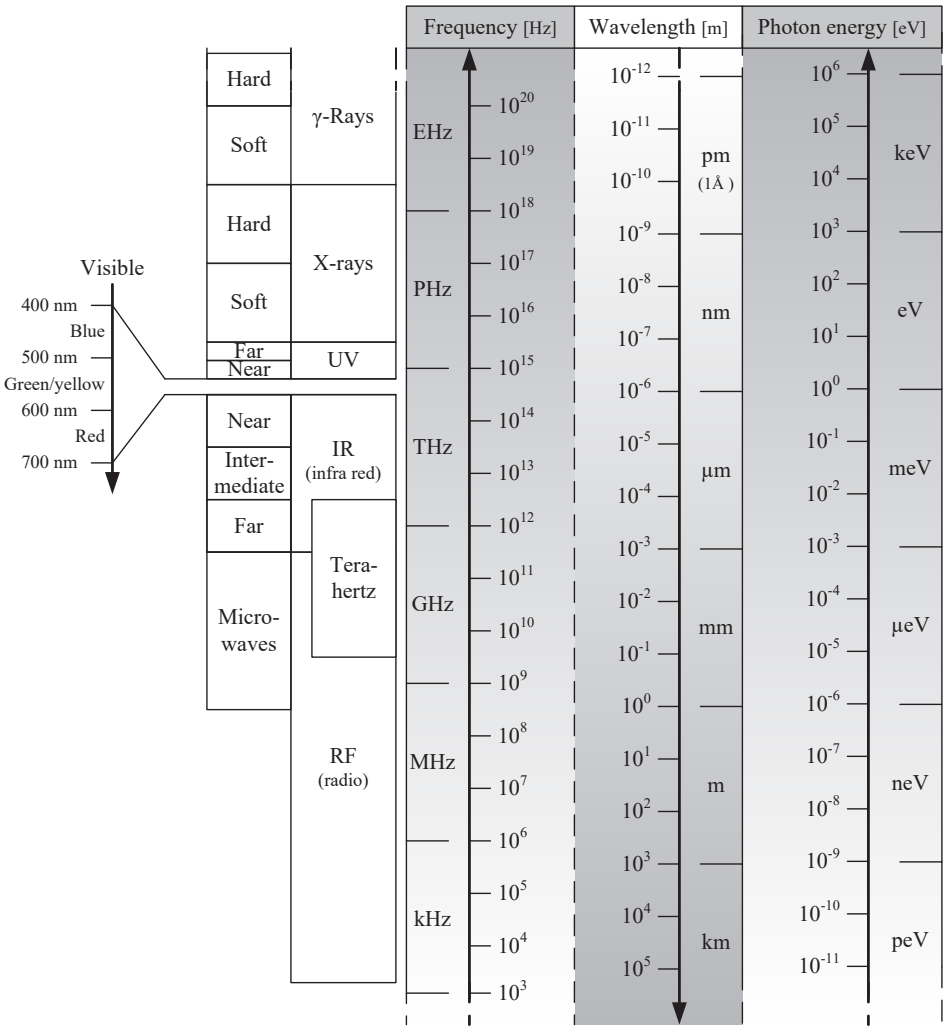

Figure 35. The electromagnetic spectrum between 1 kHz and 100 EHz (Berwanger et al. 2014).

Infrared region is subdivided as shown in Table 3. NIR is close to the visible range (can be detected by sensing matrix of an ordinary camera), sometimes SWIR range devices are called NIR (Lahtela et al. 2019). Longer waves require dedicated optics and detectors. LWIR and MWIR (less common) regions are used for thermography – a remote measurement of object temperature by thermal cameras (maximum of black body radiation at 300 K occurs at 10 µm wavelength). FIR overlaps with terahertz region assigned to radiation between 0,1 THz to 10 THz (30 µm to 3 mm). At terahertz region technology transits from optics to radio electronics. Terahertz radiation penetrates through most materials, but is safe (non-ionizing), unlike X-rays. Terahertz is reflected by metals and absorbed by water. Terahertz pulsed imaging (TPI) produces an image with both amplitude and phase information of the transmitted signal. Infrared spectroscopy includes Raman spectroscopy which measures rather weak Raman scattering – the returned radiation wavelength differs slightly (by a Raman shift) from the incident monochromatic laser beam and depends on molecule structure in the sample. (Berwanger et al. 2014.)

Table 3. Subdivision of the infrared spectrum (Berwanger et al. 2014).

Name	Abbreviation	Wavelength, µm
near infrared	NIR	0,7 – 1,4
short-wavelength infrared	SWIR	1,4 – 3
mid-wavelength infrared	MWIR	3 – 8
long-wavelength infrared	LWIR	8 – 15
far infrared	FIR	15 – 1000

3.1.8 Feeding and routing

The database was not filled with many examples of feeding and routing mechanisms due to the challenge in capturing their distinct features, but several issues need to be disclosed because of their influence on sensor-based separation. Vibrating table feeder, flat conveyor belt (or chute) and air nozzle bar are typical auxiliary structures for sensor operation (WRAP 2010), see Figure 36.

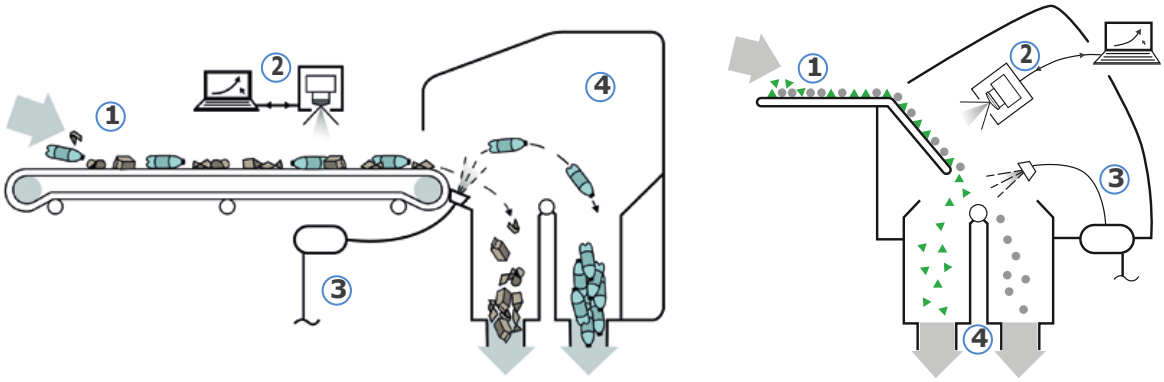

Figure 36. HSI-based sorting layout with conveyor and with chute: 1 – feeding conveyor (left), vibratory feeder(right), 2 – machine-vision and sensors, 3 – separation with compressed air, 4 – separation chamber (Picvisa n.d.)

The feeder must ensure uniform monolayer on the belt with sufficient distance between particles to avoid co-ejection. The latter can be accomplished with acceleration belt – conveyor belt that moves faster than the feed stream on the vibrating table, so that particles are spread out (Yu 2014). Feeding from a hopper, by a screw or rotary drum are some alternatives, but they have not gained wide use in automatic separation (Yu 2014).

Air nozzle bars are used for either whole piece ejection (like PET bottle) or for flakes and granules in size ranges of, for example, 10-60 mm or 1-15 mm (Picvisa n.d.). Several studies have shown the following deficiencies of the technology:

- influence region for ejection of a 10 mm by 10 mm square or cubic particle by a single air jet is about 25 mm wide (Pascoe et al. 2015) which indicates the need for significant gaps between particles,
- in 6-10 and 10-15 mm size intervals the ejection efficiency can reach 98% with 5-8% particles falsely co-ejected (Fitzpatrick et al. 2015), in 5-8 mm size interval 96% particles are ejected with 3-10% co-ejection (Pieper et al. 2018),
- co-ejection increases with throughput and proportion of target particles (Pascoe et al. 2015),
- pneumatic valve switch time must stay below 4-5 ms for accurate ejection (Pascoe et al. 2015),
- area occupied on the belt hardly exceeds 5% (Yu 2014),
- up to 80-93% of energy is wasted in compressed air equipment (Máša & Kuba 2016).

Control of air flow through nozzles requires dedicated solenoid valves. Currently they come at width of 10 mm (3,125 mm for Binder+Co Clarity Glass), switching-on time 2 ms, switching power 5 W, mean time between failure 5 billion cycles, operating pressure up to 8 bar (Festo Valves n.d.), single valve costs ~50 € (Landefeld n.d.). An industrial colour sorter (1 t/h, 64 valves) price starts from ~10 k€ (Color Sorter Group), although custom separation conveyor for research purposes can be rather compact, see Figure 37.

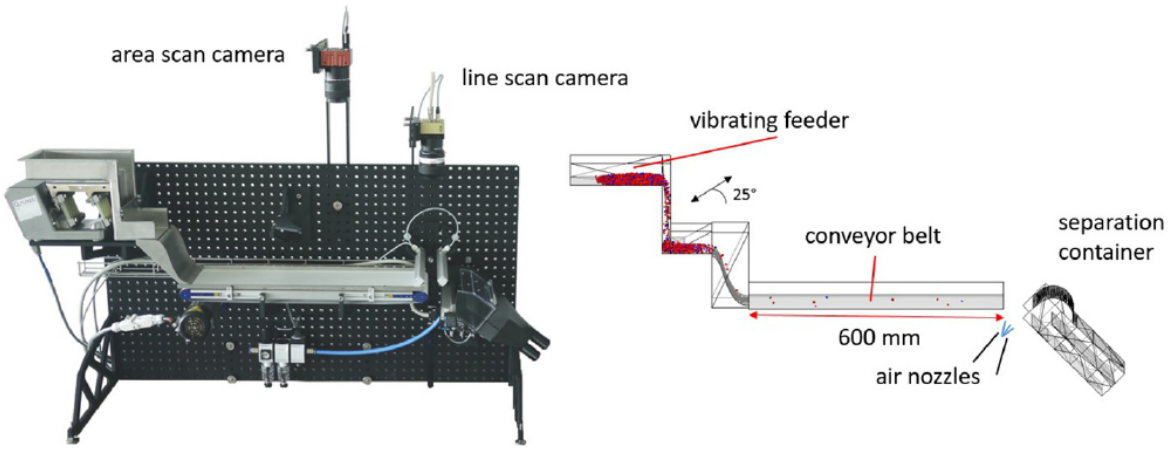

Figure 37. TableSort – installation for rapid prototyping of sorting systems, includes: a feed hopper, conveyor belt, air supply, air nozzle bar, rack for sensor and illumination mounting (Pieper et al. 2018).

Despite multidimensional (spatial and spectral) data obtained from sensors, NIR, XRT and other sorters usually accomplish only binary separation. Therefore, MRF with multi-fraction waste infeed may need to use about 10 NIR sorters together (WRAP 2010). There are systems, however, that can produce multiple fractions after single classification unit, see Figures 38-41.

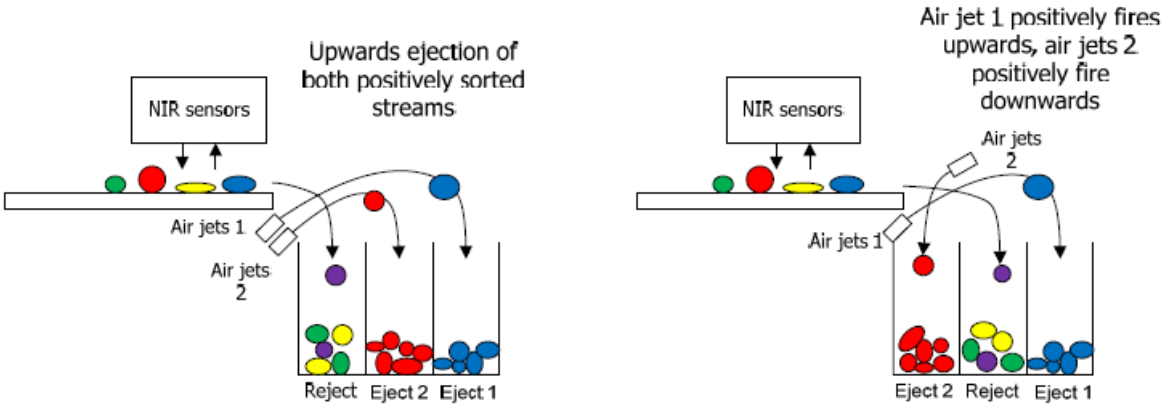

Figure 38. Ternary sorting (WRAP 2010), commercial example – Binder+Co Clarity Glass (n.d.).

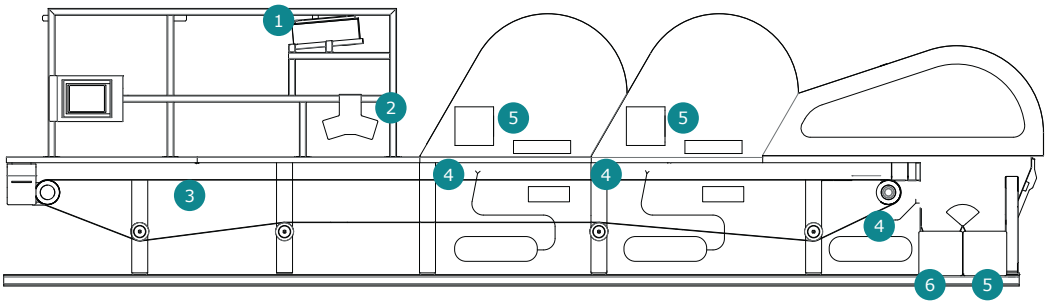

Figure 39. Perforated conveyor belt allows to position air nozzles underneath the belt and sort whole items into 4-6 fractions, transported sideways by auxiliary conveyors (Binder+Co n.d.), a similar construction is possible with pneumatic hammers under conveyor belt (Pat. WO 01/64359 2001).

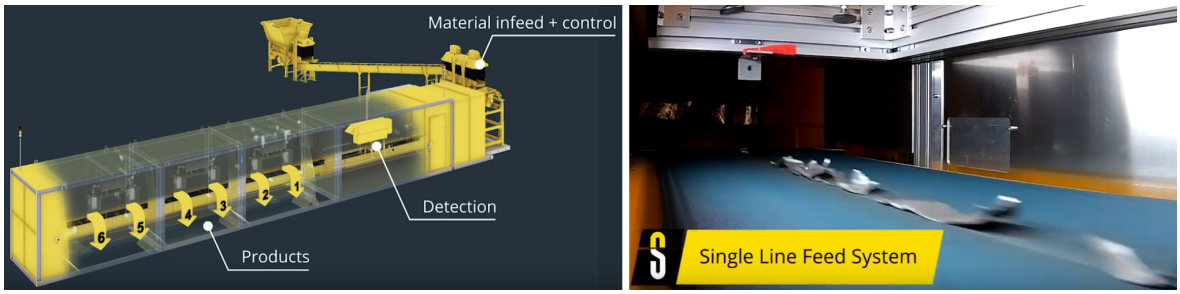

Figure 40. Steinert Line Sorting System uses single line distribution on the flat belt with air nozzles blowing items sideways into 4-6 fractions (Steinert LSS 2018), adapted from Steinert Global (2018).

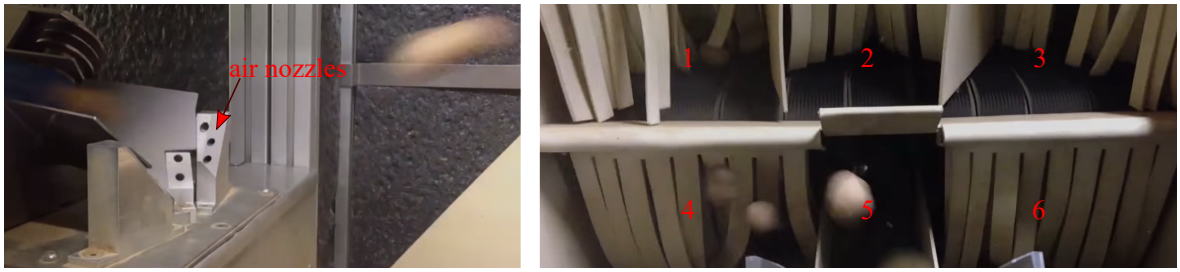

Figure 41. Example from the food industry. Trough conveyor (flat belts in V-arrangement) feeds vegetables (potatoes or carrots, up to 30 pieces per second) in a single line, air nozzles deflect them into 4-6 compartments (Visar Sortop 2016), adapted from Visar Sorting (2016).

An alternative approach is the use of robotic manipulators with 3-4 degrees of freedom and 2-finger gripper (Kujala et al. 2015) or vacuum suction cup at the end AMP Robotics n.d..

Machine learning algorithms with an extra 3D camera are needed to achieve about 90% picking success rate with 1-2 picks per second (Kujala et al. 2015).

Powersort 360 sorting equipment is one of a kind design of feeder and sensor arrangement, see Figure 42. High-speed analyzer (laser spectrometer) scans along 360deg circle line, the laser beam and analyzed signal are directed by a rotating mirror (5000-15000 revolutions per minute) (Pat. US 2017/0259305 2017). The material stream (flakes 8-75 mm) is distributed along the whole circumference (4 m), falling from 8 separate feeding compartments, so that 8 binary sorting processes run independently from each other in parallel. Routing into inner or outer collecting sectors is done by air nozzles right after scanning (30 mm below). 10 t/h throughput is achieved within 20 m^2 floor space (Meyer et al. 2017).

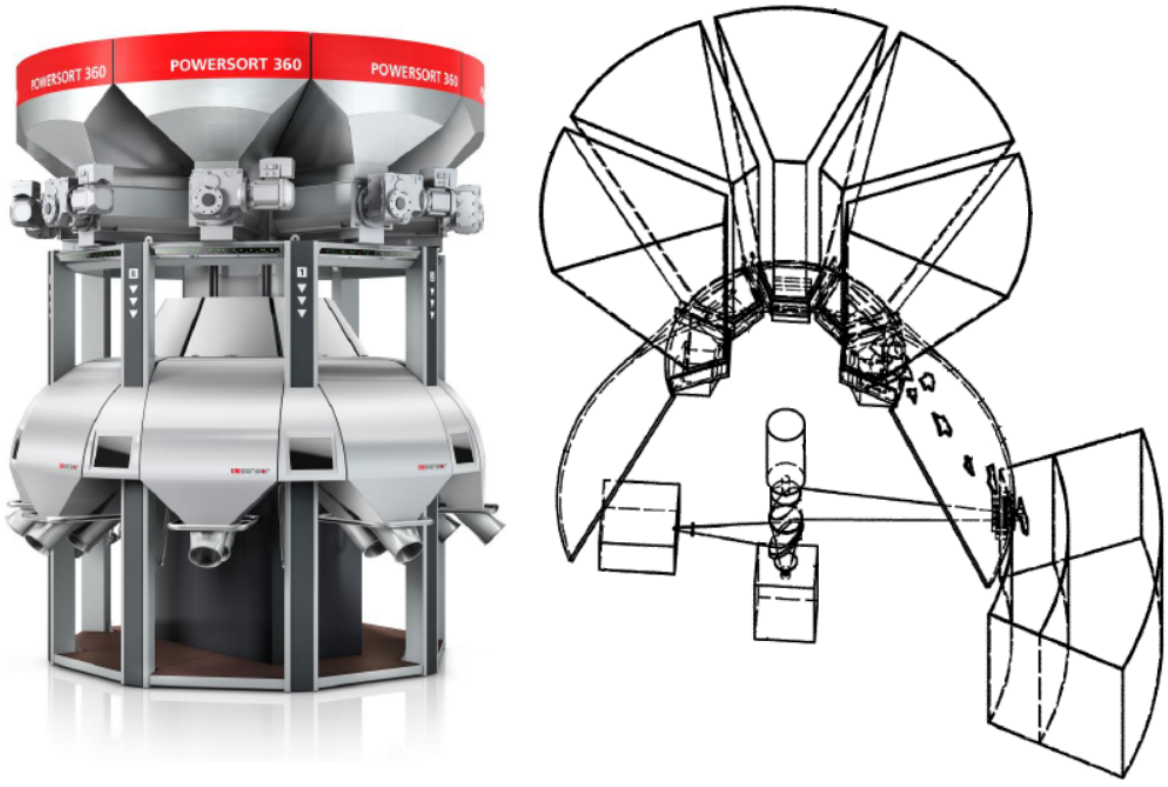

Figure 42. Powersort 360 separator: exterior (left) and schematic principle (right), adapted from Meyer et al. (2017) and Pat. US 2017/0259305 (2017).

3.1.9 Optical reflectance spectroscopy

Hyperspectral cameras are industrially applied in the sorting of glass (UV and visual spectrum) and plastic or paper waste (visual and NIR) (Picvisa n.d.). Although separation purity and recovery rates may exceed 95% with automatic separation alone, often subsequent

hand picking lines are arranged to increase efficiency from 60-70% to 90-95% (WRAP 2010). Cameras for shorter wavelengths may have higher frame rate and spatial resolution – about 1-3 mm in visual range and 5-7 mm in NIR (Binder+Co Clarity Glass n.d.). Recent studies aimed at expansion of NIR sorters target material categories (see Figure 43): identification of wood composites and wood treated with preservatives (Mauruschat et al. 2016), sorting of mineral aggregates in CDW (Vegas et al. 2015). In the latter case investment in equipment was estimated to be from 95-140 k€ (for 0,6 m wide belt) to 230-320 k€ (2,8 m). HSI in the visual range has shown 97% accuracy to distinguish steel, lead, copper, aluminium, brass alloys (Picón et al. 2012).

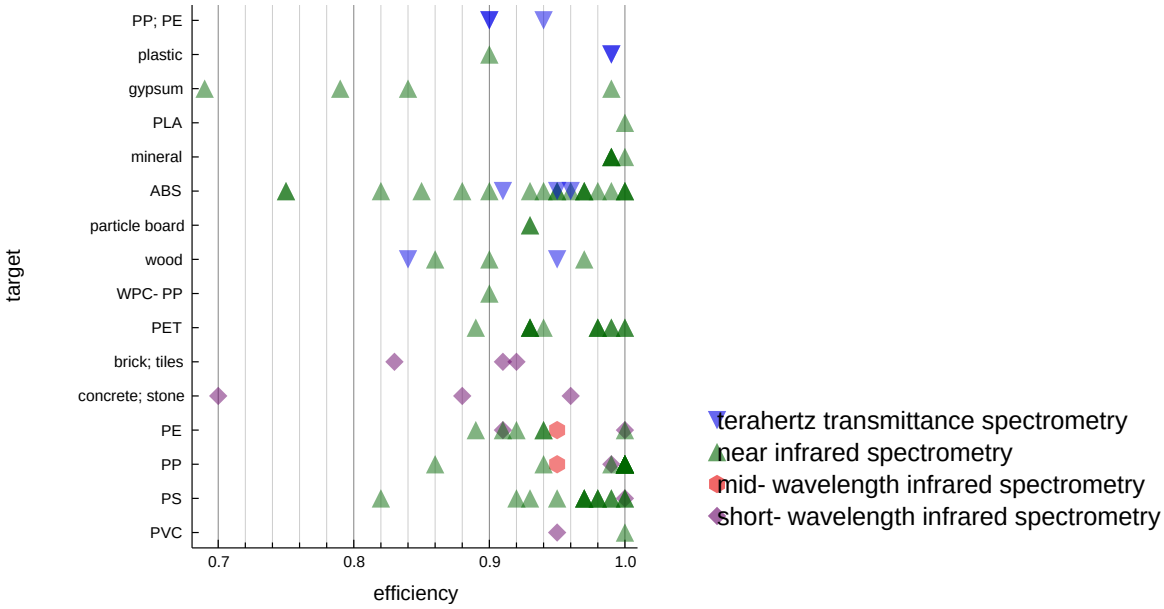

Figure 43. Observed efficiency for IR and THz sorting, from the database. WPC denotes wood-plastic composite.

Although the accuracy of spectral material classification may get close to 100%, limitation of optical sensors remains low depth of penetration, so misclassification occurs because of labels, coatings and contaminants. Another issue is sorting of materials with the addition of black soot that absorbs radiation in the wide range from UV to IR, but a commercial solution (UniSort BlackEye by Steinert) emerged recently with the use of MWIR HSI (Beel 2017). A general review of commercial optical (mostly) separators was done in Demingling the mix (2011), but spectral analysis equipment used in research are shown in Figure 44.

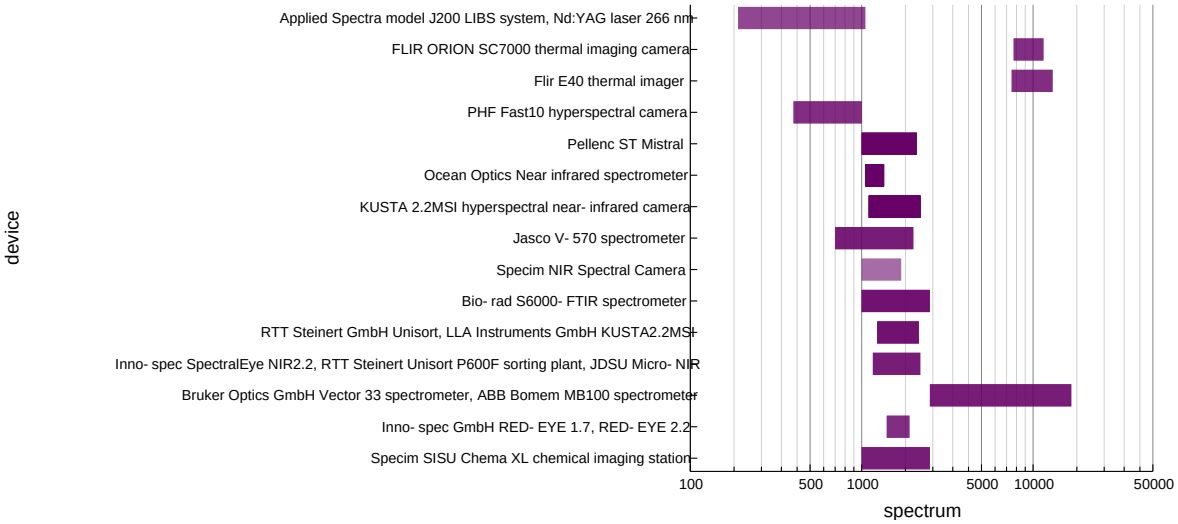

Figure 44. Spectral equipment used in research, wavelength in nm, from the database.

3.1.10 Thermal imaging

Information from a single channel ("grayscale") thermal (LWIR) cameras were found to be sufficient to distinguish materials in some cases, see Figure 46. Different IR emissivity of materials after heating to 55°C makes sorting of MSW into iron, wood, plastic/paper and aluminium/stainless steel categories (Gundupalli et al. 2017b), as well as WEEE into the printed circuit board (PCB), metal, plastic and glass categories (Gundupalli et al. 2018) possible with an accuracy above 85%. The technique is robust against dust because radiation can pass through it. The distinct feature of these experiments is classification of whole, relatively large items, see the comparison with other sensor techniques in Figure 45.

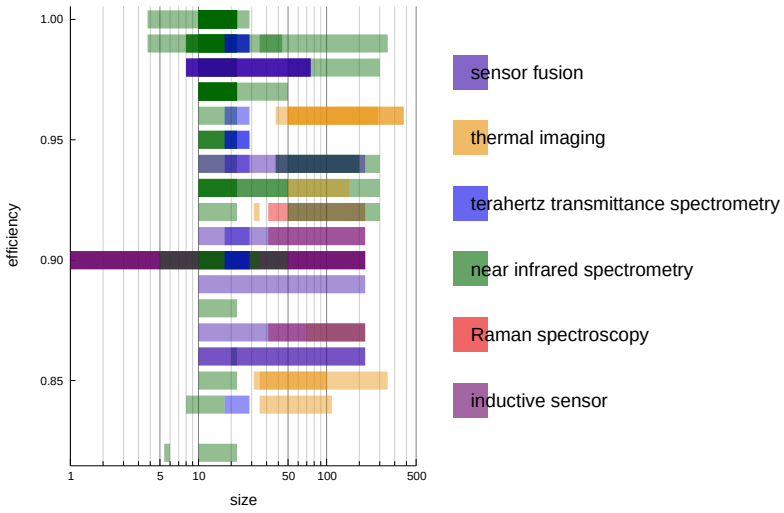

Figure 45. Sensor technology efficiency for different particle size ranges, from the database.

Another approach makes use of the difference in microwave energy absorption by plastics. Rubber samples, as well as PP, PVC and ABS plastics, were distinguished with an average accuracy 75% (Huang et al. 2018).

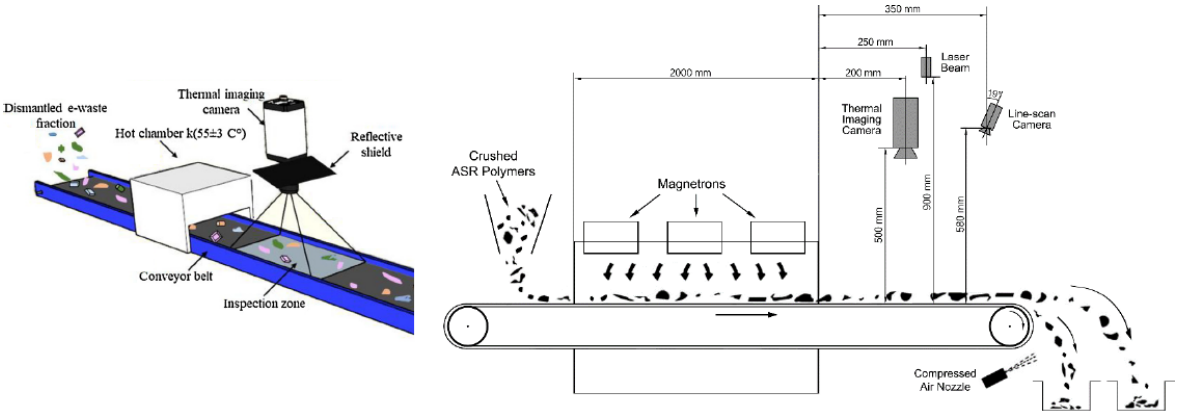

Figure 46. Separation layouts with thermal cameras: (left) with hot air chamber (Gundupalli et al. 2018) and (right) with microwave heating (Huang et al. 2018).

3.1.11 Transmittance imaging

Dual energy XRT is implemented in commercial solutions where detection of relatively heavy elements can be used for classification: cast and wrought aluminium, stone and wood, PVC and other plastics, inert and leaded glass, plastics with and without flame retardants (Steinert XSS T n.d.; Pellenc ST Xpert n.d.). X-rays go through materials, so they can detect inclusions, like metal fasteners in wood. However, a cheaper (and safer) way to see through provides THz imaging: a 25 k€ THz vision system (no spectroscopy) can replace a 70 k€ X-ray system (TeraSense n.d.). TPI with the use of phase information was suggested to classify black plastics (Brandt et al. 2016). Wavelength in millimetre range limited the spatial resolution, so an extra visible light camera was used to determine boundaries between flakes. Visible or UV light transmission is used industrially for sorting of transparent materials – glass, clear PET (Picvisa n.d.).

3.1.12 Fluorescence, LIBS, Raman spectroscopy

Detection of certain substances can be realized when these substances have distinct fluorescence spectrum. Lignin content can be estimated because of 650 nm peak in fluorescence under excitation with 532 nm laser (Ramasubramanian et al. 2005). The developed sensor can distinguish grades of paper, even though red ink produces false positive

results. XRF and LIBS technologies were found effective to detect wood with CCA treatment (Solo-Gabriele et al. 2004), but LIBS could perform measurements at a longer distance (~10 cm) because of the longer focal region. Fast elemental analysis of samples by LIBS was applied in industrial sorter of aluminium alloys on the basis of quantitative analysis of alloying elements: copper, iron, magnesium, silicium, zinc, chromium (Steinert LSS 2018). High power laser spectrometer in Powersort 200 and Powersort 360 separators by Unisensor Sensorsysteme makes 1 million measurements of Raman scattering and LIF response per second and achieves 98% separation accuracy for plastic shredder residue, including black one (Meyer et al. 2017). The high-speed laser produces sharp spectral image by sequential point measurements, unlike NIR cameras.

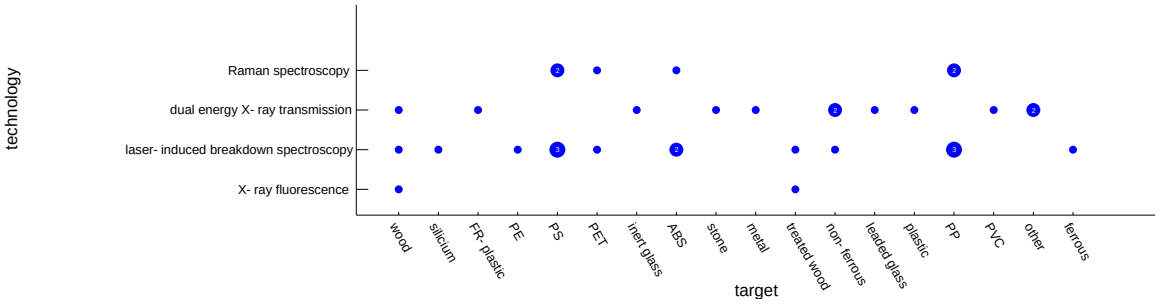

Figure 47. X-ray, Raman and LIBS techniques used for identification of different materials, bubble size indicates instance count, from the database.

Elemental analysis is less suitable for categorization of organics (composed mostly of carbon and hydrogen atoms), but some numerical approaches were proposed to classify plastic types (Anzano et al. 2011; Kim & Choi 2019), also black plastics (Roh et al. 2018). Raman spectroscopy, despite its operation in IR region (Tsuchida et al. 2009), can be made suitable for black plastics with help of advanced algorithms like neural networks (Roh et al. 2017). Laboratory LIBS equipment may cost below 30 k€, Raman spectrometer 10-25 k€ (StellarNet n.d.).

3.1.13 Acoustic emission and sensor fusion

Acoustic vibration induced in materials may be recognized by advanced algorithms and classify broad categories of materials: metal, plastic, glass, cardboard (Korucu et al. 2016). However, when information about particle size is provided (by 3D laser scan camera), plastics can be distinguished by type using the dominant frequency of the impact sound (Huang et al.

2017), see Figure 48. Combination of various sensors, like inductive with optical ones are used in industrial sorters (Picvisa n.d.), examples of laboratory experiments are summarized in Table 4.

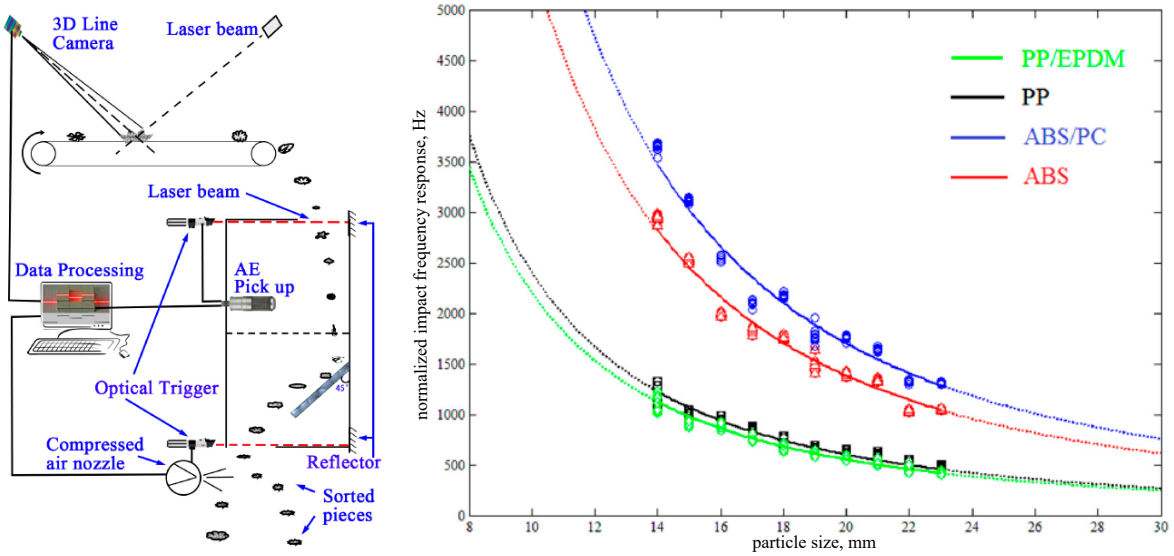

Figure 48. Layout of acoustic emission based separator (left) and plastic flakes sound frequency after impact, adapted from Huang et al. (2017).

Table 4. Sensor fusion for material separation, laboratory trials.

Publication	Sensors	Result
Ramasubramanian et al. (2012)	measurement of lignin content (fluorescence), gloss, colour, bending stiffness (an air jet impinges sheet and ultrasonic sensor measures deflection)	newsprint, white free sheets, coated sheets, board, coloured free sheets are distinguished, fuzzy logic showed better accuracy (80-100%) than neural network
Koyanaka & Kobayashi (2010, 2011)	weightmeter under conveyor and 3D camera	wrought aluminium, cast aluminium and magnesium alloy chunks classified based on their apparent density with purity and recovery close to 90%, 35 k€ equipment had 200 kg/h throughput
Takezawa et al. (2015)	XRT and inductive sensor	aluminium 1200, 2024, 3004, 5052, 6061, 8000 alloys classified
Kutila et al. (2005)	colour camera and inductive sensor	copper, steel and brass classified with efficiency about 80%

3.2 Technologies to adapt and to create

In the following new separation principles and auxiliary technologies are suggested, their feasibility and limitations discussed.

3.2.1 Coandă effect

Coandă effect is adherence of fluid jet to a convex surface. The effect has numerous practical applications, some of those may find use in recycling. Coandă screen (see Figure 49) removes sediment from water at a high throughput by deflecting water with a grid of triangular bars (May 2015), a slightly different layout is used to remove grit (0,2 mm) from water (HUBER n.d.). The technology can be useful in returning water to high throughput wet separators like hydrocyclones. Classification of fine powders (0,003-0,2 mm) by size is accomplished in Coandă classifier by deflecting an air jet (Powder Systems n.d.). The technology might be scaled up to sort waste by weight.

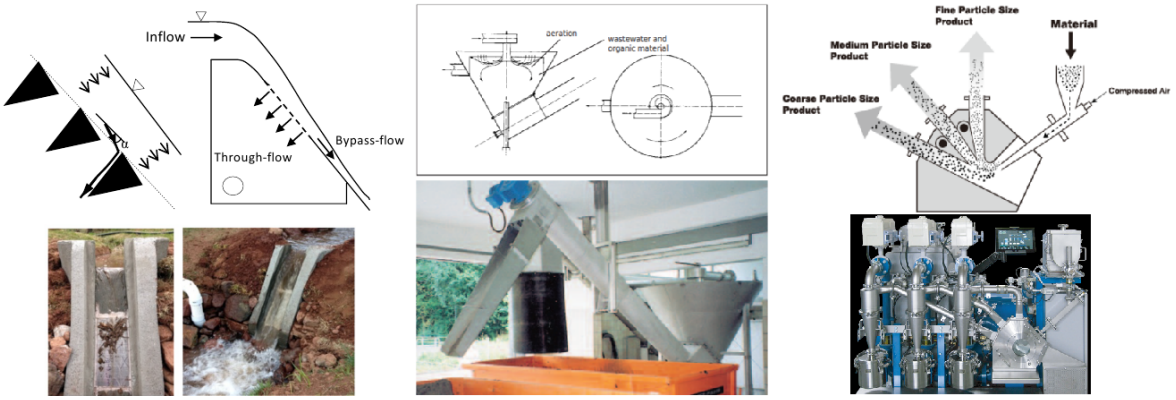

Figure 49. Coandă effect in use (left to right): laboratory scale (230 €) Coandă screen, (May 2015), Coandă effect grit removal (HUBER n.d.), laboratory Coandă classifier (Powder Systems n.d.).

3.2.2 Robotic grippers

Advancements in robotic grippers can be partly introduced in recycling. Vacuum suction cups have alternatives like Bernoulli gripper and Coandă ejector. Both produce suction by blowing pressurized air, thus simplifying design and improving performance in case of porous materials like textile Fantoni et al. (2014). Bernoulli gripper spreads air in radial directions to attract an object by reduced pressure in the jet. Even though commercial grippers are used in contactless handling of silicon wafers (Festo Bernoulli grippers OGGB n.d.), the adaptable design proposed by (Petterson et al. 2010) can lift objects with arbitrary shape. In recycling,

flat Bernoulli gripper might selectively pick up thin foil materials, while adaptable gripper might pick up arbitrary objects and simultaneously blow out the dust from them. Coandă ejector resembles the suction cup, except that air is sucked in by a small amount of accelerated air flow, the ejector can be made of simpler planar shape (Lien & Davis 2008).

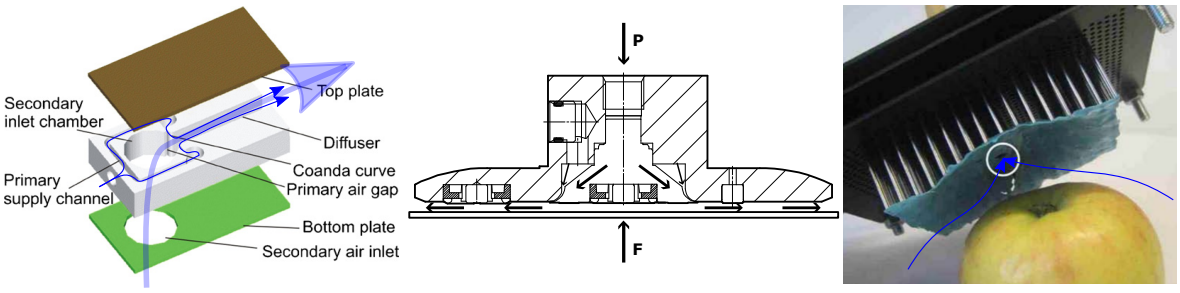

Figure 50. Vacuum grippers (left to right): planar Coandă ejector (adapted from Lien & Davis (2008)), commercial Bernoulli gripper (adapted from Festo (n.d.)), Bernoulli gripper for convex shapes (adapted from Petterson et al. (2010)).

Challenges with the handling of textiles have led to the invention of grippers with a peculiar design that might get used in the recycling of mineral wool or other porous materials like foams. Needle gripper is a commercially available solution that grasps textiles with pneumatically operated needles (FIPA Needle Grippers n.d.). Cryogripper sprays a tiny amount of water first and adheres to the sheet when the Peltier element freezes the water (Seliger et al. 2000).

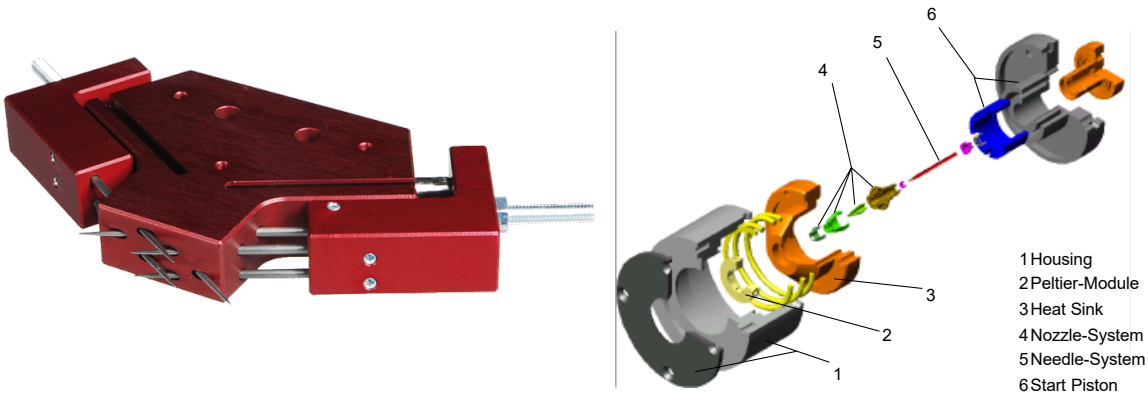

Figure 51. Left: needle gripper (FIPA Needle Grippers n.d.); right: cryogripper prototype elements (Seliger et al. 2000).

The grippers mentioned might need a redesign, so that they operate within conveying mechanisms rather than as the end effector of a robotic manipulator. Innovative forms

of versatile grippers (Figure 52) may have potential in recycling if they withstand handling of coarse and dirty objects.

Figure 52. FlexShapeGripper: hydraulic fluid inside the silicone "chameleon tongue" grips objects by drawing them inward (Festo FlexShapeGripper n.d.).

3.2.3 Security scanning and non-destructive evaluation

Security scanning and waste separation have some common features: a stream of items of diverse origin are looked through for detection and ejection based on some fuzzy criteria. In addition to X-rays, security scanners make use of gamma rays and fast neutron radiography to see through cargo containers and distinguish between heavy and light metals, organics, explosives. (Sowerby & Tickner 2005). High cost (up to 1 M€) and use of radioactive substances promotes search of alternatives.

Measurement of reflection, transmission and phase change of signals in the radio frequency range (including WiFi) may detect metals and water (Wang et al. 2018a) as well as distinguish materials from each other (Wang et al. 2017b). However, research is still in early stage and ~1 dm wavelength limits the spatial resolution accordingly.

In contrast, a new NIR imaging was proposed a decade ago to see objects concealed behind clothes and thin materials (Diamond 2008). It uses lock-in amplification – a technique to detect modulated signal in a very strong noise. A similar approach was used for NIR transmittance multispectral imaging. Four NIR laser sources of different wavelengths were modulated by a square wave at individual frequencies (hundreds of kilohertz), combined and passed through the sample. Transmitted signal was detected by a photodiode and extracted by

the lock-in amplifier, see Figure 53. The technique was applied for non-destructive evaluation (NDE) of food: 2-3 mm size glass, metal contaminants were seen behind 2-3 cm of cheese. Signal intensity for the four channels was measured for one pixel at a time (1×1 mm), but the use of multiple photodiodes and laser sources can lead to a real-time imaging device (Senni et al. 2016). This technology can be seen as an alternative to both NIR HSI (with lower spectral resolution) and X-ray, THz transmittance imaging (for detection of inclusions).

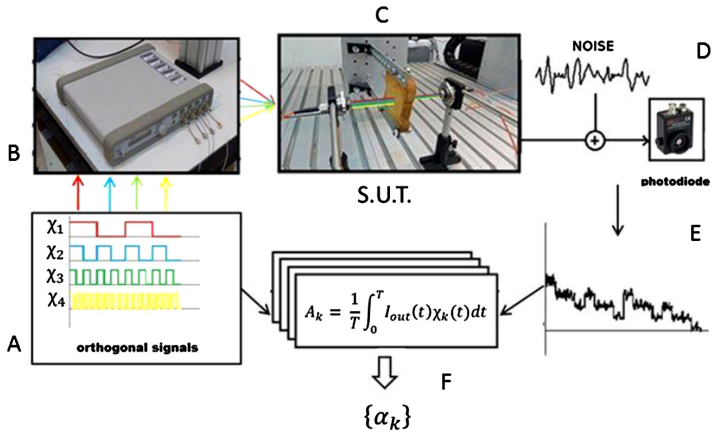

Figure 53. Flow chart of multispectral laser imaging (Senni et al. 2016).

3.2.4 Low-cost MWIR HSI

HSI is getting widespread use but remains expensive laboratory equipment. However, researchers manage to build HSI equipment themselves from single components. Sigernes et al. (2018) made an HSI camera for visible and NIR ranges with hardware cost below 600 €. MWIR optics and detectors are made of different material than consumer photo cameras, resulting in a cost of about 0,1 € per pixel. Kilgus et al. (2018) proposed use of microbolometer detector for capturing MWIR in HSI. A bolometer is an unspecific radiation sensor that works by heating up from the incoming radiation and changing its resistance. Miniaturization and increase in sensitivity of bolometers have lead to their use in uncooled microbolometer LWIR thermal cameras, although the sensor is sensitive to MWIR as well. A 160×120 pixel camera with 9 Hz frame rate able to take images in MWIR range (in a narrow bandwidth at once due to filter) was made with hardware cost below 500 €, decreasing the cost down to 0,01 € per pixel (Kilgus et al. 2018).

Neither 9 Hz frame rate nor single-wavelength images are not sufficient for material identification on a conveyor belt. However, a push broom scanner with diffraction grating

instead of a tunable filter can be assembled from the following hardware:

- 1200 € 320×256 pixel lensless microbolometer, 60 Hz (FLIR n.d.),
- 150 € diffraction grating (Thorlabs n.d.),
- 150 € CaF_2 lens, 2 pieces (Thorlabs n.d.),
- 50 € concave mirror (substitutes a more expensive lens) (Thorlabs n.d.),
- 100 € slit (Thorlabs n.d.),

about 2000 € in total. The layout is given in Figure 54: the light enters the front lens, passes through a narrow slit (taking one scan line), reflects from the concave mirror and falls in parallel beam onto dispersive element – reflective diffraction grating. Rays of different wavelengths get focused on the microbolometer, resulting in 320 spatial pixels and 256 spectral pixels (or vice versa).

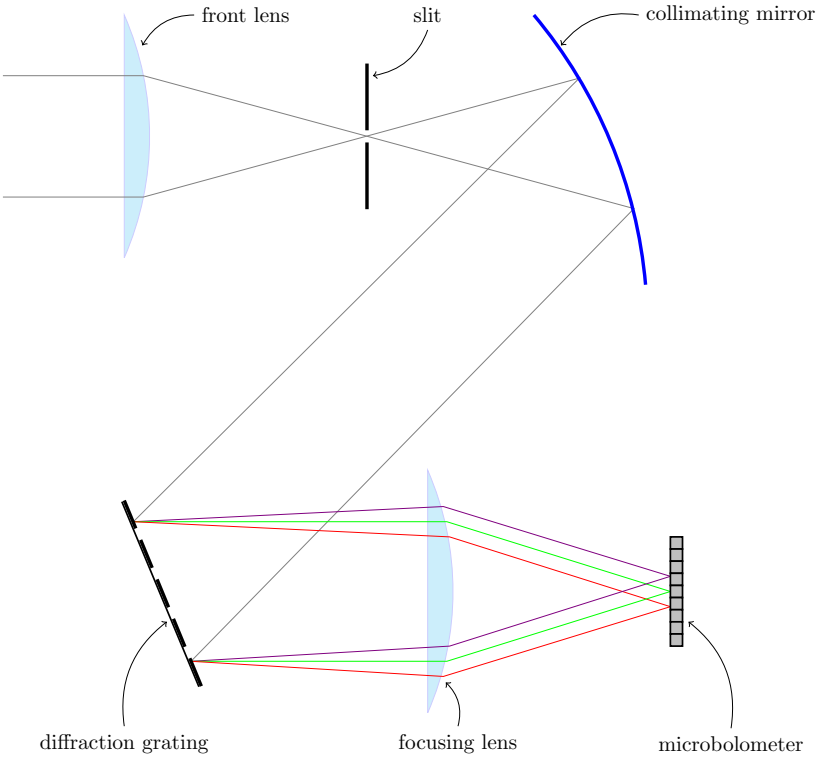

Figure 54. Push broom low-cost MWIR HSI camera possible layout

The performance of the camera will definitely stay behind the industry-leading Specim MWIR HSI cameras (~100 k€ (Keinänen 2019)) with maximum 800 Hz frame rate but should be able to distinguish black plastics. 60 Hz frame rate can yield up to 1 cm resolution with 0,6 m/s conveyor speed.

3.2.5 Thermoplastic needle grabber

Bollegraaf company offers PaperSpike and FilmGrabber machines that separate hard cardboard from paper and catch films from the waste stream (Bollegraaf n.d.). The operation principles of these machines are closely related, namely, materials are selectively pierced or caught by spikes or hooks, see Figure 55.

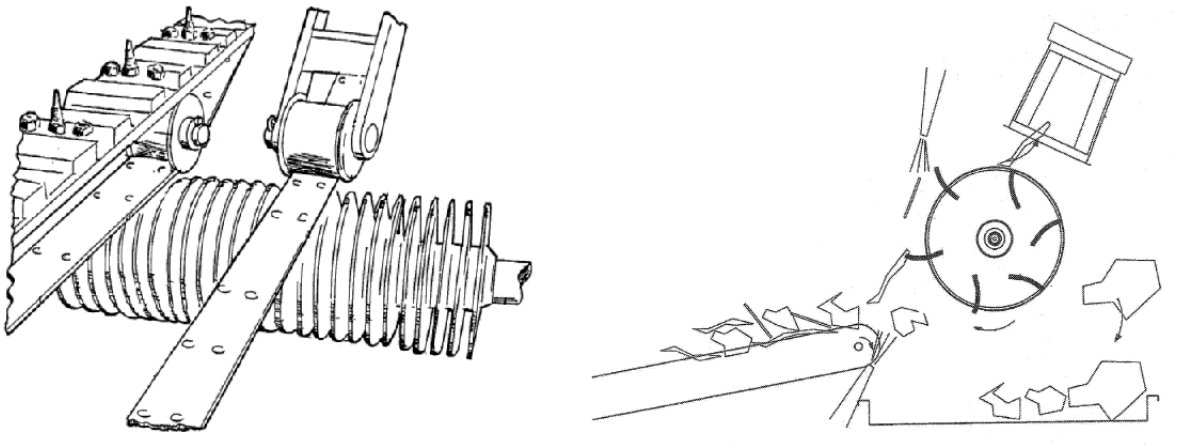

Figure 55. Core elements of PaperSpike (left) and FilmGrabber (right), adapted from Pat. EP 1291092 (2003) and Pat. EP 1970130 (2008), respectively.

In the PaperSpike machine, cardboard sheets are pierced and retained on spikes while paper sheets fall off. The relatively low melting temperature of thermoplastics compared to other materials of similar density (like wood and wood-derived materials), so a machine analogous to PaperSpike or FilmGrabber could be designed with heated spikes that would selectively pierce chunks of plastic. The idea is partly justified by the existence of Vicat hardness or Vicat softening temperature test. In the test procedure, a thermoplastic specimen is placed in a heated bath with steadily increasing temperature. A flat-ended steel probe of 1 mm^2 cross-section is pressed with a specified load against the specimen until the depth of penetration reaches 1 mm (ASTM D1525-00 2000). Various plastics have different Vicat hardness (see Figure 56), so the proposed method might even be suitable for coarse separation between plastics of low softening temperature (PE, PP, PS) and high softening temperature (PET). It is to be noted that mineral fillers in plastics may raise their Vicat hardness.

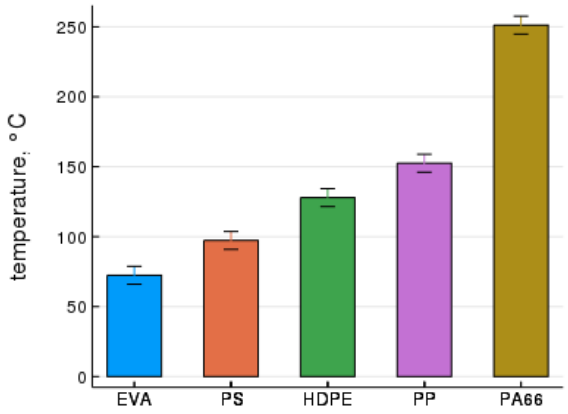

Figure 56. Vicat softening temperature of several polymers under loading 1 N and heating rate 120°C/h. Error bars show between-laboratories reproducibility limit (2,8×standard deviation among 7-10 laboratories). Data from ASTM D1525-00 (2000). EVA – ethylene-vinyl acetate.

The most feasible embodiment of the principle is hard to predict, but electrically heated needles might be in the form of rotating sharp-ended screws. Screwing the heated needle in the material will work for grabbing and unscrewing – for releasing. Spring-mounted individual electrical motor for every screw might be the feasible solution. Attachment on a robot arm might be simpler than implementing a solely mechanic construction.

3.2.6 Oxygen in magnetic density separation

Among separation methods that use magneto-Archimede's effect, only technology using ferrofluid has reached pilot scale operation. Water-based solutions of paramagnetic salts are still demonstrated in small scale experiments. Regardless of how far these techniques are developed, they will be facing problems of insufficient wetting and extra buoyancy created by attached air bubbles. Yet there is gas with strong paramagnetic properties – oxygen. Oxygen has a low density at room temperature and atmospheric pressure and rather weak interaction with the magnetic field. However, its density can be increased by rising pressure and lowering temperature, but volumetric magnetic susceptibility is proportional to density and inversely proportional to the absolute temperature (Néel's law). Pure oxygen is highly flammable, so it is better used at concentrations below 30% (Catherall et al. 2005). Given that the air contains at least 20% oxygen by weight, it might be advantageous to use compressed air as separation medium in a magnetic field, thus eliminating the need for extra wetting and drying stages and benefiting from low viscosity. Unfortunately, requirements for both magnetic field and

air pressure are very high and imply usage of superconducting magnets (see Figure 57).

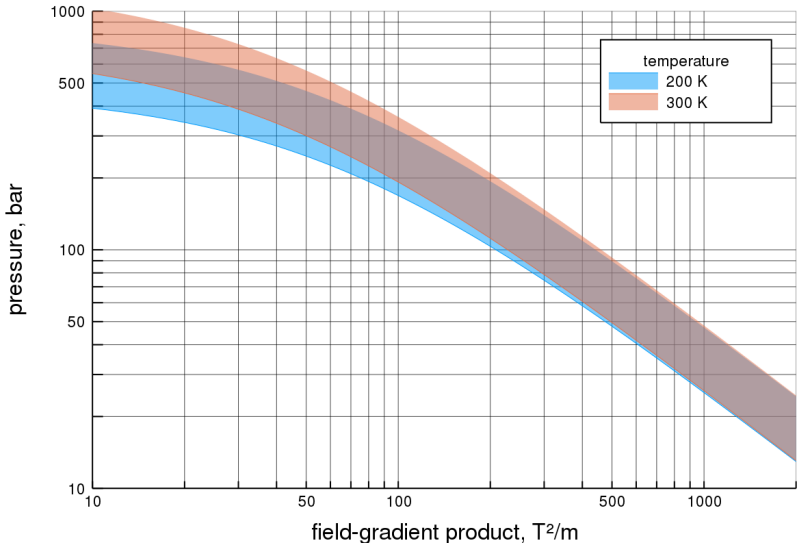

Figure 57. Air pressure and magnetic field-gradient product necessary to levitate materials from 800 to 1500 kg/m^3, air considered ideally compressible.

Air compression ratio sufficient for levitation can be computed by equation (derived from Catherall et al. (2005)):

$$r = \frac{T}{T_0} \frac{\rho_m g - \frac{\chi_m}{\mu_0} B \frac{dB}{dz}}{\rho_0 g - \frac{T}{T_0} \frac{\chi_0}{\mu_0} B \frac{dB}{dz}} \tag{6}$$

In the equation r – compression ratio, T and T_0, K – absolute temperature for levitation and initial temperature, ρ_m and ρ_0, kg/m^3 – material density and air density at initial conditions (1 bar, 300 K), χ_m and χ_0 – magnetic susceptibility for material and air, $B\frac{dB}{dz}$, T^2/m – magnetic field-gradient product, μ_0, H/m – magnetic permeability of free space and g, m/s^2 – acceleration of free fall.

High pressure complicates feeding into the separation chamber. According to Craven (2014) high-pressure feeding of solids works at pressure levels below 100 bar (with only dust screw feeding up to 200 bar). However, air can be liquefied for higher density and magnetic susceptibility. With density close to water (870 kg/m^3) and 7 times lower viscosity, it has favourable properties for magnetic density separation except for requirement for cryogenic temperatures, to which all processed materials have to cool down (-195 °C). In liquid air at

$|B\frac{dB}{dz}| = 10\ \mathrm{T}^2/\mathrm{m}$ materials with $\rho_m < 1700\ \mathrm{kg/m}^3$ will float.

Air liquefaction is a standard industrial process, although energy-consuming. In mass production, liquid air may cost 50 €/t (Akhurst et al. 2013) and with 0,64 kg liquid air freezing 1 kg PVC it yields 32 € liquid air costs per 1 t PVC (calculated based on Bradley & Radebaugh (2013)). If heat exchange between frozen outcoming and warm incoming waste streams is implemented, then the consumption of liquid air and energy can be decreased significantly.

Use of liquid air justifies application of high-temperature superconducting magnets to create a strong magnetic field over a broad space. The cost of equipment is still high in this case, so potentially this technology is feasible when there are extra benefits of using cryogenic temperatures, like cryocomminution of PCBs (Zhou et al. 2016) or dry cleaning with dry ice or liquid nitrogen (Máša & Kuba 2016).

3.2.7 Electrostatics for routing

So far electric forces were used for separation of different materials. Good performance was achieved in the separation of several plastic mixtures that are not separable by density. However, tribocharging and other electrostatic forces can be changed in polarity and magnitude by contaminants and additives. On the other hand, electrostatic forces are used in widespread devices for very targeted delivery of certain materials – in printers for application of toner from drum to paper.

Laser printers use electrophotography technique to print text and images on paper with resolution of several hundreds dots per inch. Stages of electrophotography include:

1. Charging – the electrostatic charge is uniformly applied over the surface of the drum.
2. Exposure – the drum has a conductive core and photosensitive insulating outer layer. Laser radiation makes outer layer conductive and previously accumulated charge flows away in those lit areas defined by illumination pattern (from image).
3. Development – toner particles are tribocharged by agitation and then applied to the drum. They stick to only those regions where the opposite charge remains.
4. Transfer – drum with toner particles attached is pressed against paper. Subsequent actions fix toner on paper and prepare drum for further operation.

This principle can be transferred to sensor-based separation of fine particles, substituting air ejection system with too low resolution. Instead, a selectively charged drum can be used to pick up target particles from a conveyor belt surface. Conveyor belt should presumably carry some limited charge to force particles to stay in place. In such system information from the camera can be directly applied to the drum to remove target particles pixel by pixel. Concern about the feasibility of such system is to do with the tiny size of toners used in printers – in the order of 10 μm. Firstly, capacity can be estimated from that of a typical laser printer – 200 pages per minute (top performance), 70 mg of toner per 5% covered page (Wyhof 1997). It yields toner consumption at about 15 kg/h. The consumption is proportional to the layer thickness which is minimized in printers for toner savings. Since scanning sensors need a monolayer distribution of material, the layer thickness is proportional to the particle size. For the toner particle of size $d = 10$ μm the force needed to detach from the drum is $F = 250$ nN (Cassidy et al. 2003). The mass must have the order of $m = 10$ ng. Consequently, ratio between the electrostatic and gravity force is $\frac{F}{mg} \approx 25000$.

Since the amount of charge is proportional to the surface area, $F \propto d^2$ and mass is proportional to the volume, $m \propto d^3$, then $F/m \propto 1/d$. Therefore, it should be possible to increase particle size 1000 times (to 10 mm) and keep the prevalence of electrostatic force over gravity. The throughput will increase accordingly if all technologies involved can keep up with each other.

Another electrostatic technology can be applied for feeding and routing particles of bigger size – electroadhesion. Narrow conductive strips in a dielectric are connected to a high voltage source with alternating polarity (Figure 58). When the voltage is on, objects (both conductive and non-conductive) in close proximity from electrodes acquire induced charges and attracts to the electrodes. The Grabit Inc. company offers electroadhesive grippers and conveyors. Electroadhesive grippers start to replace vacuum grippers with great savings of energy (Bain 2017). In turn, electroadhesive conveyors may (Pat. US 2013/0294875 2013):

- feed items upwards at a slope of 40°
- because of short-range attraction, items slide with respect to each other until they destack and stick to the belt, in recycling this can be a way for creating a monolayer
- electrodes in the belt can be selectively energized and de-energized, thus creating attraction only at a certain area, letting items to slide or fall elsewhere, which can be used for sorting (currently suggested for parcels)

- in recycling, attraction to the belt may solve the problem of light items like foils or foams affected by aerodynamic force on high-speed running belts

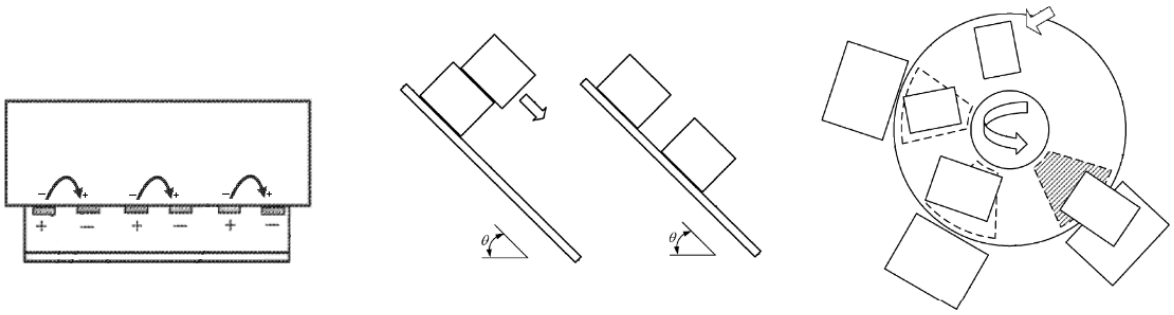

Figure 58. Electroadhesive conveying devices (left to right): charge induction and attraction, parcel destacking on an electroadhesive conveyor, parcel sorting on a carousel by switching off electroadhesive sectors in the right time, adapted from Pat. US 2013/0294875 (2013).

3.2.8 Thermoplastics foaming

Foaming of plastics used within differential density alteration method can be applied to recover fine plastic particles, too small for NIR separators (<3-5 mm). The same blowing agent like carbon dioxide may get absorbed in ABS, PS, PE and PP in range of 1-10% by weight (Lin et al. 2014), so 5-10 fold increase in volume might be possible. Crystalline polymers (PE, PP) tend to absorb less gas than amorphous polymers, which may act as a distinct property for separation. Absorption under pressure of 15-40 bars lasts for hours, so it is hardly feasible to implement for continuous operation, but for small particles process duration could possibly be decreased. Precise handling of small foam particles might require the development of electrostatic routing mechanisms.

3.2.9 Refractive index from image

Specular light reflection from convex objects let estimate refractive index of material the object is made of. The measurement includes illumination of an object at different angles with different wavelength sources (possibly polarized). Six-sensor spectral camera allowed Tominaga & Tanaka (2003) to estimate material properties and construct a photorealistic computer image of the object (a plastic container) afterwards. Saman & Hancock (2011) used an ordinary camera with polarization filter to take multiple photos of an illuminated object (like tomato or apple) and to compute the refractive index for that. Yang et al. (2016) measured reflection of laser sources from flat objects and estimated refractive index of glass, quartz, aluminium and copper at different wavelengths. Accuracy and sensitivity of the

method are illustrated by the fact that for copper plate estimated index diverged only 5-10% from the reference value, but the estimate for aluminium plate was close to the value of aluminium oxide, so the reflection was generated by thin oxide layer rather than aluminium itself.

Refractive index is a material-specific property, although the refractive index of plastics falls in quite narrow interval 1,3-1,7, being close to 1,5 mostly. However, metals differ a lot and may have the refractive index below 1, see reference values for 700 nm (red) light (Polyanskiy n.d.):

- silver 0,17
- copper 0,21
- brass 0,45
- aluminium 1,6
- iron 2,87

All results were obtained in a controlled laboratory environment, so their application in industrial scale is arguable. However, tailored solutions for the distinction of certain materials might get developed, use of ordinary cameras and suitability for complex shapes are some advantages.

3.3 Case study: CDW pilot separation line

Following the current research interest of LUT University, it was decided to study possible equipment layouts for research on mechanical separation of plastic from construction and demolition waste. The equipment should be reasonably versatile for multiple use cases and possibly self-contained, without too many pre- and postprocessing stages like water treatment.

3.3.1 Input and output streams

CDW lacks sustainable management solutions, see the current processing scenario in Figure 59. Cumulative results of previous studies on CDW content in Finland are presented in Figure 60. Plastic, metal, aggregates and cellulose materials (wood, cardboard, paper) are the largest fractions by weight. Wood materials include pure wood, coated (painted) wood, impregnated wood, plywood; aggregates include gypsum, concrete, bricks (Liikanen et al. 2018). Waste is often covered in dust and contains moisture due to open field storage.

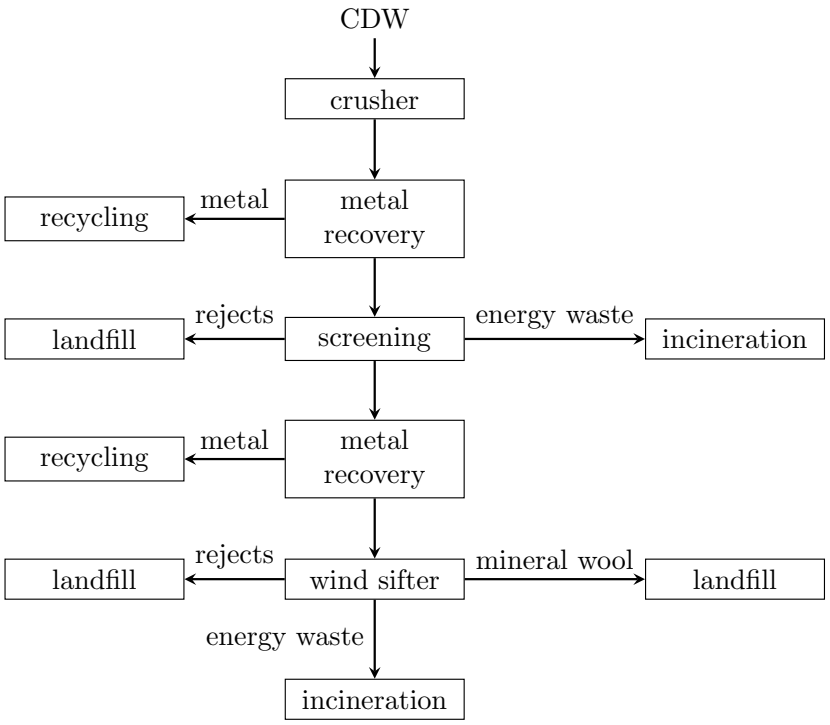

Figure 59. Current CDW processing, adapted from Liikanen et al. (2018)

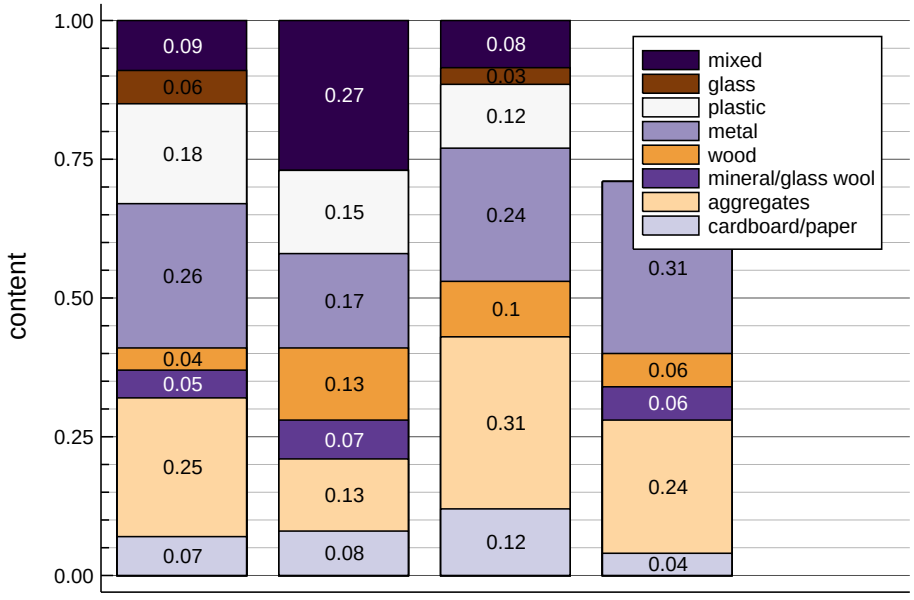

Figure 60. Materials content in CDW studies, data from Liikanen et al. (2018).

Plastics types found in CDW are shown in Figure 61. Plastics constitute 12-18% of CDW by weight. PE and PP dominate in most cases, a large share of ABS in the first example might be due to unrepresentative sample (Lahtela et al. 2019). PVC contributes up to 10% by mass and needs special care because of its detrimental effect on other polymers in reprocessing. PS

contributes 4-6% by weight and may have a large volume as foamed insulation material. A significant share (15-30%) belongs to unidentified plastics, caused mostly by dark pigment, so separation process must be able to handle that.

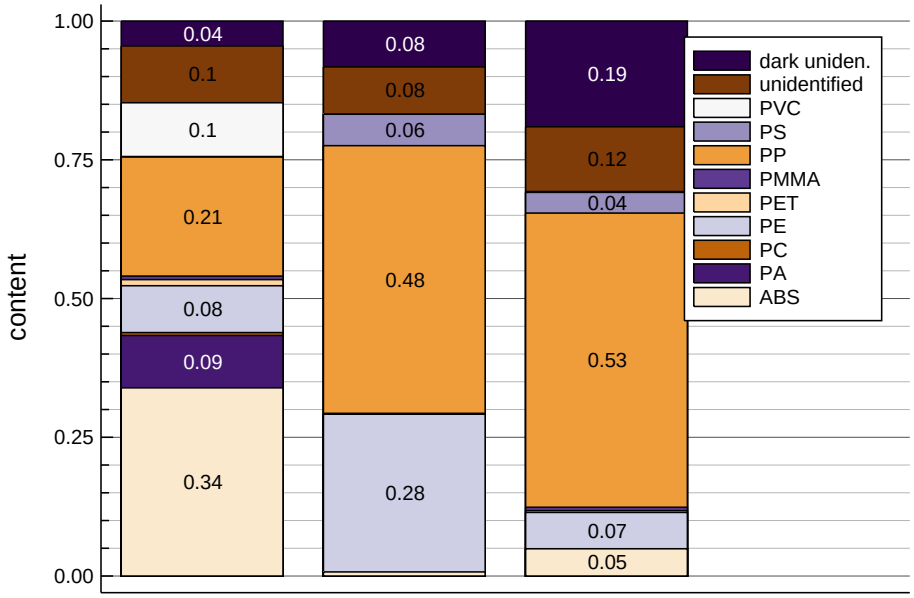

Figure 61. Plastics share in CDW plastic fraction, data from Lahtela et al. (2019). Unidentified and dark unidentified polymers were not classified by SWIR (1600-2400 nm) analyzer.

3.3.2 Technology selection

Separation can be done in two stages:

1. recovery of plastics,
2. separation of plastics by types.

Selection of direct sorting methods needs an examination of material properties. Exemplary CDW material density ranges are shown in Figure 62. It becomes apparent that plastics together with some dense wood materials (like particle boards) can be segregated by density from foam, mineral and metal fractions. Properties like high electrical resistance and diamagnetism are not characteristic for plastics only.

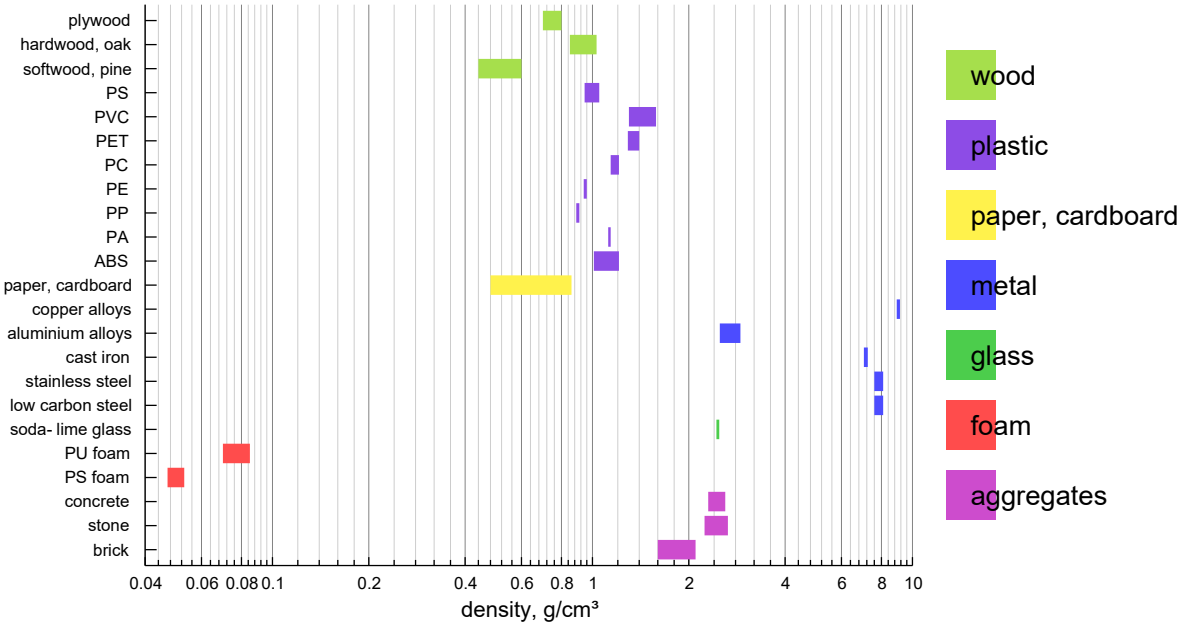

Figure 62. CDW materials density ranges, data from Ashby (2012). PP may have 20% filling with talc with increase in density up to 1,2 g/cm^3 (Ragaert et al. 2017).

Wet density separation methods are not favourable because of extra equipment. Comparative infographics about dry density-based separation technologies was shown in Figures 20 and 21. Active pulsing and zigzag air classifiers have similar performance to pneumatic jigging, however, pneumatic jigging works well for coarser particles (4-20 mm), consumes less air (it is used for agitation only) and has higher efficiency at closer densities.

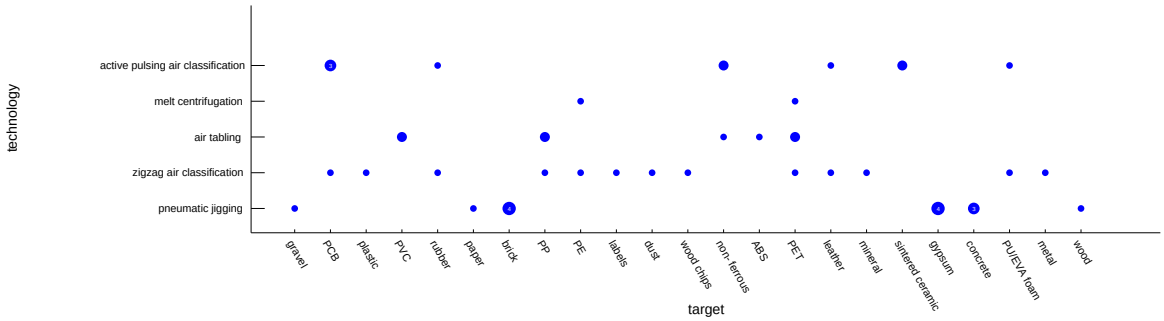

Figure 63. Target materials for dry density separation, bubble size measures instance count, from the database.

The downside for pneumatic jigging is a shorter list of known target materials in waste separation (Figure 63). On the other hand, pulsating water jig was successfully used in presorting of MSW into the light, middle and heavy fraction in a pilot polyolefin separation

line (Bauer et al. 2018), see the layout in Figure 64. Construction of both jigs is quite similar, so pneumatic jig can be turned into water jig without too vigorous intervention.

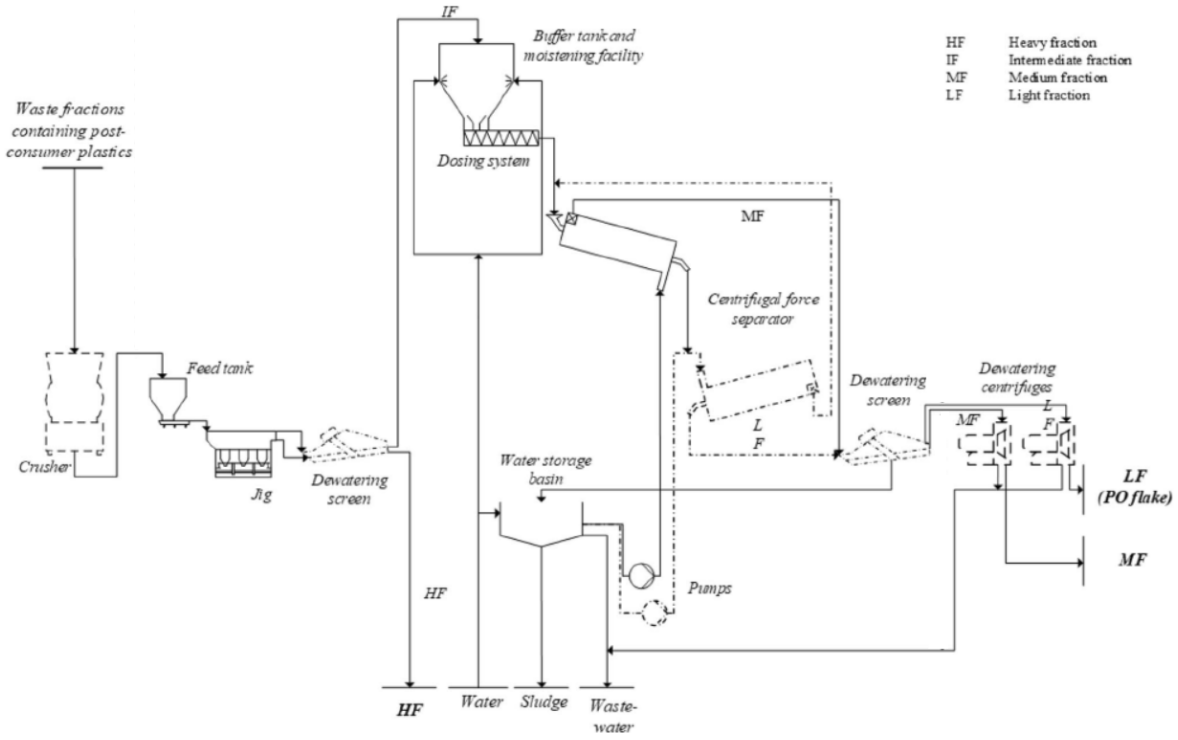

Figure 64. Layout of pilot (65 kg/h) polyolefin (PO) separation line, with crushing and dewatering equipment (Bauer et al. 2018).

Auxiliary equipment for the chosen process would be crusher (down to ~20 mm), mesh screen for fines removal (~4 mm), air cyclone for air cleaning and plastic cleaner before subsequent separation. Since the process is dry, mechanical cleaning by centrifugal equipment is preferred, like that produced by Pla.to Technology with 100-200 kg/h throughput at 25-37 kW power (Pla.to Technology 2018), other solutions were examined by Xia & Zhang (2018). Another way of extracting plastics from CDW stream could be suggested thermoplastic needle grabber, but such technology does not exist yet.

Target plastics have overlapping densities, so further sorting by type should be done by some other property. It is possible with froth flotation (water is used, though), triboelectrostatic separation and (perhaps, little data available) with charge-decay electrostatic separation, see Figure 65. Triboelectrostatic separation is sensitive to surface contaminants and mineral additives like talc, so robust operation with CDW is unlikely. Charge decay is dependent on material electrical resistivity, but there is significant overlap in the target plastics specific

resistivity, see Figure 66. Direct sorting has limited applicability in fine multifraction separation, although froth flotation or precise separation by density (hydrocyclone, decanter centrifuge, magnetic density separation) might work with limited success.

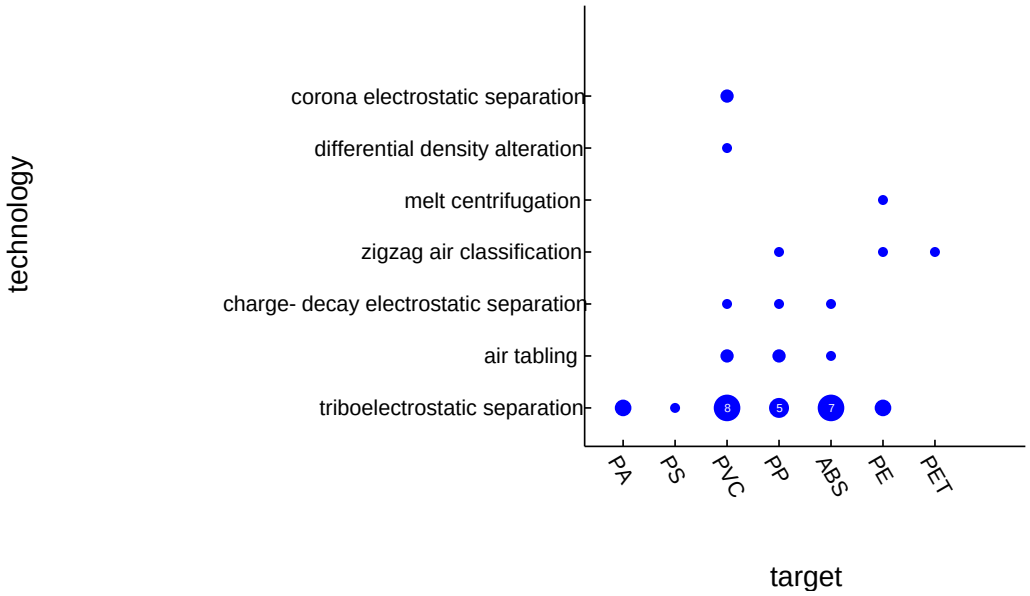

Figure 65. Dry separation technologies used for target plastics, bubble size indicates instance count, from the database.

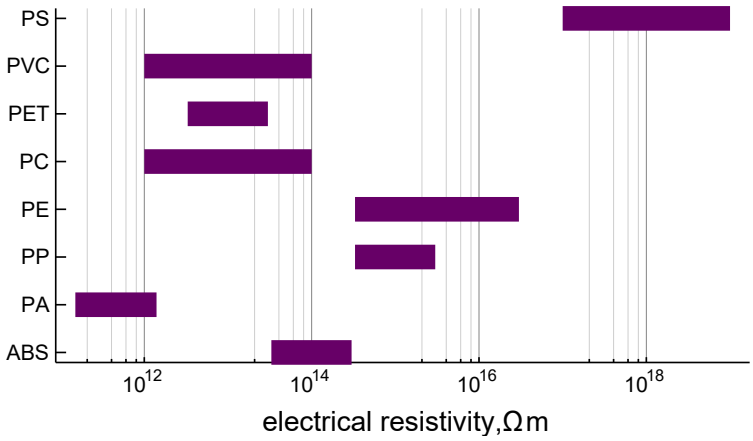

Figure 66. CDW plastics specific electrical resistivity, data from Ashby (2012).

Sensors may distinguish plastic types at once, but macrosorting into general categories will reduce the required volume to sort into high purity fractions. Municipal solid waste items were sorted by thermal imaging after hot chamber (Gundupalli et al. 2017b), so it may be applied for CDW. In this particular case, heating may provide the following benefits:

- reduction of moisture content, which is favourable for subsequent spectral techniques,
- heated objects might emit sufficient MWIR radiation for subsequent HSI,
- collapse of foam insulation material and contraction of plastic films, making them easier to handle.

For the latter effect to work short-time hot (~100°C) air blow is required that will soften thin and low-density plastic items, but heat moderately bulk items. Surface colour and roughness may influence material emissivity, but the simplicity of thermal imaging may outweigh that. Separation by acoustic properties is also feasible, see Figure 67. Plastics should have a distinct impact sound response, problems with hollow items may arise because of complicated modes of vibration and difficulty with thickness estimates. Perhaps sensor fusion can be implemented with those two technologies for better accuracy.

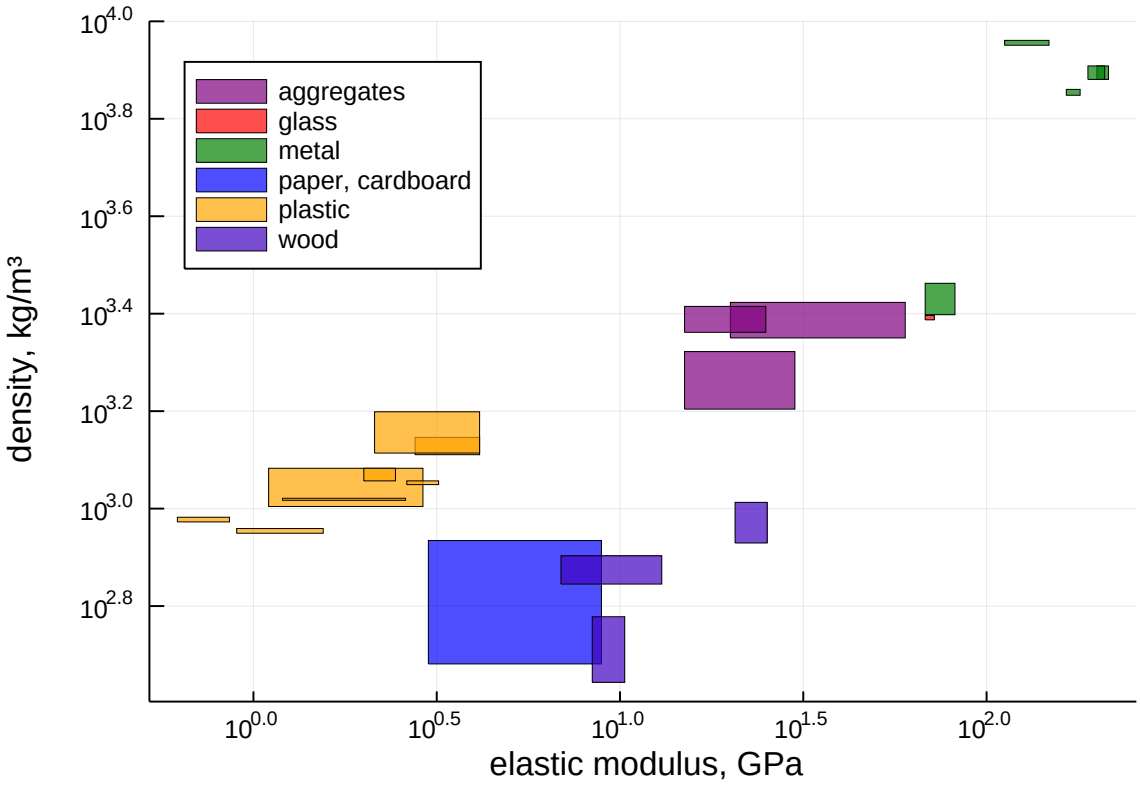

Figure 67. CDW materials acoustic properties estimates based on mechanical properties (foams excluded for their very low parameters), data from Ashby (2012).

Presence of black plastics and their organic nature limits the choice of sensors to:

- MWIR HSI,
- Raman scattering,
- LIBS,

- laser spectroscopy (LIF and Raman scattering).

LIBS does not seem to have an industrial implementation for plastics sorting, whereas laboratory equipment needs software and takes single point probes, so an extra light or NIR camera is desirable for object homogeneity and boundary estimation. MWIR HSI and laser spectroscopy industrial equipment has a quite high capacity and works with particles <75 mm. Implementation of all techniques in a laboratory scale needs development of classification algorithm. In a custom installation, for MWIR HSI speaks its imaging capability and possibility to implement it at low cost, but for Raman scattering and LIBS – availability of laboratory analysis equipment at a lower price than MWIR HSI camera.

A less sensitive, but still viable distinction between plastic items can be seen in thermal imaging after microwave heating of plastics. CDW plastics absorb microwave energy differently, although PP and PE, ABS and PET have similar dissipation factors (overall it depends on frequency), see Figure 68.

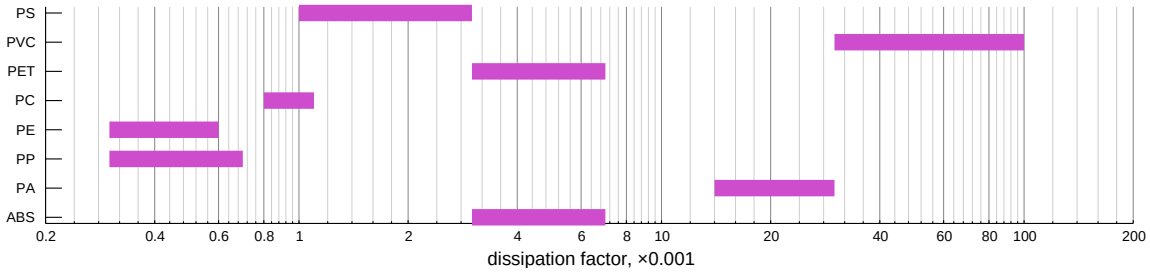

Figure 68. CDW plastic microwave energy absorption estimate from dissipation factor, data from Ashby (2012).

For laboratory scale sorting a single line conveyor feed should provide high enough throughput with the advantage of simpler multi-way routing (in Visar-style or Steinert LSS-style, recall Figures 41 and 40). Implementation of an electroadhesive routing might be highly advantageous.

4 DISCUSSION

The carried out technology review is summarized as follows.

4.1 Technology landscape

Density-based separation can be effective when every material in the stream has a value distinct from all the rest. If it is not the case (see Figure 69), the method is simply not suitable. Hydrocyclone and decanter centrifuge are the most reliable wet separation techniques, practically insensitive to variation in particle size, shape and wetting because of high centrifugal acceleration. Waste dewatering is an issue, though. Decanter centrifuge may get it done by design, but hydrocyclone should benefit from bringing in new technologies, like Coandă screen. Water jigging has better tuning capabilities for different density ranges (even more than two) without change of separation medium, but it is dependent on particle size and wetting. Multidune shows promising results, but it is in early research.

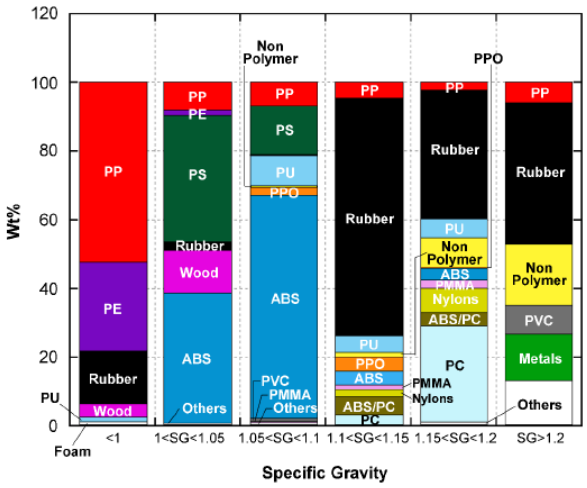

Figure 69. Fractions in automobile shredder residue within selected density ranges (Huang et al. 2018). PPO denotes polyphenylene oxide.

Among dry separation techniques, pneumatic jigging possesses good tunability without excessive air consumption like active pulsing air and zigzag classifiers do. It is dependent on particle size and shape, like all air classification methods, but when ~90% product purity is enough it works reasonably well. For both dry and wet separation methods industrial equipment is available or it can be made relatively easily (from vortex pumps, air compressors, butterfly valves), except decanter centrifuge.

Plastics foaming for differential density alteration as well as supercritical density separation have not gained widespread use presumably because operation with elevated pressure and temperature adds up complexity to the process. Magnetic manipulation with medium density was shown to be effective with consistent feed material composition. However, it creates secondary problems (wetting, fluid reuse) characteristic to very basic sink-float separation without the possibility for similar intensification.

Magnetic and eddy current separation evolve by using progress in material science (stronger magnets) and by implementing active control (electromagnets). With the latter, a single device can be made to serve for both ferrous and non-ferrous materials separation.

Froth flotation and triboelectrostatic separation use surface effects of solid-liquid and solid-solid interaction, respectively. Both methods can be very selective for a particular material, but at the same time they need

- small particle size (<10 mm),
- clean surfaces,
- controlled environment (wetting and froth agent, low air humidity).

If no disturbing factors are present in the waste stream (like certain plastic additives), pre- and post-treatment steps are taken, both technologies are feasible.

Application of direct sorting technologies resembles picking a problem for an existing solution. In contrast, sensor hardware and software can be tailored to the problem statement.

Sensor equipment has high modularity and sensor fusion is a powerful technique, practically unavailable in direct sorting. With proper feeding and routing technologies multi-fraction separation task can be done at once: either with single line conveying and a set of air nozzles for every component or a robot arm. Robot picking is an algorithmically more challenging problem and robots struggle to work with small items (below ~50mm), whereas air blowing may become energy consuming with large and heavy items. In laboratory scale, air blow jets arranged along or around a single line conveyor should be enough for most of the tasks.

HSI with optical sensors is in the lead in the industry, however, it got strong competitors from high-speed single point measuring equipment (LIBS, Raman and LIF spectroscopy) that outperform the former in the separation of dark materials. Raman and LIF spectroscopy, as

well as MWIR HSI camera, are better suited for analyzing organic materials, whereas X-ray and LIBS methods work better with substances containing heavy elements. THz spectral technology is still on the way to industrial implementation and it has a resolution limited by the wavelength. Thus, Raman spectroscopy is a favourable option for dark plastic sorting in a laboratory. A complementary IR or visible light camera is needed for machine vision.

Some low-cost sensor methods (thermal imaging, acoustic emission) were suggested that may work well for macrosorting of commingled waste into general categories. Macrosorting with sensors could help recycle bulk wood materials without crushing them down to chips.

4.2 New and borrowed ideas

Rating of the proposed ideas is shown in Table 5. Easiness of development refers to the current state of technology development (and the remaining development path) and risks if the proposed principle is not possible to implement in an economical way. The effect coordinate estimates how significantly (and broadly) proposed technology will influence recycling upon successful development. The clear winner is the electroadhesive routing: the technology is already commercialized, it just needs a suitable embodiment and control to make routing of waste fractions versatile, energy efficient and accurate. In several direct sorting devices division in sectors is used for multiple fraction output (recall Figures 15 and 23), but it is challenging to implement this with actuators, except the carousel arrangement presented in Figure 58. Simple basic principle (easy experimentation) and minimum moving parts (unlimited lifetime) make this idea a promising direction for research.

Table 5. Potential of proposed ideas

Criteria	Easy development	Difficult development
Strong effect	• electroadhesive routing	• low-cost MWIR HSI • NIR transmission imaging
Weak effect	• Coandă screen • new robotic grippers	• electrophotography principle • separation by Vicat hardness • separation by refractive index • separation in liquid air • thermoplastic foaming

Readily available technologies from other fields like Coandă screen and new robotic grippers

are easy to test and adapt, but their application scope will be limited. Further development of IR imaging may bring new sensors techniques, but the development is in early stage and positive results are not guaranteed. The bottom right quadrant of the table contains ideas with a high risk of failure in both development and application.

4.3 Pilot CDW separation line

The pilot separation line for CDW should start with a presorting stage: either crusher with pneumatic jigging or whole item separation by thermal imaging. Before separation by plastic type dry cleaning is needed, which, in turn, requires waste comminution down to flakes. Fine separation is better achieved with spectral analysis technologies, presumably Raman spectroscopy or MWIR HSI camera. An extra induction sensor or colour camera may help to control the flow and detect incompletely liberated particles.

Studies by Neto et al. (2017) and Vegas et al. (2015) suggest that optical sorters can be economically viable in the separation of aggregates from CDW, the increase in equipment cost does not play a huge role. Consequently, sensor-based sorting is reasonable for even higher value CDW fraction, such as plastics.

4.4 Tools review

Tools used in the present study were the creation of the technology database and extracting filtered facts from it as well as the creation of informative plots from them. The implemented algorithm for data storage and factualization proved its usefulness, although some contradictions have to be noted. Facts contained in the database are biased to a certain extent by:

- subjectivity in the selection of literature sources,
- better detail level of scientific publications rather than information from industry (this offsets particle size ranges to lower values, but separation rates – to higher values),
- limited resources for collection of information,
- some information is inevitably lost because of exclusion of observations that do not fit well in the database format.

Nevertheless, such processing helps to make generalized conclusions with a transparent reasoning. The database approach has an advantage against pure text review that it can be updated and expanded over time without starting the process all over again and therefore its

analytical power will grow steadily.

The database may get an improved interface for more intricate queries and better formatting of plots, although it is quite usable already (none of the plots from the database was specially edited before insertion in this report). A very broad scope of reviewed technologies has made it challenging to compute purity and recovery rates of the suggested separation line layout. In Jansen et al. (2015) publication it was suggested that collected information about state of the art equipment yield rates allows to plan MRF layouts, but the scope in that case was just sorting of plastic packaging waste.

Some important topics remained practically uncovered (and outside the scope), such as waste comminution and liberation, auxiliary equipment (cleaning, dewatering), feeding, routing and enriching technologies were presented with very few documented examples. The study indicates a considerable gap between academic and industrial knowledge: commercial solutions for sorting of black plastics were known since the year 2011 at least (Demingling the mix 2011), but little awareness is shown in academia working on the same problem.

Idea generation has succeeded along the following paths:

- found from effects: supercritical fluid density separation, Coandă screen;
- search across fields: low-cost HSI, NIR transmission imaging, electrostatics for routing;
- from material properties: Vicat hardness separation, refractive index separation;
- extension of existing methods: separation in liquid air, thermoplastics foaming.

The minority of them are feasible, but it is typical for invention search.

Lists of effects accompanying reviewed technologies indicate the presence of similar principles in different technologies like asymmetric vibrations, agitating fan. Although most of the physical effects are quite exotic for application in waste processing (acoustic tweezers, vortex ring) they give an insight into the level of science and technology and some may eventually get their use (superconducting magnets, Cheerio effect, Brazil nut effect).

5 CONCLUSION

Separation technologies become more and more selective as downcycling is less acceptable nowadays. Newer direct sorting techniques get capabilities for the fine tuning towards every range of materials properties. However, they come to their limit when a single material property is not sufficient for sorting into narrow material categories. Sensors become a viable alternative with improved speed, resolution, computational power and versatility, as a consequence. At the same time, gained experience in direct sorting methods can be used for more efficient material routing after sensor-based classification like it was proposed for electrostatics.

The multitude of technologies with similar classification capacity makes a systematic selection challenging. The proposed database approach allows to look at technologies as "black boxes" with some performance figures and features and make decisions based on that. However, an expert review of the detailed textual technology description is still necessary to get to the final conclusion after database screening has narrowed down the available options.

Results of this work will come to test by future research at LUT University. The collected information could be used for further situation-specific conclusions and decisions. With no doubts, waste separation techniques will develop and become more profitable and widespread. However, despite technological advancement in waste treatment, the best waste management is no waste at all. This is the strategy everybody can follow right now, being conscious about thrifty use of resources, regardless of their origin, primary or secondary.

REFERENCES

Abbasi, M., Salarirad, M.M. and Ghasemi, E., 2010. Selective separation of PVC from PET/PVC mixture using floatation by tannic acid depressant. Iranian Polymer Journal 19 (7), 2010, pp. 483-489.

Akhurst, M., Arbon, I., Ayres, M., Brandon, N., Bruges, R., Cooper, S., Ding, Y., Evison, T., Goode, N., Grünewald, P. and Heyes, A.L., 2013. Liquid Air in the energy and transport systems: Opportunities for industry and innovation in the UK. The Centre for Low Carbon Futures, published 09.05.2013, 134 p.

Allmineral pneumatic allair® jig 2019 [web document]. [Referred 20.02.2019]. Available: http://www.allmineral.com/fileadmin/user_upload/allmineral/pdf/product-factsheets-2019/allmineral_productinfo_allair_012019.pdf

Ambros, W.M., Sampaio, C.H., Cazacliu, B.G., Miltzarek, G.L. and Miranda, L.R., 2017. Usage of air jigging for multi-component separation of construction and demolition waste. Waste Management, 60, pp. 75-83.

AMP Robotics n.d. [web document]. [Referred 26.02.2019]. Available: https://www.amprobotics.com

Andersson, M., Söderman, M. & Sandén, B. 2017. Are scarce metals in cars functionally recycled? Waste Management, 60, pp. 407-416.

Ando, T., Hirota, N. and Maie, M., 2015. Development of recovery device for particulates in fluid by magneto-Archimedes separation. Separation and Purification Technology, 149, pp. 197-207.

Andritz. Setting Standards in Plastic Recycling, n.d. [web document]. [Referred 01.02.2019]. Available: https://www.andritz.com/resource/blob/13438/297b6952b75c42dd26e8b11e27b4c15b/se-censor-centrifuge-en-data.pdf

Anzano, J., Bonilla, B., Montull-Ibor, B. and Casas-González, J., 2011. Plastic identification and comparison by multivariate techniques with laser-induced breakdown spectroscopy. Journal of Applied Polymer Science, 121(5), pp. 2710-2716.

Apple Inc., 2018. Apple adds Earth Day donations to trade-in and recycling program. Press release [web document]. Published 19.04.2018. [Referred 19.09.2018]. Available: https://www.apple.com/newsroom/2018/04/apple-adds-earth-day-donations-to-trade-in-and-recycling-program/

Ashby, M.F. 2012. [Chapter 15:] Material Profiles. In: Ashby, M.F. Materials and the Environment (Second Edition). Boston: Butterworth-Heinemann. Pp. 459-595.

ASTM D1525-00, 2000. Standard Test Method for Vicat Softening Temperature of Plastics. West Conshohocken: ASTM International, West Conshohocken. 8 p.

Aulive Production Inspiration, 2019 [web document]. [Referred 01.02.2019]. Available: http://www.productioninspiration.com

Bain, M. 2017. Nike Is Investing in Robots That Use Static Electricity to Put Its Shoes Together [web document]. Quartz, 7 Sept. 2017. [Referred 15.02.2019]. Available: https://qz.com/1070240/nike-is-investing-in-grabits-robots-which-use-static-electricity-to-put-its-shoes-together/

Bauer, M., Lehner, M., Schwabl, D., Flachberger, H., Kranzinger, L., Pomberger, R. and Hofer, W., 2018. Sink–float density separation of post-consumer plastics for feedstock recycling. Journal of Material Cycles and Waste Management, pp. 1-11.

Beel, H. 2017. Sortierung von schwarzen Kunststoffen nach ihrer Polymerklasse mit Hyperspectral-Imaging-Technologie; Sorting of black plastics by polymer type with hyperspectral imaging technology. In: Thomé-Kozmiensky, K.J., Goldmann, D. eds. 2017. Recycling und Rohstoffe, Vol. 10. Neuruppin, Germany: TK Verlag Karl Thomé-Kozmiensky, pp. 175-192.

Berwanger, M., Gaastra, M., Köpcke, M., Warcholik, M., Knapp, H., Küch, C., Neubert, K., Fietz, N., Maul, A., Schropp, C., Raulf, K., Robben, M., Maul, A., Nagel, M., Hahn, M., Neumann, K. 2014. [Chapter 4:] Technical and physical principles of sensor technologies applied in the raw materials industry. In: Nienhaus, K., Pretz, T. and Wotruba, H. eds., 2014. Sensor technologies: impulses for the raw materials industry. Aachen: Shaker Verlag. Pp. 47-199.

Binder+Co Clarity Glass n.d. CLARITY – the innovative sorting system from Binder+Co [web document]. [Referred 26.02.2019]. Available: https://www.binder-co.com/955/CLARITY-glass

Binder+Co n.d. Clarity Multiway revolutionary recycling and sorting system [web document]. [Referred 26.02.2019]. Available: https://www.binder-co.com/App_Upload/User/en/products/downloads/Binder+Co_CLARITY_Multiway%20Sorter_EN.pdf

Bollegraaf Recycling Solutions, n.d. [web document]. [Referred 01.02.2019]. Available: https://www.bollegraaf.com/technologies/shredders

Bradley, P.E. and Radebaugh, R., 2013. Properties of Selected Materials at Cryogenic Temperatures (No. CRC Handbook of Chemistry and Physics).

Brandt, C., Kieninger, M., Negara, C., Gruna, R., Längle, T., Küter, A. and Nüßler, D., 2016. Sorting of black plastics using statistical pattern recognition on terahertz frequency domain data. 7th Sensor-Based Sorting & Control 2016.

Brighton & Hove City Council n.d. Reduce Reuse Recycle Useful Links [web document]. [Referred 15.01.2019]. Available: https://www.brighton-hove.gov.uk/content/environment/recycling-rubbish-and-street-cleaning/reduce-reuse-recycle-useful-links

Carvalho, M.T., Agante, E. and Durão, F., 2007. Recovery of PET from packaging plastics mixtures by wet shaking table. Waste Management, 27(12), pp. 1747-1754.

Cassidy, A., Grant, M. and Provatas, N., 2003. Modelling dielectric heterogeneity in electrophotography. Modelling and Simulation in Materials Science and Engineering, 12(1), pp. 91-107.

Catherall, A.T., Lopez-Alcaraz, P., Benedict, K.A., King, P.J. and Eaves, L., 2005. Cryogenically enhanced magneto-Archimedes levitation. New Journal of Physics, 7(1), art. no. 118.

Chang, K.S.P. and Myers, B.A., 2016. Using and exploring hierarchical data in spreadsheets. In Proceedings of the 2016 CHI Conference on Human Factors in Computing Systems (pp. 2497-2507). ACM.

Chang, N.B. and Pires, A., 2015. [Chapter 2:] Technology MAtrix for Solid Waste Management. In: Chang, N.B. and Pires, A. Sustainable solid waste management: a systems engineering approach. Hoboken: John Wiley & Sons. Pp. 19-97.

Coates, G. and Rahimifard, Sh., 2009. Modelling of post-fragmentation waste stream processing within UK shredder facilities. Waste Management, 29(1), pp. 44-53.

Code Beautify JSON Viewer, n.d. [web document]. [Referred 01.02.2019]. Available: https://codebeautify.org/jsonviewer

Color Sorter Group Industrial color sorter products n.d. [web document]. [Referred 26.02.2019]. Available: http://www.colorsortergroup.com/Products/Industrial-Color-Sorter-Optical-Sorting-Machine.html

Craven, J.M., 2014. Energy Efficient Solids Feed System for High Pressure Processes (Doctoral dissertation, University of Sheffield).

Crockford, D. and Carter, Z., 2018. JSONLint – The JSON Validator [web document]. [Referred 01.02.2019]. Available: https://jsonlint.com

Dahmus, J. B. and Gutowski T. G., 2006. Material Recycling at Product End-of-Life. Electronics and the Environment, 2006. Proceedings of the 2006 IEEE International Symposium, 2006, pp. 206-211.

Demingling the mix: An assessment of commercially available automated sorting technology, Second Edition 2011 [web document]. January 2011 [Referred 25.02.2019]. 4R Sustainability, Inc. 25 p. Available in PDF-file: https://plastics.americanchemistry.com/Assessment-of-Commercially-Available-Automated-Sorting-Technology/

Dholu, N., Nagel, J.R., Cohrs, D. and Rajamani, R.K., 2017. Eddy current separation of nonferrous metals using a variable-frequency electromagnet. KONA Powder and Particle Journal, 34, pp. 241-247.

Diamond, G., 2008. A low cost alternative to terahertz imaging for security and defense applications. SPIE Newsroom.

Dini, G., Fantoni, G. and Failli, F., 2009. Grasping leather plies by Bernoulli grippers. Cirp Annals, 58(1), pp. 21-24.

Dobrovszky, K. and Ronkay, F., 2014. Alternative polymer separation technology by centrifugal force in a melted state. Waste Management, 34(11), pp. 2104-2112.

Dodbiba, G., Sadaki, J., Okaya, K., Shibayama, A. and Fujita, T., 2005. The use of air tabling and triboelectric separation for separating a mixture of three plastics. Minerals Engineering, 18(15), pp. 1350-1360.

Duan, C., Sheng, C., Wu, L., Zhao, Y., He, J. and Zhou, E., 2014. Separation and recovery of fine particles from waste circuit boards using an inflatable tapered diameter separation bed. The Scientific World Journal, 2014.

Dully, S. 2011. Internetbasiertes Technologie-Scouting für Recyclingtechnologien; Internet-based technology scouting for recycling technologies. Doctoral dissertation. Heimsheim, Germany: Jost-Jetter Verlag 2011. [Referred 18.02.2019]. Available: http://dx.doi.org/10.18419/opus-4445

Eriez Magnetics, 2019. Eriez Lab Equipment, Electrostatic Separators [web document]. [Referred 25.02.2019]. Available: https://www.eriezlabequipment.com/lab-equipment/electrostatic-separators/

Fantoni, G., Santochi, M., Dini, G., Tracht, K., Scholz-Reiter, B., Fleischer, J., Lien, T.K., Seliger, G., Reinhart, G., Franke, J. and Hansen, H.N., 2014. Grasping devices and methods in automated production processes. CIRP Annals-Manufacturing Technology, 63(2), pp. 679-701.

Fekir, D.E., Miloudi, M., Miloua, F., Medles, K. and Dascalescu, L., 2017. New Propeller-Type Tribocharging Device With Application to the Electrostatic Separation of Granular Insulating Materials. IEEE Transactions on Industry Applications, 53(3), pp. 2416-2422.

Festo Bernoulli grippers OGGB, n.d. [web document]. [Referred 01.02.2019]. Available: https://www.festo.com/cat/en-gb_gb/data/doc_ENUS/PDF/US/OGGB_ENUS.PDF

Festo FlexShapeGripper, n.d. [web document]. [Referred 01.02.2019]. Available: https://www.festo.com/PDF_Flip/corp/Festo_FlexShapeGripper/en/files/assets/common/downloads/Festo_FlexShapeGripper_en.pdf

Festo Valves, n.d. [web document]. [Referred 01.02.2019]. Available: https://www.festo.com/net/SupportPortal/Files/17267

FIPA Needle Grippers, n.d. [web document]. [Referred 01.02.2019]. Available: https://www.fipa.com/en_GB/media/3298036/1025-BDS_FIPA-GR04.711-Nadelgreifer_en_Master.pdf?download&amp

Fitzpatrick, R.S., Glass, H.J. and Pascoe, R.D., 2015. CFD–DEM modelling of particle ejection by a sensor-based automated Sorter. Minerals Engineering, 79, pp. 176-184.

FLIR BOSON 320 Thermal Imaging Lensless Core, n.d. [web document]. [Referred 19.02.2019]. Available: https://www.oemcameras.com/flir-boson-320x256-no-lens.htm

Fridrich, D. and Urban, J., 2018. Hierarchical dynamic containers for fusion data. Fusion Engineering and Design, 129, p. 68.

Gent, M.R., Menéndez, M., Muñiz, H. and Torno, S., 2015. Recycling of a fine, heavy fluff automobile shredder residue by density and differential fragmentation. Waste Management, 43, pp. 421-433.

Gent, M.R., Menéndez, M., Toraño, J. and Torno, S., 2009, October. Enhanced plastics recycling by cyclone media separation. In ISWA APESB World Congress, Lisbon, Portugal (p. 10).

Goudsmit Magnetic Systems Eddy Current Separators, n.d. [web document]. [Referred 01.02.2019]. Available: https://www.goudsmitmagnets.com/data/repository/documents/Brochure_Eddy_current_non_ferrous_separator_EN.pdf

Goudsmit Magnetic Separators for Recycling, n.d. [web document]. [Referred 01.02.2019]. Available: https://www.goudsmitmagnets.com/data/repository/documents/Brochure_Recycling_EN.pdf

Gundupalli, S. P., Hait, S. and Thakur, A. 2017a. A review on automated sorting of source-separated municipal solid waste for recycling. Waste Management, 60(C), pp. 56-74.

Gundupalli, S.P., Hait, S. and Thakur, A., 2017b. Multi-material classification of dry recyclables from municipal solid waste based on thermal imaging. Waste Management, 70, pp. 13-21.

Gundupalli, S.P., Hait, S. and Thakur, A., 2018. Classification of metallic and non-metallic fractions of e-waste using thermal imaging-based technique. Process Safety and Environmental Protection, 118, pp. 32-39.

Guo, J., Li, X., Guo, Y., Ruan, J., Qiao, Q., Zhang, J., Bi, Y. and Li, F., 2016. Research on Flotation Technique of separating PET from plastic packaging wastes. Procedia Environmental Sciences, 31, pp. 178-184.

Hamos EKS Plastic/Plastic Separators n.d. [web document]. [Referred 01.02.2019]. Available: https://www.hamos.com/infocenter/brochure.html#hamos/6

He, Y., Duan, C., Wang, H., Zhao, Y. and Tao, D., 2011. Separation of metal laden waste using pulsating air dry material separator. International Journal of Environmental Science & Technology, 8(1), pp. 73-82.

Hellemans, A., 2013. Sorting plastic waste: a magnetic game [web document]. Published 13.06.2013 [Referred 24.02.2019]. Available: http://www.youris.com/environment/recycling/sorting_plastic_waste_a_magnetic_game.kl

Herbold Meckesheim – Washing lines for washing, separating, drying n.d. [web document]. [Referred 01.02.2019]. Available: https://www.herbold.com/en/machines/washing-separating-drying-2/

Huang, J., Tian, C., Ren, J. and Bian, Z., 2017. Study on impact acoustic—Visual sensor-based sorting of ELV plastic materials. Sensors, 17(6), art. no. 1325.

Huang, J., Zhu, Z., Tian, C. and Bian, Z., 2018. Feasibility Study on S-Band Microwave Radiation and 3D-Thermal Infrared Imaging Sensor-Aided Recognition of Polymer Materials from End-of-Life Vehicles. Sensors, 18(5), art. no.1355.

HUBER Coanda Grit Classifier RoSF3 n.d. [web document]. [Referred 28.02.2019]. Available: https://www.huber-technology.com/products/grit-separation-and-treatment/grit-classifiers/huber-coanda-grit-classifier-rosf3.html

Huerta, D.A., Sosa, V., Vargas, M.C. and Ruiz-Suárez, J.C., 2005. Archimedes' principle in fluidized granular systems. Physical Review E, 72(3), p.031307.

Introducing JSON. ECMA-404 The JSON Data Interchange Standard, 2017 [web document]. [Referred 01.02.2019]. Available: https://www.json.org

Ip, K., Testa, M., Raymond, A., Graves, S. & Gutowski, T. 2018. Performance evaluation of material separation in a material recovery facility using a network flow model. Resources, Conservation & Recycling, 131, pp. 192-205.

Ito, M., Tsunekawa, M., Ishida, E., Kawai, K., Takahashi, T., Abe, N. and Hiroyoshi, N., 2010. Reverse jig separation of shredded floating plastics—separation of polypropylene and high density polyethylene. International Journal of Mineral Processing, 97(1-4), pp. 96-99.

Jansen, M., van Velzen, E.T. and Pretz, T., 2015. Handbook for sorting of plastic packaging waste concentrates: separation efficiencies of common plastic packaging objects in widely used separaion machines at existing sorting facilities with mixed postconsumer plastic packaging waste as input (No. 1604). Wageningen UR-Food & Biobased Research. 30 p.

Julia in a nutshell, n.d. [web document]. [Referred 01.02.2019]. Available: https://julialang.org

Jupyter Project, 2019 [web document]. [Referred 01.02.2019]. Available: https://jupyter.org

Karmana, E., Eiler, B., Mainiero, D., Bedner, M. and Enick, R., 1997. The microsortation of high loadings of post-consumer mixed polyolefins using liquid carbon dioxide in a slightly agitated, batch apparatus. Resources, conservation and recycling, 20(3), pp. 143-152.

Keinänen, M. 2019. Information to my thesis [private e-mail]. Sender: Markku Keinänen, professor of biological and biomedical imaging in University of Eastern Finland. Receiver: Luka Ivanovskis. Sent 26.02.2019.

Kilgus, J., Zimmerleiter, R., Duswald, K., Hinterleitner, F., Langer, G. and Brandstetter, M., 2018. Application of a Novel Low-Cost Hyperspectral Imaging Setup Operating in the Mid-Infrared Region. In Multidisciplinary Digital Publishing Institute Proceedings (Vol. 2, No. 13, p. 800).

Kim, E. and Choi, W.Z., 2019. Real-time identification of plastics by types using laser-induced breakdown spectroscopy. Journal of Material Cycles and Waste Management, 21(1), pp. 176-180.

Kinoshita, T., Okamoto, K., Yamaguchi, K. and Akita, S., 2006. Separation of plastic mixtures using liquid-fluidized bed technology. Chemosphere, 63(6), pp. 893-902.

Korucu, M.K., Kaplan, Ö., Büyük, O. and Güllü, M.K., 2016. An investigation of the usability of sound recognition for source separation of packaging wastes in reverse vending machines. Waste Management, 56, pp. 46-52.

Koyanaka, S. and Kobayashi, K., 2010. Automatic sorting of lightweight metal scrap by sensing apparent density and three-dimensional shape. Resources, Conservation and Recycling, 54(9), pp. 571-578.

Koyanaka, S. and Kobayashi, K., 2011. Incorporation of neural network analysis into a technique for automatically sorting lightweight metal scrap generated by ELV shredder facilities. Resources, Conservation and Recycling, 55(5), pp. 515-523.

Kujala, J.V., Lukka, T.J. and Holopainen, H., 2015. Picking a conveyor clean by an autonomously learning robot. arXiv preprint arXiv:1511.07608.

Kutila, M., Viitanen, J. and Vattulainen, A., 2005, November. Scrap metal sorting with colour vision and inductive sensor array. In International Conference on Computational Intelligence for Modelling, Control and Automation and International Conference on Intelligent Agents, Web Technologies and Internet Commerce (CIMCA-IAWTIC'06), Vol. 2, pp. 725-729.

Lahtela, V., Hyvärinen, M. and Kärki, T., 2019. Composition of Plastic Fractions in Waste Streams: Toward More Efficient Recycling and Utilization. Polymers, 11(1), art. no. 69.

Landefeld Festo MHJ9-QS-4-MF Solenoid valve, n.d. [web document]. [Referred 01.02.2019]. Available: https://www.landefeld.com/artikel/en/mhj9-qs-4-mf-553118-solenoid-valve/OT-FESTO028001

Li, J., Gao, K. and Xu, Z., 2017. Charge-decay electrostatic separation for removing Polyvinyl chloride from mixed plastic wastes. Journal of Cleaner Production, 157, pp. 148-154.

Lien, T.K. and Davis, P.G.G., 2008. A novel gripper for limp materials based on lateral Coanda ejectors. CIRP annals, 57(1), pp. 33-36.

Liikanen, M., Helppi, O., Havukainen, J. and Horttanainen, M., 2018. Rakennusjätteen koostumustutkimus–Etelä-Karjala. LUT Scientific and Expertise Publications/Tutkimusraportit–Research Reports 82.

Lin, G.G., Lin, D.J., Wang, L.J. and Kuo, T.W., 2014. Absorption and foaming of plastics using carbon dioxide. Research on Chemical Intermediates, 40(6), pp. 2259-2268.

Lee, B.W. and Orr, D.E., 2009. The TriboElectric Series [web document]. AlphaLab, Inc. [Referred 25.02.2019]. Available: https://www.alphalabinc.com/triboelectric-series/

Lungu, M., 2005. Separation of small nonferrous particles using an angular rotary drum eddy-current separator with permanent magnets. International Journal of Mineral Processing, 78(1), pp. 22-30.

Lungu, M. and Neculae, A., 2018. Eddy current separation of small nonferrous particles using a complementary air-water method. Separation Science and Technology, 53(1), pp. 126-135.

Lungu, M. and Rem, P., 2002. Separation of small nonferrous particles using an inclined drum eddy-current separator with permanent magnets. IEEE Transactions on magnetics, 38(3), pp. 1534-1538.

Lupo, E., Moroni, M., La Marca, F., Fulco, S. and Pinzi, V., 2016. Investigation on an innovative technology for wet separation of plastic wastes. Waste management, 51, pp. 3-12.

Mallampati, S.R., Heo, J.H. and Park, M.H., 2016. Hybrid selective surface hydrophilization and froth flotation separation of hazardous chlorinated plastics from E-waste with novel nanoscale metallic calcium composite. Journal of Hazardous Materials, 306, pp. 13-23.

Manida, S.N., 2001. Archimede's law for accelerating bodies. Zakon Arhimeda dlya uskorenno dvizhushihsya t'el. Imperia matematiki. Mezhdunarodny fiziko-matematichesky zhurnal dlya yunoshestva, 2001(2), pp. 18-26.

Máša, V. and Kuba, P., 2016. Efficient use of compressed air for dry ice blasting. Journal of Cleaner Production, 111, pp. 76-84.

Matmatch – Find Materials & Suppliers n.d. [web document]. [Referred 30.09.2019]. Available: https://matmatch.com/

Mauruschat, D., Plinke, B., Aderhold, J., Gunschera, J., Meinlschmidt, P. and Salthammer, T., 2016. Application of near-infrared spectroscopy for the fast detection and sorting of wood–plastic composites and waste wood treated with wood preservatives. Wood Science and Technology, 50(2), pp. 313-331.

May, D., 2015. Sediment Exclusion from Water Systems Using a Coanda Effect Device. International Journal of Hydraulic Engineering, 4(2), pp. 23-30.

MBA Polymers 1998. Development of Hydrocyclones for Use in Plastics Recycling. American Plastics Council, Inc. 42 p.

Mellor, W., Wright, E., Clift, R., Azapagic, A. & Stevens, G. 2002. A mathematical model and decision-support framework for material recovery, recycling and cascaded use. Chemical Engineering Science, 57(22), pp. 4697-4713.

Meyer, J., Fey, D. and Krieg, S. 2017. Kunststoff-Sortierung aus Schredderrückständen mit Hochleistungs-Laserspektroskopie; Plastic sorting from shredder residues with high-performance laser spectroscopy. In: Thomé-Kozmiensky, K.J., Goldmann, D. eds. 2017. Recycling und Rohstoffe, Vol. 10. Neuruppin, Germany: TK Verlag Karl Thomé-Kozmiensky, pp. 193-198.

Negari, M.S., Movahed, S.O. and Ahmadpour, A., 2018. Separation of polyvinylchloride (PVC), polystyrene (PS) and polyethylene terephthalate (PET) granules using various chemical agents by flotation technique. Separation and Purification Technology, 194, pp. 368-376.

Neto, R.O., Gastineau, P., Cazacliu, B.G., Le Guen, L., Paranhos, R.S. and Petter, C.O., 2017. An economic analysis of the processing technologies in CDW recycling platforms. Waste Management, 60, pp. 277-289.

Oxford Creativity TRIZ Effects Database, n.d. [web document]. [Referred 01.02.2019]. Available: https://www.triz.co.uk/how/triz-effects-database

PacNext 2014. Top 10 Packaging Challenges for Recycling in a Material Recovery Facility [web document]. [Referred 07.09.2018]. Available: http://www.pac.ca/assets/pac-next_top10mrf-finalcompressed.pdf

Pascoe, R.D., Fitzpatrick, R. and Garratt, J.R., 2015. Prediction of automated sorter performance utilising a Monte Carlo simulation of feed characteristics. Minerals Engineering, 72, pp. 101-107.

Pascoe, R.D. and O'Connell, B., 2003. Flame treatment for the selective wetting and separation of PVC and PET. Waste Management, 23(9), pp. 845-850.

Pat. EP 1291092. 2003. Verfahren und Maschine zum Aussondern der Pappanteile aus einem Altpapier-Gemenge. Process and machine to separate cardboard from paper waste. Appl. 02017176.5, 2002-07-31. Publ. 2003-03-12.

Pat. EP 1970130. 2008. Apparatus and method for separating plastic film from waste. Machinefabriek Bollegraaf Appingedam B. V. (Legtenberg, H.J.). Appl. 08152839.0, 2008-03-17. Publ. 2008-09-17. 11 p.

Pat. EP 2679310. Method and apparatus for separation of mixture. Ube Industries, Ltd., Osaka University (Nishijima, S. and Mishima, F.). Appl. 12749423.5, 2012-02-21. Publ. 2014-01-01. 32 p.

Pat. US 2013/0294875. 2013. Electroadhesive conveying surfaces. SRI International (Prahlad, H., Pelrine, R.E., McCoy, B.K. and Low, T.P.). Appl. 13/886052, 2013-05-02. Publ. 2013-11-07. 31 p.

Pat. US 2017/0259305. 2017. Sorting installation and method for separatnig material fractions. Unisensor Sensorsyteme GmbH (Bohleber, J. and Schmidt, A.). Appl. 15/504907, 2015-08-19. Publ. 2017-02-17. 11 p.

Pat. US 5462973. 1995. Separation of polyethylene terephtalate and polyvinyl chloride using supercritical carbon dioxide. Hoechst Celanese Corporation (Serad, G.A. and Thornburg, T.S.). Appl. 274508, 1994-07-13. Publ. 1995-10-31. 4 p.

Pat. US 6335376. 2002. Apparatus and method for enhancing partitioning of different polymeric materials from a mixture by density differential alteration. MBA Polymers, Inc. (Allen., L. E. and Arola, D.F.) Appl. 09/320190, 1999-05-26. Publ. 2002-01-01. 18 p.

Pat. WO 01/64359. 2001. Separating device for solid particles. Technische Universiteit Delft

(de Jong, T., Kattentidt, H. and Schokker, E.). Appl. PCT/NL01/00118, 2001-02-12. Publ. 2001-09-07. 14 p.

Peeters, J.R., Vanegas, P., Tange, L., Van Houwelingen, J. and Duflou, J.R., 2014. Closed loop recycling of plastics containing Flame Retardants. Resources, Conservation and Recycling, 84, pp. 35-43.

Pellenc ST Xpert – the XRT sorting machine for metals and ELVs n.d. [web document]. [Referred 01.02.2019]. Available: http://www.pellencst.com/wp-content/uploads/PellencST_Xpert_ENG_WEB_1-2.pdf

Petterson, A., Ohlsson, T., Caldwell, D.G., Davis, S., Gray, J.O. and Dodd, T.J., 2010. A Bernoulli principle gripper for handling of planar and 3D (food) products. Industrial Robot: An International Journal, 37(6), pp. 518-526.

Picón, A., Bereciartua, A., Echazarra, J., Ghita, O., Whelan, P.F. and Iriondo, P.M., 2012. Real-time hyperspectral processing for automatic nonferrous material sorting. Journal of Electronic Imaging, 21(1), art. no. 013018.

Picvisa Machine Vision Systems Products n.d. [web document]. [Referred 26.02.2019]. Available: http://picvisa.com/en/pc/21-productos

Pieper, C., Pfaff, F., Maier, G., Kruggel-Emden, H., Wirtz, S., Noack, B., Gruna, R., Scherer, V., Hanebeck, U.D., Längle, T. and Beyerer, J., 2018. Numerical modelling of an optical belt sorter using a DEM–CFD approach coupled with particle tracking and comparison with experiments. Powder Technology, 340, pp. 181-193.

Pla.to Technology Dry cleaning 2018 [web document]. [Referred 20.02.2019]. Available: https://www.plato-technology.de/fileadmin/user_upload/PDF/Pla.to_Dry_Cleaning_EN_2018.pdf

Polyanskiy, M.N., n.d. Refractive index database [web database]. [Referred 09.01.2019]. Available: https://refractiveindex.info

Powder Systems Co., Ltd. Small Classifier Laboratory Use HPC-ZERO [web document]. [Referred 28.02.2019]. Available: https://www.powder.co.jp/EN/products/02/

Pretz, T. and Julius, J., 2008. Stand der Technik und Entwicklung bei der berührungslosen Sortierung von Abfällen; State of technology and development for contactless sorting of waste. Österreichische Wasser-und Abfallwirtschaft, 60(7-8), pp. 105-112.

Ragaert, K., Delva, L. and Geem K. V. 2017. Mechanical and chemical recycling of solid plastic waste. Waste Management, 69, pp. 24-58.

Ramasubramanian, M.K., Venditti, R.A., Ammineni, C. and Mallapragada, V., 2005. Optical sensor for noncontact measurement of lignin content in high-speed moving paper surfaces. IEEE Sensors Journal, 5(5), pp. 1132-1139.

Ramasubramanian, M.K., Venditti, R.A. and Gillella, P.K., 2012. Sensor systems for high speed intelligent sorting of waste paper in recycling. TAPPI J, 11(2), pp. 33-39.

Reinsch, E., Frey, A., Albrecht, V., Simon, F. and Peuker, U.A., 2014. Die Anwendung der Elektrosortierung beim Recycling von Kunststoffen; Application of electrosorting for recycling of plastics. Chemie Ingenieur Technik, 6(86), pp. 784-796.

Reuter, M.A. and Kojo, I.V., 2012. Challenges of metals recycling. Materia, 2(2012), pp. 50-57.

Roh, S.B., Oh, S.K., Park, E.K. and Choi, W.Z., 2017. Identification of black plastics realized with the aid of Raman spectroscopy and fuzzy radial basis function neural networks classifier. Journal of Material Cycles and Waste Management, 19(3), pp. 1093-1105.

Roh, S.B., Park, S.B., Oh, S.K., Park, E.K. and Choi, W.Z., 2018. Development of intelligent sorting system realized with the aid of laser-induced breakdown spectroscopy and hybrid preprocessing algorithm-based radial basis function neural networks for recycling black plastic wastes. Journal of Material Cycles and Waste Management, pp. 1-16.

Salama, A., Richard, G., Medles, K., Zeghloul, T. and Dascalescu, L., 2018. Distinct recovery of copper and aluminum from waste electric wires using a roll-type electrostatic separator. Waste Management, 76, pp. 207-216.

Saman, G. and Hancock, E., 2011, September. Refractive index estimation using photometric stereo. In 2011 18th IEEE International Conference on Image Processing, pp. 1925-1928.

Sekito, T., Matsuto, T. and Tanaka, N., 2006. Application of a gas–solid fluidized bed separator for shredded municipal bulky solid waste separation. Waste management, 26(12), pp. 1422-1429.

Seliger, G., Stephan, J. and Lange, S., 2000. Non-rigid part handling by new gripping device. In Proc 8th Intl Conf Manuf Eng, ICME2000, Sydney, Australia (pp. 423-427).

Senni, L., Burrascano, P. and Ricci, M., 2016. Multispectral laser imaging for advanced food analysis. Infrared Physics & Technology, 77, pp. 179-192.

Shapiro, M. and Galperin, V., 2005. Air classification of solid particles: a review. Chemical Engineering and Processing: Process Intensification, 44(2), pp. 279-285.

Sigernes, F., Syrjäsuo, M., Storvold, R., Fortuna, J., Grøtte, M.E. and Johansen, T.A., 2018. Do it yourself hyperspectral imager for handheld to airborne operations. Optics express, 26(5), pp. 6021-6035.

Silveira, A.V.M., Cella, M., Tanabe, E.H. and Bertuol, D.A., 2018. Application of tribo-electrostatic separation in the recycling of plastic wastes. Process Safety and Environmental Protection, 114, pp. 219-228.

Singh, N., Hui, D., Singh, R., Ahuja, I. P. S., Feo, L. and Fraternali, F., 2017. Recycling of plastic solid waste: A state of art review and future applications. Composites Part B, 115(C), pp. 409-422.

Solo-Gabriele, H.M., Townsend, T.G., Hahn, D.W., Moskal, T.M., Hosein, N., Jambeck, J. and Jacobi, G., 2004. Evaluation of XRF and LIBS technologies for on-line sorting of CCA-treated wood waste. Waste Management, 24(4), pp.413-424.

Sowerby, B. and Tickner, J., 2005. Scanner for the detection of contraband in air cargo containers. The Physicist"Australian Institute of Physics, 42(10).

Stadtschnitzer, A. and Flachberger, H., 2008. Beitrag zur Auswahl von Verfahren der Dichtesortierung. Contribution to selection of density sorting processes. BHM Berg-und Hüttenmännische Monatshefte, 153(6), pp. 211-216.

Steinert starts operation of the first industrial LIBS system for separating aluminium scrap alloys 2018 [web document]. Published 09.06.2018. [Refferred 26.02.2019]. Available:

https://steinertglobal.com/news-events/news-in-detail/news/steinert-starts-operation-of-the-first-industrial-libs-system-for-separating-aluminium-scrap-alloys/

STEINERT Global 2018. Discover STEINERT LSS for Sorting Aluminium Alloys. YouTube, 2 Oct. 2018. Available: https://www.youtube.com/watch?v=aH-DBFUVhdQ

Steinert XSS T X-Ray Sorting System n.d. [web document]. [Referred 01.02.2019]. Available: https://steinertglobal.com/fileadmin/user_upload/_steinert/_downloads/_magnete-sensorsortierer/_sensorsortierung/XXS_T/STE_XSS_T_EN.pdf

StellarNet US Online Quotation Generator n.d. [web document]. StellarNet, Inc. [Referred 28.02.2019]. Available: https://www.stellarnet.us/online-quotation-generator/

Super, M.S., Enick, R.M. and Beckman, E.J., 1993. Density-based separation of thermoplastics found in the post-consumer waste stream. Resources, Conservation and Recycling, 9(1-2), pp. 75-88.

Takezawa, T., Uemoto, M. and Itoh, K., 2015. Combination of X-ray transmission and eddy-current testing for the closed-loop recycling of aluminum alloys. Journal of Material Cycles and Waste Management, 17(1), pp. 84-90.

TeraSense n.d. Terahertz Equipment for THz Imaging [web document]. [Referred 15.01.2019]. Available: http://terasense.com

Teqmine, n.d. [Teqmine webpage]. [Referred 01.02.2019]. Available: https://teqmine.com

Thanh Truc, N.T. and Lee, B.K., 2016. Sustainable and selective separation of PVC and ABS from a WEEE plastic mixture using microwave and/or mild-heat treatment with froth flotation. Environmental science & technology, 50(19), pp. 10580-10587.

Thorlabs – Optical elements, n.d. [Thorlabs webpage]. [Referred 01.02.2019]. Available: https://www.thorlabs.com/navigation.cfm?guide_id=7

Tominaga, S. and Tanaka, N., 2003. Refractive index estimation and color image rendering. Pattern Recognition Letters, 24(11), pp. 1703-1713.

Tsuchida, A., Kawazumi, H., Kazuyoshi, A. and Yasuo, T., 2009, October. Identification of shredded plastics in milliseconds using Raman spectroscopy for recycling. In IEEE SENSORS, 2009, pp. 1473-1476.

Tsunekawa, M., Hori, K., Hiroyoshi, N. and Ito, M., 2005a. Technological Developments in Wet Gravity Separation Processes. Mining and Materials Processing Institute of Japan, 121(10/11), pp.467-473.

Tsunekawa, M., Naoi, B., Ogawa, S., Hori, K., Hiroyoshi, N., Ito, M. and Hirajima, T., 2005b. Jig separation of plastics from scrapped copy machines. International Journal of Mineral Processing, 76(1-2), pp. 67-74.

Ueda, Y., Mishima, F., Akiyama, Y. and Nishijima, S., 2014. Fundamental Study of Plastic Separation Utilizing Magnetic Force. IEEE Transactions on Applied Superconductivity, 24(3), pp. 1-5.

van Kooy, L., Mooij, M. and Rem, P., 2004. Kinetic gravity separation. Physical Separation in Science and Engineering, 13(1), pp.25-32.

van Schaik, A. & Reuter, M. A. 2010. Dynamic modelling of E-waste recycling system performance based on product design. Minerals Engineering, 23(3), pp. 192-210.

Vegas, I., Broos, K., Nielsen, P., Lambertz, O. and Lisbona, A., 2015. Upgrading the quality of mixed recycled aggregates from construction and demolition waste by using near-infrared sorting technology. Construction and Building Materials, 75, pp. 121-128.

Visar Sorting 2016. Optical Sorter Visar Sortop Potatoes EN. YouTube, 5 July 2016. Available: https://www.youtube.com/watch?v=zYimxuEAEtk

Visar Sortop 2016. Potatoes Optical Sorter [web document]. [Referred 20.11.2018]. Available: http://www.visar-europe.com/visar-sorting/images/stories/Prospectus/Prospectus_Potatoes_janv_2016_EN.pdf

Vrancken, C., Longhurst, P. J. & Wagland, S. T. 2017. Critical review of real-time methods for solid waste characterisation: Informing material recovery and fuel production. Waste Management, 61, pp. 40-57.

Wang, C., Liu, J., Chen, Y., Liu, H. and Wang, Y., 2018a. Towards In-baggage Suspicious Object Detection Using Commodity WiFi. In 2018 IEEE Conference on Communications and Network Security (CNS), pp. 1-9.

Wang, D., Ma, X., Zhi, X. and Zhang, S., 2013. Research review of scrap metals eddy current separation technology. Sensors & Transducers, 158(11), pp. 242-248.

Wang, C.Q., Wang, H., Wu, B.X. and Liu, Q., 2014. Boiling treatment of ABS and PS plastics for flotation separation. Waste Management, 34(7), pp. 1206-1210.

Wang, C.Q., Wang, H., Fu, J.G. and Liu, Y.N., 2015. Flotation separation of waste plastics for recycling—A review. Waste Management, 41, pp. 28-38.

Wang, C.Q., Wang, H. and Huang, L.L., 2017. A novel process for separation of polycarbonate, polyvinyl chloride and polymethyl methacrylate waste plastics by froth flotation. Waste Management, 65, pp. 3-10.

Wang, H., Wang, J., Zou, Q., Liu, W., Wang, C. and Huang, W., 2018b. Surface treatment using potassium ferrate for separation of polycarbonate and polystyrene waste plastics by froth flotation. Applied Surface Science, 448, pp.219-229.

Wang, J., Xiong, J., Chen, X., Jiang, H., Balan, R.K. and Fang, D., 2017, October. TagScan: Simultaneous target imaging and material identification with commodity RFID devices. In Proceedings of the 23rd Annual International Conference on Mobile Computing and Networking (pp. 288-300). ACM.

Wolf, M. I., Colledani, M., Gershwin, S. B. & Gutowski, T. 2010. Modeling and design of multi-stage separation systems. Sustainable Systems and Technology (ISSST), 2010 IEEE International Symposium on, pp. 1-6.

WRAP 2009. Separation of mixed WEEE plastics final report (WRAP Project MDD018 and MDD023) [web document]. [Referred 07.09.2018]. Available: http://www.wrap.org.uk/sites/files/wrap/Separation%20of%20mixed%20WEEE%20plastics%20-%20Final%20report.pdf

WRAP 2010. Good practice of Near Infrared sorting of plastic packaging (WRAP Project MDP033) [web document]. [Referred 16.10.2018]. Available: http://www.wrap.org.uk

Wyhof, J., 1997. Page Yield of Printer Cartridges. System Support Series 112. [Referred 18.02.2019]. Available: https://arbikas.com/pub/media/storage/articles/SSS112TECHPageYield.pdf

Xia, D. and Zhang, F.S., 2018. A novel dry cleaning system for contaminated waste plastic purification in gas-solid media. Journal of Cleaner Production, 171, pp. 1472-1480.

Yang, B., Yan, C., Zhang, J. and Zhang, H., 2016. Refractive index and surface roughness estimation using passive multispectral and multiangular polarimetric measurements. Optics Communications, 381, pp. 336-345.

Yu, H., 2014. Metal Recovery via Automated Sortation. Doctoral dissertation. Worcester Polytechnic Institute. [Referred 18.02.2019]. Available: https://web.wpi.edu/Pubs/ETD/Available/etd-041714-211407/unrestricted/HaoYu.pdf

Zhang, H. and Chen, M., 2017. Triboelectrostatic separation for PP and ABS plastics in end of life passenger vehicles. Journal of Material Cycles and Waste Management, 19(2), pp. 884-897.

Zhou, C., Pan, Y., Lu, M. and Yang, C., 2016. Liberation characteristics after cryogenic modification and air table separation of discarded printed circuit boards. Journal of Hazardous Materials, 311, pp. 203-209.

DATA PARSER

dataparser.jl code listing

```
using CategoricalArrays, DataFrames, JSON, Missings

#produce facts from the json-database
function factualize!(terms, heap, df::DataFrame, facts=Dict{String,Any}())

    facts = copy(facts)
    next = nothing #next entry point for factualization

    if isa(heap, Dict)
        if ~haskey(facts, "technology")
            for (k, v) in heap
                facts["technology"] = k
                factualize!(terms, v, df, facts)
            end
            return nothing
        end

        for k in keys(heap)
            if k ∉ terms
                println("wrong keyword found: ", k)
            end
        end

        for (k, v) in heap
            if k in ["instances", "trials"]
                facts[k[1:end-1]] = nrow(df)>0 ? df[end, Symbol(k[1:end-1])] : 0
                next = heap[k] #entry point for next-level parsing
            elseif k in ["device", "effects", "factors", "note", "property", "remark"]
                if ~isa(v, Array)
                    v = [v]
                end
                facts[k] = haskey(facts, k) ? vcat(facts[k], v) : v
            else #override in any case
                facts[k] = v
            end

            if k == "reference"  #extract year as a number
                facts["year"] = missing
                if isa(v, Array)
                    for s in v
                        try
                            facts["year"] = parse(Int, s[end-3:end])
```

```
                    catch
                    end
                end
                facts["reference"] = join(v, "; ")
            else
                try
                    facts["year"] = parse(Int, v[end-3:end])
                catch
                end
            end
        end
    end

    if next ≠ nothing
        factualize!(terms, next, df, facts)
        return nothing
    end
else #array - go through elements (instances or trials) and parse them
    if haskey(facts, "trial")
        cnt = "trial"
    else
        cnt = "instance"
    end
    for i in heap
        facts[cnt] += 1
        factualize!(terms, i, df, facts)
    end
    return nothing
end

#let's find out what how experimental results and conditions map to each other
fields = Dict{String, Any}()
for k in ["accuracy", "efficiency", "input", "materials", "shape", "size",
    "spectrum", "parameter", "purity", "recovery", "waste"]

    f = get(facts, k, [missing])
    if isa(f, String)
        f = [f]
    end
    fields[k] = hcat(f...) #make everything a 2D array
end

#materials go rightward, trials go downward
if size(fields["materials"], 1) > 1
    fields["materials"] = permutedims(fields["materials"], [2,1])
end

#these are min-max types of fields
```

```
fields["param"] = fields["parameter"]
delete!(fields, "parameter")
for k in ["param", "size", "spectrum"]
    if size(fields[k], 1) == 2
        fields[k*"_min"] = fields[k][1:1,:]
        fields[k*"_max"] = fields[k][2:2,:]
    elseif size(fields[k], 2) == 2
        fields[k*"_min"] = fields[k][:,1:1]
        fields[k*"_max"] = fields[k][:,2:2]
    else
        fields[k*"_min"] = fields[k*"_max"] = fields[k]
    end
    if k == "param" && size(fields[k], 1) == size(fields["materials"], 1)
        fields[k*"_min"] = fields[k*"_max"] = fields[k]
    end
    delete!(fields, k)
end

#let's review what kind of dimensions we have for experimental results
dims = Set(1)
for v in values(fields)
    push!(dims, size(v, 1))
    push!(dims, size(v, 2))
end

if length(dims) > 3
    println("dimension mismatch in ", facts["reference"])
    return nothing
end

#all results will be in the table of ntrial x nmat size
nmat = size(fields["materials"], 2) # == ncol
ntrial = 1 # == nrow
for v in values(fields)
    m = minimum(size(v))
    n = maximum(size(v))

    if m==nmat
        ntrial = max(ntrial, n)
    elseif n==nmat
        ntrial = max(ntrial, m)
    else
        ntrial = max(ntrial, n)
    end
end

#every field should become aligned so that size(v) == (ntrial, nmat)
for (k, v) in fields
```

```
    if (size(v, 1) == nmat || size(v, 2) == ntrial) && nmat ≠ ntrial
        fields[k] = permutedims(v, [2,1])
    end
end

for (k,v) in fields
    if k in ["input", "materials", "param_min", "param_max"]
        v = hcat(v, fill(missing, size(v, 1), nmat-size(v, 2)))
        fields[k] = repeat(v, ntrial ÷ size(v, 1), 1)
    elseif k in ["shape", "size_min", "size_max",
        "spectrum_min", "spectrum_max", "waste"]
        #multiply both trial-wise and material-wise
        fields[k] = repeat(v, ntrial ÷ size(v, 1), nmat ÷ size(v, 2))
    elseif k in ["accuracy", "efficiency", "purity", "recovery"]
        #fill out with missing
        v = vcat(v, fill(missing, ntrial-size(v, 1), size(v, 2)))
        fields[k] = hcat(v, fill(missing, ntrial, nmat-size(v, 2)))
    end
end

#putting fact into the dataframe, line by line
if ~haskey(facts, "instance")
    facts["instance"] = nrow(df)>0 ? df[end, :instance]+1 : 1
end

oldtrial = nrow(df)>0 ? df[end, :trial] : 0
for m in 1:nmat
    for i in 1:ntrial
        facts["trial"] = oldtrial+i
        for (k, v) in fields
            if k in ["materials", "param_min", "param_max", "param_dif"]
                continue
            end
            facts[k] = v[i, m]
        end
        facts["target"] = fields["materials"][i, m]
        #to trash go all materials except the target one
        facts["trash"] = join(fields["materials"][i, [1:m-1;m+1:end]], "&")
        if facts["trash"] == ""
            facts["trash"] = missing
        end

        #parameter - value of the target property for the target material
        #parameterΔ - distance to the closest trash material
        facts["param_min"] = fields["param_min"][i, m]
        facts["param_max"] = fields["param_max"][i, m]
        if ~ismissing(facts["param_min"]) && ~ismissing(facts["param_max"])
            mindif = Inf
```

```
                p1 = 0.5*(facts["param_min"] + facts["param_max"])
                for j in [1:m-1;m+1:nmat]
                    p2 = 0.5*(fields["param_min"][i, j] + fields["param_max"][i, j])

                    dif = abs(p1-p2)
                    if ~ismissing(dif) && dif < mindif
                        mindif = dif
                    end
                end
                facts["param_dif"] = mindif < Inf ? mindif : missing
            end

            #finally, push a new line to the dataframe
            push!(df, [get(facts, String(k), missing) for k in names(df)])

            # make efficiency equal to geometric mean of
            # accuracy, recovery and purity (what is available)
            if ismissing(df[end, :efficiency])
                x=1.0
                n=0
                for i in [:accuracy, :recovery, :purity]
                    if ~ismissing(df[end, i])
                        x*= df[end, i]
                        n+=1
                    end
                end
                if n>0
                    df[end, :efficiency] = round(x^(1/n), digits=2)
                end
            end
        end
    end

    return df
end

function makecategorical!(df, guide, catcols)

    for c in catcols
        allowed = collect(getkeys(guide[String(c)]))
        for i in eachindex(df[c])
            if ~(ismissing(df[i,c]) || df[i,c] in allowed)
                println("unknown term  $c  in")
                println(df[i,:reference])
            end
        end

        categorical!(df, c)
```

```
        levels!(df[c], allowed)
    end
end

function matsplit!(df, allowed=nothing, splitcols=[:target, :trash])
    for c in splitcols
        a = Array{Union{Missing, Array{String,1}},1}(undef, nrow(df))
        for i in 1:nrow(df)
            if ismissing(df[i,c])
                a[i] = missing
            else
                a[i] = split(df[i,c], "&")
            end

            if ~isnothing(allowed) && ~ismissing(a[i])
                for s in a[i]
                    if ~haskey(allowed, s)
                        println("unknown term  $s  in")
                        println(df[i,:reference])
                        return nothing
                    end
                end
            end

        end
        df[c] = a
    end
end

function getkeys(tree::Dict{String,Any})
    key = keys(tree)
    for (k,v) in tree
        if isa(v, Dict)
            key = union(key, getkeys(v))
        end
    end
    return key
end

struct Taxonomy
    id::Dict{String,Int64} #name=>index pairs for distance matrix
    n::Array{String,1} #names ordered as in distance matrix
    d::Array{Int64,2}  #distance matrix
    len::Int64
    function Taxonomy(data::Dict{String,Any}, rootname::String)
        names = [collect(getkeys(data[rootname])); rootname]
        len = length(names)
```

```
        id = Dict{String,Int64}()
        for i in eachindex(names)
            id[names[i]] = i
        end

        BIG = 1234567
        d = fill(BIG, len, len)
        d[1 : size(d,1)+1 : end] .= 0

        getconnections!(rootname, data[rootname], id, d)

        #find shortest paths in material hierarchy by Floyd-Warshall algorithm
        for k in 1:len, i in 1:len, j in 1:len
            d[i,j] = min(d[i,j], d[i,k] + d[k,j])
        end

        #replace infinities with -1
        for i in eachindex(d)
            d[i] = d[i]<BIG ? d[i] : -1
        end

        new(id, names, d, len)
    end
end

function Base.getindex(tax::Taxonomy, x::String, y::String)
    return tax.d[tax.id[x], tax.id[y]]
end

function Base.in(x::String, tax::Taxonomy)
    return haskey(tax.id, x)
end

function getconnections!(rootname::String, tree::Dict{String,Any},
    id::Dict{String,Int64}, d::Array{Int64,2})

    for (k,v) in tree
        d[id[k], id[rootname]] = 1
        if isa(v, Dict)
            getconnections!(k, v, id, d)
        end
    end
end

function xisy(tax::Taxonomy, x::String, y::String)
    if x ∉ tax || y ∉ tax
        return missing
    end
```

```
    return tax[x,y] ≥ 0
end

function alias(tax::Taxonomy, x::Union{String, Missing}, depth::Int=-1)
    if ismissing(x) || x ∉ tax || depth<0
        return x
    end
    level = findmax(tax.d[tax.id[x], :])[1]
    return level < depth ? x : tax.n[findfirst(isequal(level-depth), tax.d[tax.id[x], :])]
end

function alias(tax::Taxonomy, x::Array{String,1}, depth::Int=-1)
    return unique(map(y->alias(tax, y, depth), x))
end

function loadall()
    tech = DataFrame(
        accuracy = Union{Missing, Float64}[], #override
        action = Union{Missing, String}[], #override
        brief = Union{Missing, String}[], #override
        continuity = Union{Missing, String}[], #override
        cost = Union{Missing, String}[], #override
        device = Union{Missing, String, Array{String,1}}[], #concat
        effects = Union{Missing, Array{String,1}}[], #concat
        efficiency = Union{Missing, Float64}[], #override
        factors = Union{Missing, Array{String,1}}[], #concat
        input = Union{Missing, Float64}[], #override
        instance = Int64[],
        maturity = Union{Missing, String}[], #override
        medium = Union{Missing, String}[], #override
        note = Union{Missing, Array{String,1}}[], #concat
        param_min = Union{Missing, Float64}[], #override
        param_max = Union{Missing, Float64}[], #override
        param_dif = Union{Missing, Float64}[], #override
        property = Union{Missing, Array{String,1}}[], #concat
        pressure = Union{Missing, String}[], #override
        purity = Union{Missing, Float64}[], #override
        recovery = Union{Missing, Float64}[], #override
        reference = Union{Missing, String}[], #override
        remark = Union{Missing, Array{String,1}}[], #concat
        shape = Union{Missing, String}[], #override
        size_min = Union{Missing, Float64}[], #override
        size_max = Union{Missing, Float64}[], #override
        spectrum_min = Union{Missing, Float64}[], #override
        spectrum_max = Union{Missing, Float64}[], #override
        target = Union{Missing, String}[], #override
        technology = Union{Missing, String}[], #unique
        temperature = Union{Missing, String}[], #override
```

```
        trash = Union{Missing, String}[], #override
        trial = Int64[],
        waste = Union{Missing, String}[], #override
        year = Union{Missing, Int}[] #override
    )

    data = JSON.parsefile("data.json"; dicttype=Dict, inttype=Int64)

    factualize!(keys(data["guide"]), data["technologies"], tech)
    makecategorical!(tech, data["guide"],
        [:action, :continuity, :maturity, :medium, :pressure, :temperature])
    categorical!(tech, [:brief, :technology])

    mat = Taxonomy(data, "materials")
    matsplit!(tech, mat.id)

    return(data, tech, mat)
end
```

DATA FILTER

datafilter.jl code listing

```
using DataFrames, Interact, Plots, XLSX
gr()

function getall(x)
    levels(vcat(skipmissing(x)...))
end

function allchecked(options, label)
    checkboxes(options, value=options, label=label)
end

function multichoice(a::AbstractArray, n::Int)
    options = getall(a)
    [autocomplete(options) for i in 1:n]
end

function initcontrol(tech::DataFrame, mat::Taxonomy, nopts::Int=5)
    ymin = findmin(getall(tech[:year]))[1]
    ymax = findmax(getall(tech[:year]))[1]
    maxdepth = findmax(mat.d)[1]

    ctrl = Dict(
        :accuracy=>spinbox(0:0.01:1, value=0, label="accuracy>"),
        :action=>allchecked(levels(tech[:action]), "action"),
        :continuity=>allchecked(levels(tech[:continuity]), "continuity"),
        :effects=>multichoice(tech[:effects], nopts),
        :efficiency=>spinbox(0:0.01:1, value=0, label="efficiency>"),
        :factors=>multichoice(tech[:factors], nopts),
        :input_min=>spinbox(0:0.01:1, value=0),
        :input_max=>spinbox(0:0.01:1, value=1, label="<input<"),
        :maturity=>allchecked(levels(tech[:maturity]), "maturity"),
        :medium=>allchecked(levels(tech[:medium]), "medium"),
        :param_min=>spinbox(value=0),
        :param_max=>spinbox(value=findmax(collect(skipmissing(tech[:param_max])))[1],
            label="<parameter<"),
        :param_dif=>spinbox(value=findmax(collect(skipmissing(tech[:param_dif])))[1],
            label="parameter Δ<"),
        :property=>multichoice(tech[:property], nopts),
        :pressure=>allchecked(levels(tech[:pressure]), "pressure"),
        :purity=>spinbox(0:0.1:1, value=0, label="purity>"),
        :recovery=>spinbox(0:0.1:1, value=0, label="recovery>"),
        :shape=>allchecked(levels(tech[:shape]), "shape"),
```

```
        :size_min=>spinbox(),
        :size_max=>spinbox(label="<size (mm)<"),
        :spectrum_min=>spinbox(),
        :spectrum_max=>spinbox(label="<spectrum (nm)<"),
        :target=>[autocomplete(mat.n) for i in 1:nopts],
        :temperature=>allchecked(levels(tech[:temperature]), "temperature"),
        :technology=>multichoice(tech[:technology], nopts),
        :year_min=>spinbox(ymin:ymax, value=ymin),
        :year_max=>spinbox(ymin:ymax, value=ymax, label="<year<"),

        :showcol=>[checkbox(label=n) for n in names(tech)],
        :showline=>spinbox(0:nrow(tech), value=parse(Int, ENV["LINES"]),
            label="Show lines: "),
        :dropempty=>[checkbox(label=n) for n in names(tech)],
        :alias=>slider(0:maxdepth, value=maxdepth, label="material category level"),

        :keyword=>textbox(value="", label="search keyword"),
        :upd=>button("update"),

        :xlabel=>dropdown(names(tech), value=:pressure, label="x-axis"),
        :ylabel=>dropdown(names(tech), value=:temperature, label="y-axis"),
        :grouping=>dropdown([:none; names(tech)], label="grouping"),
        :pltype=>dropdown(["bubble", "scatter", "range"], label="plot type"),

        :fname=>textbox(value="dataexport"),
        :ex2excel=>button("export to Excel"),
        :refid=>spinbox(1:typemax(Int64), value=1),
        :getref=>button("open reference line #"),
        :iname=>textbox(value="plotimage"),
        :ex2image=>button("save plot")
    )

    return ctrl
end

function filtdashboard(ctrl::Dict{Symbol,Any})
    display(hbox(vbox(hbox(ctrl[:recovery], ctrl[:purity]),
        hbox(ctrl[:accuracy], ctrl[:efficiency]),
        hbox(ctrl[:param_min], ctrl[:param_max]),
        ctrl[:param_dif],
        hbox(ctrl[:input_min], ctrl[:input_max]),
        hbox(ctrl[:size_min], ctrl[:size_max]),
        hbox(ctrl[:spectrum_min], ctrl[:spectrum_max]),
        hbox(ctrl[:year_min], ctrl[:year_max]),
        ctrl[:alias],
        ctrl[:keyword]),
        hbox(vbox(ctrl[:action], ctrl[:pressure]),
            vbox(ctrl[:shape], ctrl[:temperature]),
```

```
            vbox(ctrl[:continuity], ctrl[:maturity]),
            ctrl[:medium])))

    display(hbox(vbox(vcat(highlight("effects"), ctrl[:effects])),
            vbox(vcat(highlight("factors"), ctrl[:factors])),
            vbox(vcat(highlight("property"), ctrl[:property])),
            vbox(vcat(highlight("technology"), ctrl[:technology])),
            vbox(vcat(highlight("target"), ctrl[:target]))))

    display(highlight("exclude missings in the following columns:"))
    display(checkboxgrid(ctrl[:dropempty]))

    return nothing
end

function filt(params::Dict{Symbol,Any}, tech::DataFrame, mat::Taxonomy, output::Symbol)
    #set amount of lines shown via environment variable
    ENV["LINES"] = params[:showline][]

    df = deepcopy(tech)

    #exclude missings where needed
    musthave = [x[] for x in params[:dropempty]]
    df = sum(musthave)==0 ? df : df[completecases(df[musthave]),:]

    #apply aliasing to materials
    depth = params[:alias][]
    for c in [:target, :trash]
        df[c] = map(x->alias(mat, x, depth), df[c])
    end

    #boolean with allowed rows
    pass = fill(true, nrow(df))

    #filter options
    for val in [:action, :continuity, :maturity, :medium, :pressure, :shape, :temperature]
        pass .&= map(x->coalesce(x in params[val][], true), df[val])
    end
    #filter minima
    for val in [:accuracy, :efficiency, :purity, :recovery]
        pass .&= map(x->coalesce(x ≥ something(params[val][], -Inf), true), df[val])
    end
    #filter maxima
    for val in [:param_dif]
        pass .&= map(x->coalesce(x ≤ something(params[val][], Inf), true), df[val])
    end
    #filter intervals
    for subval in [:input, :param, :size, :spectrum, :year]
```

```
    val = Symbol(subval, :_min)
    c = val in names(df) ? val : subval
    pass .&= map(x->coalesce(x ≥ something(params[val][], -Inf), true), df[c])
    val = Symbol(subval, :_max)
    c = val in names(df) ? val : subval
    pass .&= map(x->coalesce(x ≤ something(params[val][], Inf), true), df[c])
end

#filter multioptions
for val in [:effects, :factors, :property, :technology]
    allowed = Set([""])
    for x in params[val]
        push!(allowed, x[])
    end
    allowed = setdiff(allowed, [""])

    if ~isempty(allowed)
        pass .&= map(x-> ~isempty(intersect(allowed,
            Set(ismissing(x) || isa(x, Array) ? coalesce(x, allowed) : [x]))), df[val])
    end
end

#filter materials with taxonomy
for val in [:target]  # :trash could be here as well
    allowed = Set([""])
    for x in params[val]
        push!(allowed, x[])
    end
    allowed = setdiff(allowed, [""])

    if ~isempty(allowed)
        pass .&= map(df[val]) do x
            present = Set{String}(coalesce(x, allowed))
            for p in present, a in allowed
                if xisy(mat, p, a)
                    return true
                end
            end
            return false
        end
    end
end

#search for the keyword
keyword = lowercase(ctrl[:keyword][])
if ~isempty(keyword)
    pass .&= map(x-> occursin(keyword, lowercase(join(vcat(x...), ";"))), eachrow(df))
end
```

```
    toshow = [x[] for x in params[:showcol]]

    #let's output
    if output == :table
        return sum(pass)*sum(toshow)>0 ? unique(df[pass,toshow]) : df[pass,toshow]
    elseif output == :filter
        return df[pass,:]
    elseif output == :plot
        grouping = params[:grouping][]==:none ? [] : params[:grouping][]
        if sum(pass) == 0
            return "nothing to plot"
        end

        df = df[pass,:]
        if params[:pltype][] == "bubble"
            bubbleplot(df, params[:xlabel][], params[:ylabel][], grouping)
        elseif params[:pltype][] == "scatter"
            scatterplot(df, params[:xlabel][], params[:ylabel][], grouping)
        elseif params[:pltype][] == "range"
            xlabel = Symbol(String(params[:xlabel][])[1:end-4])
            rangeplot(df, xlabel, params[:ylabel][], grouping)
        else
            return nothing
        end
    else
        return nothing
    end
end

function checkboxgrid(c, h=4)
    len = length(c)
    return hbox([vbox([c[j] for j in i:min(i+h-1, len)]) for i in 1:h:len])
end

function dfdashboard(ctrl)
    display(hbox(ctrl[:showline], highlight("Show columns: ")))
    display(checkboxgrid(ctrl[:showcol]))
    display(hbox(ctrl[:ex2excel], ctrl[:fname]))
    display(hbox(ctrl[:getref], ctrl[:refid]))

    return nothing #(fname, ex2excel, refid, getref)
end

function plotdashboard(ctrl)
    display(hbox(ctrl[:xlabel], ctrl[:ylabel], ctrl[:grouping], ctrl[:pltype]))
    display(hbox(ctrl[:ex2image], ctrl[:iname]))
    #map((x...)->filt(Dict(zip(keys(ctrl),x)), mat), values(ctrl)...)
```

```
    return nothing #(fname, ex2image)
end

function makexcel(fname::String, tb::DataFrame)
    if isempty(tb)
        return nothing
    end
    try
        a = copy(tb)
        for i in names(a)
            a[i] = map(x-> isa(x, Union{Number, String, Missing}) ? x : join(x, "; "),
                Array(a[i]))
        end
        XLSX.writetable(fname*".xlsx",
            data=( DataFrames.columns(a), DataFrames.names(tb) ), overwrite=true)
    catch
        println("oops, ", fname, ".xlsx was not saved")
    end
    return nothing
end

function refopen(refid::Int, df::DataFrame)
    try
        refs = df[refid,:reference]
        if ismissing(refs)
            return nothing
        elseif ~isa(refs, Array)
            refs = [refs]
        end
        for s in refs
            for ext in [".pdf", ".png"]
                fname = "ref\\" * s * ext
                try
                    run(`cmd /c start "" /max $fname`);
                catch
                end
            end
        end
    catch
    end
    return nothing
end
```

DATA PLOTTER

dataparser.jl code listing

```
using Plots
gr()

function logticks(lims::NTuple{2,Float64})
    decirow = Float64[1,5]
    row = decirow

    mult = 1
    while row[1]>lims[1]
        mult/=10
        row = [mult.*decirow; row]
    end
    mult = 1
    while row[end]<lims[2]
        mult*=10
        row = [row; mult.*decirow]
    end
    first = findlast(x-> x<=lims[1], row)
    last = findfirst(x-> x>=lims[2], row)
    row = row[first:last]

    str = [string(x<1 ? x : Int(x)) for x in row]

    return (row, str)
end

function bubbleplot(df::DataFrame, xlabel::Symbol, ylabel::Symbol, grouping=[];
    binary::Bool=false, annotate::Bool=true)

    try
        m = copy(df[completecases(df[[xlabel,ylabel]]), [xlabel; ylabel; grouping]])

        for c in [xlabel, ylabel]
            m[c] = map(i-> isa(i, Array) ? i : [i], m[c])
        end

        cnt = Dict{Tuple{String, String}, Int64}()

        if grouping ≠ []
            present = Set{Tuple}()
            for r in eachrow(m)
                for x in r[xlabel], y in r[ylabel]
```

```
            if haskey(cnt, (x,y))
                if (x,y,r[grouping]) ∉ present
                    cnt[(x,y)] += 1
                end
            else
                cnt[(x,y)] = 1
            end
            push!(present, (x,y,r[grouping]))
        end
    end
else
    for r in eachrow(m)
        for x in r[xlabel], y in r[ylabel]
            if haskey(cnt, (x,y))
                cnt[(x,y)] += 1
            else
                cnt[(x,y)] = 1
            end
        end
    end
end

x = [i[1][1] for i in cnt]
y = [i[1][2] for i in cnt]
cnt = [i[2]  for i in cnt]
maxcnt = findmax(cnt)[1]

if binary
    for i in eachindex(cnt)
        cnt[i] = cnt[i]>0 ? 1 : 0
    end
end
scale = 10 / √(findmax(cnt)[1])

xlongest = 0
for s in levels(x)
    xlongest = max(xlongest, length(s))
end
ylongest = 0
for s in levels(y)
    ylongest = max(ylongest, length(s))
end

#plot dimensions
left_margin = ylongest*3Plots.px
bottom_margin = xlongest*3Plots.px
xn = length(levels(x))
yn = length(levels(y))
```

```
        width = max(xn*50 + 7*ylongest + 25, 250)
        height = max(yn*50 + 7*xlongest + 25, 250)

        # count numbers inside largest bubbles
        if annotate && ~binary
            sa = map(i-> (i>maxcnt/2 ? text(string(i),:white,5) : ""), cnt)
        else
            sa = nothing
        end

        plt = scatter(x, y, markersize=scale .*.√cnt,
            color=:blue, grid=false, legend=false,
            xticks=:all, yticks=:all, xrotation=-60,
            left_margin=left_margin, bottom_margin=bottom_margin,
            msw=0,
            size=(width, height),
            xlims=[0,xn+1], ylims=[0,yn+1],
            series_annotations=sa, tick_dir=:in,
            aspect_ratio=1,
            xlabel=xlabel, ylabel=ylabel
        )

        return plt
    catch
        return "wrong input"
    end
end

function rangeplot(df::DataFrame, xlabel::Symbol, ylabel::Symbol, grouping=[])
    try
        xmin = Symbol(xlabel,:_min)
        xmax = Symbol(xlabel,:_max)

        m = df[completecases(df[[ylabel;xmin;xmax;grouping]]), [xmin;xmax;ylabel;grouping]]
        for c in names(m)
            m[c] = map(x-> isa(x, Array) ? join(x,"; ") : x, m[c])
        end
        groups = isa(grouping, Symbol) ? levels(m[grouping]) : ["all"]
        ngroup = length(groups)
        if ngroup>1
            linecolor = [findfirst(x-> i==x, groups) for i in m[grouping]]
        else
            linecolor = fill(1, nrow(m))
        end

        #remove zeros because of log scale
        foreach(i -> m[i,xmin] < 1e-3 && (m[i,xmin] = 0.1*m[i,xmax]), eachindex(m[xmin]))
        #make single points like short intervals
```

```
foreach(i -> m[i,xmin]/m[i,xmax] > 0.99 && (m[i,xmin] = 0.9*m[i,xmax]),
    eachindex(m[xmin]))

yreal = isa(m[1,ylabel], Number)
xticks = logticks((findmin(m[xmin])[1], findmax(m[xmax])[1]))
density = √(length(levels(m[ylabel])) / length(m[xmin])) #heuristic for markeralpha

#some magic here to make plotting ranges as separate lines (series)
xs = permutedims(hcat(m[xmin], m[xmax]))
ys = permutedims(hcat(m[ylabel], m[ylabel]))

#plot optimal dimensions
ylongest = yreal ? 4 : findmax(length.(levels(ys)))[1]
left_margin = (ylongest*1+10)Plots.px
bottom_margin = 10Plots.px
xn = 5*length(levels(xticks))
yn = length(levels(ys))
width = max(xn*60 + 5*ylongest + 25, 250)
height = max(yn*30 + 25, 250)

plt = plot()
for c in 1:ngroup
    plot!(plt, xs[:,linecolor.==c], ys[:,linecolor.==c],
        legend=false, xscale=:log10, yticks=:all,
        grid=:x, minorgrid=:x, gridalpha=0.5, minorgridalpha=0.2,
        lw=20, lc=c, la = density,
        palette=:darkrainbow, clims=(1,ngroup),
        xticks=xticks, xlim=(xticks[1][1], xticks[1][end]), xlabel=xlabel,
        ylabel=ylabel, size=(width,height),
        left_margin=left_margin, bottom_margin=bottom_margin
    )
end
oldw = width

if ngroup>1 #we need a legend (outside the plot)
    ylongest = findmax(length.(groups))[1]
    yn = length(groups)
    width = 10+7*ylongest

    leg = scatter()
    for c in 1:ngroup
        scatter!(leg, [0], [c], ma=0.6, msw=0, ms=20, shape=:rect,
            palette=:darkrainbow, clims=(1,ngroup),
            axis=false, grid=false, legend=false,
            annotation=(0,c, groups[c], :left), size=(width,height),
            ylim=(0,yn+1), xlim=(-1,ylongest))
    end
    return plot(plt, leg, layout=(1,2), size=(oldw+width, height))
```

```
        end
        return plt
    catch
        return "wrong input"
    end
end

function scatterplot(df::DataFrame, xlabel::Symbol, ylabel::Symbol, grouping=[])
    try
        m = df[completecases(df[[ylabel;xlabel;grouping]]), [xlabel;ylabel;grouping]]
        for c in names(m)
            m[c] = map(x-> isa(x, Array) ? join(x,"; ") : x, m[c])
        end

        groups = isa(grouping, Symbol) ? unique(m[grouping]) : ["all"]
        ngroup = length(groups)

        if ngroup>1
            color = [findfirst(x-> i==x, groups) for i in m[grouping]]
        else
            color = fill(1, nrow(m))
        end

        xreal = isa(m[1,xlabel], Number)
        yreal = isa(m[1,ylabel], Number)

        #grids only for numerical values
        grid = false
        if xreal
            if yreal
                grid = :xy
            else
                grid = :x
            end
        elseif yreal
            grid = :y
        end

        density = 1/√ngroup #heuristic to estimate reasonable markeralpha

        xs = m[xlabel]
        ys = m[ylabel]

        #arsenal of good markers
        shp = [:diamond, :hexagon, :utriangle, :dtriangle, :rtriangle, :ltriangle,
            :pentagon, :heptagon, :star4, :star5, :star6]
        shp = repeat(shp, ceil(Int, ngroup/length(shp))) #more markers just in case
```

```
        #plot optimal dimensions
        xlongest = xreal ? 1 : findmax(length.(levels(xs)))[1]
        ylongest = yreal ? 4 : findmax(length.(levels(ys)))[1]

        left_margin = (ylongest*2+10)Plots.px
        bottom_margin = (xlongest*2+10)Plots.px
        xn = xreal ? 20 : length(levels(xs))
        yn = yreal ? 20 : length(levels(ys))
        width = max(xn*30 + 5*ylongest + 25, 250)
        height = max(yn*30 + 5*xlongest + 25, 250)

        plt = scatter()
        for c in 1:ngroup
            scatter!(plt, xs[color.==c], ys[color.==c], lab=groups[c],
                legend=false, xticks=:all, yticks=:all,
                grid=grid, minorgrid=grid, gridalpha=0.5, minorgridalpha=0.2,
                ma=density, msw=0, ms=8, shape=shp[c],
                palette=:darkrainbow, clims=(1,ngroup),
                xlabel = xlabel, ylabel = ylabel,
                xrotation = xreal ? 0 : -60,
                size=(width,height), left_margin=left_margin, bottom_margin=bottom_margin
            )
        end
        oldw = width

        if ngroup>1 #we need a legend (outside the plot)
            ylongest = findmax(length.(groups))[1]
            width = 10+7*ylongest

            leg = scatter()
            for c in 1:ngroup
                scatter!(leg, [0], [c], ma=0.6, msw=0, ms=8, shape=shp[c],
                    palette=:darkrainbow, clims=(1,ngroup),
                    axis=false, grid=false, legend=false,
                    annotation=(0,c, groups[c], :left),
                    size=(width,height), ylim=(0,yn+1), xlim=(-1,ylongest))
            end
            return plot(plt, leg, layout=(1,2), size = (oldw+width, height))
        end
        return plt
    catch
        return "wrong input"
    end
end
```